



REPUBLIQUE ALGERIENNE DEMOCRATIQUE ET POPULAIRE
MINISTRE DE L'ENSEIGNEMENT SUPERIEUR ET DE LA RECHERCHE SCIENTIFIQUE

UNIVERSITE ABOU-BEKR BELKAID – TLEMCCEN

THÈSE

Présentée à :

FACULTE DES SCIENCES – DEPARTEMENT DE PHYSIQUE

Pour l'obtention du diplôme de :

DOCTORAT EN SCIENCES

Spécialité : Physique des Polymères

Par :

Mme KHOBZAOUI Souhila

Sur le thème

Caractérisation et Etude des Propriétés Physiques des Composites Bentonite/Acrylamide [BC/AM]

Soutenue publiquement le 25/06/2022 à Tlemcen devant le jury composé de :

Mr BOUSSAID Abdelhak	Professeur	Université de Tlemcen	Président
Mr TENNOUGA Lahcene	Professeur	Ecole (ESSA) Tlemcen	Directeur de Thèse
Mr BENABADJI Ismet Kamel	Professeur	Université de Tlemcen	Co-Directeur de Thèse
Mr MEDJAHED Kouider	Professeur	Université de Tlemcen	Examineur
Mme CHEMOURI Hafida	Maître de Conférences A	Ecole (ESSA) Tlemcen	Examinatrice
Mme ABDELLI Imane	Maître de Conférences A	Ecole (ESSA) Tlemcen	Examinatrice

**Laboratoire d'Application des Electrolytes et des Polyélectrolytes Organiques
(LAEPO)BP 119, 13000 Tlemcen - Algérie**

Dedicated to My mother and my father. For their existence in my life.

My dearest treasure MOHAMED ILYAN

My precious pearl EMNA

To my husband BENABDELMOUMENE AHMED

My brothers, especially to K. DEROUICH for his encouragements. To my sisters

My second mother Khadidja and my cousin's S, A, M, F, F.

To Amina NACERI, B BASMA, B SIHEM, B ZAHRA, B OUAFA, B LYNA

My nephews and my nieces.

To my family and all those who are dear.

Wonder is the Beginning of All Science – Aristotle

It's always darkest before the dawn

Acknowledgements

First of all, I thank Almighty God who gave me the strength and faith and for getting me to this point.

I take this opportunity to express my gratitude to Pr TENNOUGA Lahcene and deceased Pr Ali Mansri, my research supervisors. My particular gratitude and recognition to Pr Tennouga, for his guidance, fruitful discussions, support and advices throughout the course. More importantly for the freedom he has given to me. My sincere regards and reverence are for him, forever.

My sincers thankfulness to Pr. BENNABADJI Ismet my co-supervisor for his support and advices during my research work.

I am extremely grateful to Dr Fernando ania for hosting me at the Macromolecular Physics Department IEM-CSIC (Madrid, Spain), during the performance of the surface mechanical experiments. He already inspired me in so many ways. He gave stimulating scientific discussions and suggestions. I truly appreciate his patience, helpfulness.

I extend my sincere thanks to, Professor Pr BOUSSAID Abdelhak, which gives me a honor by agreeing to chair the jury of this doctoral thesis. I express my sincere thanks to the committee, and jury members:

- *Pr MEDJAHED Kouider*
- *Dr CHEMOURI Hafida (MCA)*
- *Dr ABDELLI Imane (MCA)*

I acknowledge an appreciation that extends beyond any words for the love and support of my friends, particularly all LAEPO collegs (H. M , W B, W B, A B, T H, ...). I extend my deep sense of gratitude towards them. Thanks to Cindy, Fred, Katty, Kevin and others who contributed to create me the atmosphere for a calm drafting.

TABLES LIST

Chapter I

Table I.II.1 : Properties of clay mineral groups	p20
Table I.II.2 : Chemical composition of bentonite (maghnia) reported from three different references	p37
Table I.II.3 : Trace elements of bentonite	p37
Table I.II.4 : Cationic Echange of bentonite With Differents Cation.....	p37
Table I.II.5 : Particle size analysis of bentoite of maghnia (roussel).....	p37
Table I.II.6 : Physico-chemical and rheological properties of natural bentonite.....	p38
Table I.II.7 : The important physico-chemical properties of bentonite (maghnia).....	p38
Table I.II.8 : The important physico-chemical properties of bentonite (maghnia).....	p38
Tableau I.III.1 : Synthesis conditions of polyacrylamide and the weight molar	p47
Table I.III .2 : Thermo-Physical Properties Of Polyacrylamides : Experimental / Literature Data.....	p48
Table I.III.3: Thermo-Physical Properties Of Polyacrylamides : Calculated Data.....	p48

Chapter III

Table III.1: Chemical composition of bentonite BC.....	p75
Tableau III.2: Quantities used in the preparartion of PAM/BC nanocomposites.....	p76
Table III.3: EDS spectrum and elemental percent composition for the polymer composite prepared with 1% of BC	p79
Table III.4: EDS spectrum and elemental percent composition for the polymer composite prepared with 3% of BC	p79
Table III.5: EDS spectrum and elemental percent composition for the polymer composite prepared with 5% of BC	p80

Chapter IV

Table IV.1: EDS spectrum and elemental percent composition for the polymer composite prepared with 10% of BC	p94
Table IV.2: EDS spectrum and elemental percent composition for the polymer composite prepared with 25% of BC	p95
Table IV.3: EDS spectrum and elemental percent composition for the polymer composite prepared with 50% of BC	p96

Chapter V

Table V.1: Micro-hardness data of (PAM/1% wt BC) for different indentation time values for applied load of 250 mN	p107
--	------

Table V.2: Micro-hardness data of (PAM/1% wt BC) for two different load values (250 mN and 500 mN) at indentation time of 6Sp107

Table V.3: Micro-hardness data of (PAM/50% wt BC) for different indentation time values for applied load of 250 mNp108

Table V.4: Micro-hardness data of (PAM/50% wt BC) for two different load values (250 mN and 500 mN) at indentation time of 6S.....p108

FIGURES LIST

Chapter I

- Figure I.I.1 :** Schemes and images of different types of nanoreinforcements, redrafted from. Surface area/volume relations for different reinforcement geometries are also displayed...p7
- Figure I.I.2:** Schematic example of in situ polymerization process involving the synthesis of nylon-6/clay nanocomposite..... p8
- Figure I.I.3 :** Nylon-6 nanocomposite formed through in situ polymerization with ADA–MMTp9
- Figure I.I.4 :** Schematic of Fe₃O₄/MWCNT/chitosan nanocomposite synthesis by solution Mixing.....p10
- Figure I.I.5 :** Melt processing chitosan in a blend with poly(lactic acid) and poly(vinyl alcohol).....p11
- Figure I.I.6 :** Montmorillonite (MMT) exfoliation in PA-6 during WA melt compounding schematically. Note: in this case water was injected into the molten PA-6 containing pristine MMT(Na-MT).....p12
- Figure I.I.7 :** Structure of clay in nanocomposites with corresponding wide angle X-ray scattering (WAXS) and transmission electron microscopy (TEM) results.....p13
- Figure I.II.1 :** Octahedral Sheet of Clay.....p19
- Figure I.II.2 :** Tetrahedral sheet of Clay..... p19
- Figure I.II.3 :** Structure of kaollinite group..... p22
- Figure I.II.4 :** Structure of illite Micap24
- Figure I.II.5 :** Structure of smectite..... p25
- Figure I.II.6 :** Structure of Mg vermiculite.....p26
- Figure I.II.7 :** Crystal structure of cookeite LiAl₄(Si₃Al)O₁₀(OH)₈, space group Cc, projected along the b direction with perspective viewing.....p28
- Figure I.II.8 :** Multi-scale structure of montmorillonite clay.....p28
- Figure I.II.9:** Patterns of associations assumed for suspended montmorillonite strips: (a) dispersion, (b) face-to-face aggregation, (c) edge-to-face association, (d) edge-to-edge association.....p29
- Figure I.II.10:** The different types of stacking in the clays Ordered stacking (b) Semi-ordered stacking (c) Disorderly stacking.....p30
- Figure I.II.11 :** Different Modes Of Succession Of Sheets Within An Inter-Unit.....p31
- Figure I.II.12 :** Structure of bentonite p32

Figure I.II.13 : (a) Schematic illustration of the cation exchange reaction of Na^+ to Cu^{2+} in montmorillonite (b) The cylinder to the left contains a pure solution of a Cu^{2+} complex.

.....p35

Figure I.II. 14 : Acidic activation process of bentonite.....p36

Figure I.III.1 : Radicalar polymerization of polyacrylamide.....p46

Figure I.III.2 : Radicalar polymerization of polyacrylamide with a pair of redox initiator ammonium persulfate and triethanolamine.....p47

Figure I.III.3: Different kind of polyacrylamde..... p50

Fig. I.III.4 : The synthetic route of Anionic polyacrylamid..... p51

Figure I.III.5 : Hydrophobically modified cationic acrylamide copolymer..... p52

Chapter II

Figure II-1. Bragg's Law reflection..... p57

Figure II .2 : Benchtop SEM- JCM 6000 - Jeol, Leica DM Inverted Research Metallurgical Microscope, Kruss - MSZ 5600, Kruss - MMB 2300, Zeiss-Axio Scope A1p58

Figure II.3: DSC instrument Pyris 6 de Perkin Elmerp59

Figure II .4: Heat flux as a function of temperaturep60

Figure II.5 : Thermogram (a) of endothermic transformation and (b) of exothermic transformationp61

Figure II.6 : Thermogram of glass transitionp62

Figure II.7 : Adiabatic reactor..... p63

Figure II.8 : Leica VMHT MOT micro indenterp67

Figure II.9 : Microscope associated to the micro indenter p68

Figure II.10 : Typical example of a nanoindentation load-depth curve (left) and corresponding residual indent (right)Nano hardness p69

Figure II.11 : Keysight G200 nano indenter.....p71

Figure II.12 : Capture of indeter calculation during test.....p71

Chapter III

Figure III.1: SEM micrographs of (A): pure bentonite (magnification x5000) (B): PAM/BC 1% (x1000) (C): PAM/BC 3% (x1000) and (D): PAM/BC 5% (x1000).....p77

Figure III.2 : XRD scans of: (a) - BC; 2 theta from [0, 70]; I_{max} for the first peak 400cps. (b)- Composite prepared with 1% of BC; the quartz peak appears at 2 theta = 27° with $I_{max}=1000cps$. (c)- Composite prepared at 3% of BC. (d)- Composite prepared at 5% of BC.....p81

Figure III.3: DSC scan obtained for the composite prepared with 1 percent in weight of BC	p82
Figure III.4: DSC scan obtained for the composite PAM/ BC 3%	p82
Figure III.5: DSC scan obtained for the composite PAM/BC 5%	p83
Figure III.6: Glass transition temperature as a function of weight percentage of BC	p84
Figure III.7: The residual indentation on samples prepared with 1, 3 and 5 percent in weight of BC	p85
Figure III.8: Micro-hardness variation in x (parallel) and y (perpendicular) direction with percentage in weight. Average micro hardness variation with percentage in weight of BC	p85
Figure III.9: Nano-hardness (GPa) variation with displacement into surface (nm) for weight percent of BC: (a)BC=1%, (b)BC=3%, (c)BC=5% at T= 25-26°C, Relative humidity (RH)=34%	p87
Figure III.10: Modulus (GPa) variation with displacement into surface (nm), for weight percent of BC:(a)BC=1%, (b)BC=3%, (c)BC=5% at T= 25-26°C, RH=34%	p87
Figure III.11: Load (mN) variation with displacement into surface (nm)	p88
Figure III.12: (a) Storage modulus variation with percentage in weight of BC, (b) Nano hardness variation with percentage in weight of BC, (c) Tangent of curve load variation with percentage in weight of BC	p89
<u>Chapter IV</u>	
Figure IV.1: SEM micrographs of (A): pure bentonite (magnification x5000), (B): PAM/BC 10% (x100) (C): PAM/BC 25% (x1000) and (D): PAM/BC 50% (x1000)	p92
Figure IV.2 : XRD scans of: (1)- Composite prepared with 10% of BC; cps. (2)- Composite prepared at 25% of BC. (3)- Composite prepared at 50% of BC	p97
Figure IV.3: DSC scan obtained for the composite PAM/ BC 10%	p98
Figure IV.4: DSC scan obtained for the composite PAM/ BC 50%	p98
Figure IV.5: The residual indentation on samples prepared with 10, 25 and 50 percent in weight of BC	p99
Figure IV.6: Micro-hardness variation in x (parallel) and y (perpendicular) direction with percentage in weight. Average micro hardness variation with percentage in weight of BC	p99
Figure IV.7: Nano-hardness (GPa) variation with displacement into surface (nm) for weight percent of BC: (a)BC=10%, (b)BC=25%, (c)BC=50% at T= 25-26°C, Relative humidity (RH)=34%	p110
Figure IV.8: Load (mN) variation with displacement into surface (nm)	p101

Figure IV.9: Modulus (GPa) variation with displacement into surface (nm), for weight.....p101

Figure IV.10: (1) Hardness variation with percentage in weight of BC, (2) Storage modulus variation with percentage in weight of BC Nano, (3) Tangent of curve load variation with percentage in weight of BC.....p102

chapter v

Figure V.1: Residual indents at the sample surface of (PAM/ 50% wt BC) at different time indentation $t= 6s$, $t=20s$, $t=99s$p106

Figure IV.2: Residual indents at the sample surface of (PAM/ 1% wt BC) at different load applied $F=500mN$, $F=250mN$p106

Figure V.3 : Average hardness variation with indentation time for (PAM/1%wt BC) and (PAM/50wt BC).....p107

Figure V.4: Average hardness variation with load applied for (PAM/1% wt BC) and (PAM/50%wt BC).....p109

Figure V.5: Visual hardness variation with time loading for (PAM/1wt BC) and (PAM/50wt BC).....p110

ABBREVIATIONS AND SYMBOLS LIST

A

A: projected area impression

AM: Acrylamide

APS: Persulfate d'Amunium

B

BC: bleaching clay (bentonite)

D

C_p = specific heat

DSC: differentiel scannig calorimetry

d: diagonal of the indentation

E

EDS: energy dispersive X-ray spectroscopy

H

H: hardness

H_v: visual hardness

H_{//}: hardness in x direction

H_⊥: hardness in y direction

HK: Knoop hardness

HV: vickers hardness

I

I_a: crystalline intensity.

I_c: amorphous intensity.

M

Mmt: montmorillonite

P

PAM: polyacrylamide

P: load

S

Sem: scanning electron microscope

T

T_g: vitreouse temperature

W

wt: weight

X

XRD: X-ray diffraction

X_c: degree of cristanillity

TABLE CONTENT

INTRODUCTIONp1

PARTY I : BIBLIOGRAPHY AND EXPERIMENTAL TECHNIQUES

CHAPTERE I : BIBLIOGRAPHY

I-I : POLYMERS NANOCOMPOSITEp5

I-I-1- DEFINITION OF NANOCOMPOSITE MATERIAL.....p5

I-I-2- CLASSIFICATION OF NANO-COMPOSITE MATERIALS ACCORDING TO MATRIX..... p6

I-I-2-1-Nanocomposite with organic matrix.....p6

I-I-2-2- Nanocomposite with metalical matrix..... P7

I-I-2-3-Nanocomposite with ceramic matrix.....p7

I-I-3- CLASSIFICATION OF NANO-COMPOSITE MATERIALS ACCORDING TO THE FROME OF NANAOCARGE :p7

I-I-4-METHODS OF PREPARATION AND SYNTHESIS OF NANOCOMPOSITES POLYMERS.....p9

I-I-4-1-In situ polymerization :p9

I-I-4-2- Solution mixing or blendingp10

I-I-4-3-Melt belding.....p11

I-I-4-4- Melt Compoundingp12

I-I-5 : TYPES OF NANOCOMPOSITES.....p13

I-I-5-1 Microcomposite polymer.....p14

I-I-5-2 Intercalated nanocompositep14

I-I-5-3 Exfoliated nanocomposite.....p14

References.....p15

I-II- MINERALS CLAY

I-II-1 DEFINITION OF MINERAL CLAY	p20
I-II-2 CLAY MINERAL CLASSIFICATION.....	p20
➤ <u>Type 1/1(or T-O) minerals.....</u>	p22
➤ <u>Type 2/1 minerals (or T-O-T):</u>	p22
➤ <u>Minerals type 2/1/1(or T-O-T-O):</u>	p23
<u>I-II-2-1 Kaolinite group :</u>	p23
<u>I-II-2-2 Mica group.....</u>	p24
<u>I-II-2-3 Smectite group</u>	p26
<u>I-II-2-4 Vermiculite.....</u>	p28
<u>I-II-2-5 Chlorites group</u>	p29
I-II-3 MULTI-SCALE STRUCTURE OF MONTMORILLONITE CLAY.....	p31
<u>I-II.3.1. The sheet :</u>	p32
<u>I-II.3.2. The primary particle or tactoid</u>	p32
<u>I-II.3.3. The aggregate</u>	p32
I-II-4 STRUCTURE OF BENTONITE.....	p35
I-II-5 :TYPES OF BENTONITE.....	p36
<u>I-II-5-1-Calcium bentonites.....</u>	p36
<u>I-II-5-2-Sodium bentonites.</u>	p36
<u>I-II-5-3-Bentonites activated:</u>	p36
I-II-6-PROPRIETIES OF BENTONITE :	p37
<u>I-II-6-1 Physical and chemical properties of bentonite :</u>	p38
➤ <u>Cation exchange capacity (CEC)</u>	p38
➤ <u>Acidic activation of bentonite</u>	p40
<u>I-II-6-2 ; Chemical composition and some physical properties of magnesia bentonite</u> <u>performed in subsequent research studies.....</u>	p40
I-II-7 : USE AND APPLICATION OF BENTONITE.....	p43
<u>References</u>	p45

I-III POLYACRYLAMIDE PROPRIETIES

I-III-1 : DEFINITION OF THE POLYACRYLAMIDE	p49
I-III-2 : EFFECT OF INITIATOR QUANTITIES AND CONDITION OF SYNTHESIS IN THE WEIGHT MOLAR OF POLYACRYLAMIDE	p51
I-III-3 : THERMO-PHYSICAL PROPERTIES OF POLYACRYLAMIDES : EXPERIMENTAL / LITERATURE DATA.....	p52
I-III-4 : THERMO-PHYSICAL PROPERTIES OF POLYACRYLAMIDES : CALCULATED DATA	p52
I-III-5 CHEMICAL PROPERTIES OF POLYACRYLAMIDES.....	p53
I-III-6 : PHYSICAL PROPERTIES OF POLYACRYLAMIDES	p56
I-III-7 : TYPES OF POLYACRYLAMIDES	p58
<u>References</u>	p59

CHAPTER II: EXPERIMENTAL TECHNIQUES AND METHODS USED

II-1 X-RAY DIFFRACTION :	p61
<u>II-1-1 Definition of XRD</u>	p61
<u>II-1-2 : Bragg's law</u> :	p61
II.2. SCANNING ELECTRON MICROSCOPE SEM « MEB »	p62
<u>II-2-1 SEM principle</u>	p63
II-3 DIFFERENTIAL SCANNING CALORIMETRY DSC.....	p63
<u>II-3-1: DSC definition</u>	p64
<u>II-3-2- Detection of phase transitions</u>	p64
<u>II -3-3 DSC curves</u>	p65
<u>Interpretation of Dsc curves</u>	p65
II.4. ADIABATIC PROCESS	p68
<u>II-4-1. Adiabatic process definition</u>	p68
<u>II-4-2-The adiabatic reactor</u>	p68

<u>II-4-3 Adiabatic polymerisation</u>	p69
II- 5 INDENTATION TECHNIQUES:	p71
<u>II-5-1 Micro indentation techniques</u>	p71
<i>II-5-1-1 Micro indenter test</i>	p71
<i>II-5-1-2 Micro indentation working principles</i>	p71
<i>II-5-1-3 Micro hardness</i>	p72
<i>II-5-1-4 Instrumentation used</i>	p73
<u>II-5-2 Nano indentation techniques</u>	p74
<i>II-5-2-1 Definition of nanoindentation technique</i>	p74
<i>II-5-2-2 Nanoindenter Working Principles</i>	p74
<i>II-5-2-3 Nanohardness test</i>	p76
<i>II-5-2-4 Instrumentation used</i>	p77
<u>References</u>	p79

PARTY II : EXPERIMENTAL STUDIES

CHAPTER III: INFLUENCE OF NANO- STRUCTURE AND MORPHOLOGY OF THE COMPOSITE IN PAM/BC PROPERTIES

III-1 : INTRODUCTION	p82
III-2 ELABORATION AND SYNTHESIS OF PAM/BC	p82
<u>III-2-1 Materials used</u>	p82
<u>III-2-2 Reagents</u>	p83
<u>III-2-3 Operator mode of polyacrylamide bentonite nanocomposites</u>	p83
III-3 INSTRUMENTS AND CONDITIONS USED DURING TESTS	p.84
III-4. RESULTS AND DISCUSSION	p84
<u>III-4-1. SEM of polymer nanocomposites at different ratios of BC/AM</u>	p84
<u>III-4-2. XRD analyses for polymer composites with different ratio of BC/PAM</u>	p89
<u>III-4-3. DSC thermal analysis of the different samples prepared</u>	p90

III-4-4. Micro-indentation results.....p93

II-4-5. Nano-indentation results.....p95

CONCLUSION.....p99

References.....p100

CHAPTER IV: AMOUNT OF BC EFFECT ON THE PAM/BC PROPERTIES

IV-1 INTRODUCTION..... p101

IV-2. RESULTS AND DISCUSSIONS..... .p101

IV-2-1. SEM of polymer nanocomposites at different ratios of BC/AM.....p101

IV-2-2 . XRD analyses for polymer composites with different ratio of BC/PAM.....P102

IV-2-3. DSC thermal analysis of the different samples prepared.....p106

IV-2-4. Micro-indentation results..... p108

IV-2-5 Nano indentation results.....p110

CONCLUSION..... p114

CHAPTER V : LOAD APPLIED AND TIME INDENTATION EFFECT ON THE MECHANICAL BEHAVIOR OF PAM:BC NANOCOMPOSITES

V-I : INTRODUCTION..... p115

V-II : MICRO INDENTATION RESULTS.....p115

CONCLUSION..... p121

References..... p122

GENERALS CONCLUSIONS AND PERSPECTIFS.....p123



Introduction

Introduction

Nanotechnologies are recognized as a very promising and emerging multidisciplinary research branch. In the materials field, the development of polymer nanocomposites is an activity that is of growing interest and whose results could broaden the scope of application of polymers)[1]. Indeed, the evolution of polymer materials has gone through the development of organic matrix composites reinforced by micron-sized particles (e.g., talc, fibre glass, wood chips, etc.), still called fillers [2]. The specificity of these new materials lies in the fact that at least one of their dimensions is at the nanoscale (roy et al ; 1986) [3].

The nanocomposite performance depends on a number of nanoparticles features such as the size, aspect ratio, specific surface area, volume fraction used, compatibility with the matrix and dispersion. In fact, although a long time has gone in the nanocomposites materials, the dispersion state of nanoparticles remains the key challenge in order to obtain the full potential of properties enhancement (flame retardance, mechanical, barrier, thermal properties, etc.) at lower filler loading than for microcomposites. Not only can the nanoparticles themselves explain the observed effects, the impact of the interface between the matrix and particle also plays a very important role. Indeed, the extremely high surface area leads to change in the macromolecular state around the nanoparticles (e.g., composition gradient, crystallinity, changed mobility, etc.) that modifies the overall material behavior [4,5].

Almost all types of polymers, such as thermoplastics, thermosets and elastomers have been used to make polymer nanocomposites. [6].

There are a number of nanoparticles that have been reported to be used in the formulation of nanocomposites polymers and which definition can be consulted in many extensive prior literature [4, 7]. Those are generally divided in fibres (1D) platelets (2D) or particles (3D) depending on the number of dimensions they display in the nanoscale [4,8] and they generally differ from the microparticles commonly used in the composite sectors by a greater surface area. Among the polymeric matrix nanocomposites, since they are readily industrially available and low cost, nanoclays are among the most studied scientifically but are also the object of a number of commercial trials since the first work categorized as nanocomposites from Toyota leading to using nylon 6-clay hybrids in car equipment in 1989 [4,9]., nanoclays are interesting because they have a sheet structure and have a very high form factor (about 100). Their high abundance in nature also allows their more massive use in the industrial field. Bentonite is one of nanoclays widely used in different fields because of its properties [10,11].It is a type of rock that contains a lot of minerals in it that has the properties of a

typical montmorillonite namely; may inflate in water, intercalation and ion exchangers are making this material interesting organo clay used to be a catalyst nano and nano clay polymer composites [12]. A various method of nanocomposite polymer preparation have been used to be investigated in different fields, generally, they are categorized in three major routes [13, 14]: preparation with in situ polymerization, synthesis by melt blending or solution blending. After a rich bibliographical study which provided us with such important tools than essential on polyacrylamides, bentonite and polymers nanocomposites. We have deemed it necessary and essential to synthesize these polymers nanocomposites PAM/BC by a new technique of polymerization in aqueous solution. While, this work focuses more to create and innovate a new properties in order to use this one in the in medical sector.

For this reason we are interesting on improvement of mechanical properties of the polyacrylamide/bentonite nanocomposites synthesized via in situ polymerization in different percentage in weight. While, in the present study, a new adiabatic process for the polymerization of acrylamide under neutral state is used. This technique can produce polymers under ultra-rapid kinetics and without exchanging energy with the external area [11,15].

The main objective of this thesis is the fine characterization of the structure and morphology of the nanocomposites obtained by different percentage in weight of bentonite in relation to their mechanical behavior. The results obtained during this work are presented, the whole is structured around five chapters [16,17].

The first chapter contains three parts the first one is about generality of polymer nanocomposites and different kind of mineral charges with their properties afterward we describe the constituents of our material (polyacrylamide and bentonite).

The second chapter is focalized to explain the experimental techniques used in the realization of our work. we detailed in the same chapter the principal's formulas and calculation of both of micro and nano indentation techniques used in the mechanical characterization of our material.

chapter three is constituted both of micro and nano indentation results in order to study the nano structural and morphology effect on the properties of our material and their discussions.

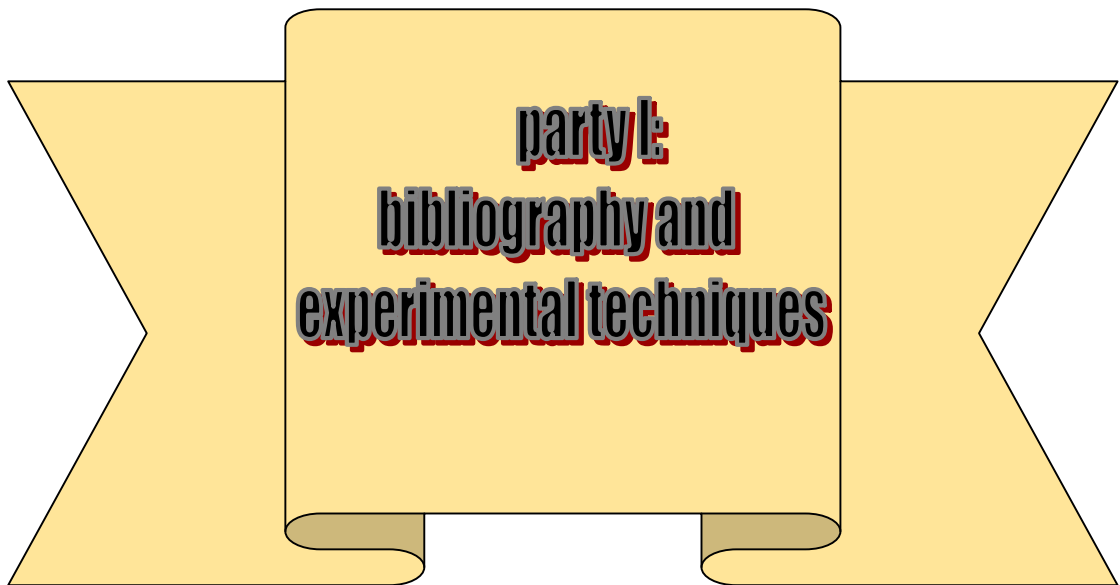
Chapter four is sacrificed for the study of the amount of the charge on the properties of our material. Fifth chapter is constituted of the micro indentation results obtained varying the time of indentation and load applied. We contributed in this section to understand the mechanical behavior of PAM/BC prepared with one and fifty percent in weight of BC

Finally, the conclusions and perspectives are presented in the last part.

References

- [1] W Gacitua, A Ballerini, J Zhang, polymer nanocomposites : synthetic and natural fillers : a review,. *Ciencia y tecnología* 7(3): 159-178(2005).
- [2] Y Kojima, A Usuki, M Kawasumi, A Okada, and Y Fukushima, Mechanical properties of nylon 6 - clay hybrid,. *J Mater Res*, 8 : 1185–1189 (1993).
- [3] M Ricaud , *Nanomatériaux : définition, identification et caractérisation des matériaux et des expositions professionnelles associées*, INRS, Hygiène et sécurité du travail, DO26(2019).
- [4] K Müller , E Bugnicourt, M Latorre, M Jorda, Y Echegoyen Sanz, J M. Lagaron , O Miesbauer , A Bianchin , S Hankin, U Bölz , G Pérez, M Jesdinszki , M Lindner , Z Scheuerer , S Castelló and M Schmid , *Review on the Processing and Properties of Polymer Nanocomposites and Nanocoatings and Their Applications in the Packaging, Automotive and Solar Energy Fields*, , *Nanomaterials (Basel)*. 7(4): 74 (2017).
- [5] G. Kanimozhi, Nibagani Naresh, Harish Kumar, N. Satyanarayana , *Review on the recent progress in the nanocomposite polymer electrolytes on the performance of lithium-ion batteries*, *Environmental Science: Nano*, 46 (6) : 7137-7174 (2022).
- [6] J cuppoletti, *Nanocomposite and polymers with analytical methods*, Ed Rijeka : InTech, 3-27 (2011).
- [7] M Hosokawa, K Nogi;, M Naito, T Yokoyama, *Nanoparticle Technology Handbook* ; Elsevier Science: Oxford, UK, (2007).
- [8] JP Hatto , *International Organization for Standardization (ISO) Part 2: Nano-Objects. Nanotechnologies—Vocabulary*, . International Organization for Standardization; Geneva, Switzerland: (2015).
- [9] A Okada, A Usuki, *Twenty years of polymer-clay nanocomposites*, *Macromol. Mater. Eng*, 291:1449–1476 (2006).
- [10] F Roopa, R. Ravishankar, M. Raj Antony, *Res J. Chem. Environ. Sci.*, 4 : 52 (2016)
- [11] S Khobzaoui, , L. Tennouga, , I. K Benabadi, A. Mansri, B. Bouras, *Preparation of rigid Bentonite/PAM nanocomposites by an adiabatic process: Influence of load content and nano-structure on mechanical properties and glass transition temperature* , *Journal of Inorganic and Organometallic Polymers and Materials*, 29 : 1111–1118(2019)
- [12] A Fisli, M and Grace. Tj Sulungbudi, *Sintesis dan karakterisasi Nanokomposit Oksida Besi-Bentonit*, , *Jurnal Sains Materi Indonesia*, 10 (2) :164 – 169 (2009).
- [13] M Alexandre, P Dubois, *Polymer-layered silicate nanocomposites: preparation, properties and uses of a new class of materials*, *Mater. Sci. Eng*, 28 : 1–63 (2000).

- [14] W VCH Verlag GmbH, C KGaA, Weinheim, Optimization of Polymer Nanocomposite Properties, ed. V. Mitta , 1–19: (2010).
- [15] B Bouras, A Mansri , L Tennouga, B Grassl Influence parameters in controlled adiabatic copolymerization of acrylamide/4-vinylpyridine (AM/4VP) system in aqueous media, , Res Chem Intermed, 41:5839–5858(2015).
- [16] W Bensalah , Gels à base d'acrylamide et de 4-VP -Application à la libération contrôlée des molécules organiques, Tlemcen Abou bekr belkaid university (2019).
- [17] A Illaik, Synthèse et caractérisation de nanocomposites polymères / hydroxydes doubles lamellaires (HDL), Pascal Blaise university (2008),



party 1:

**bibliography and
experimental techniques**



chapter I
bibliography

I-I POLYMERS NANOCOMPOSITES

The word ‘nanocomposite’ is a recent term but the concept is not new and the following paragraphs describe some generality and proprieties of these materials [1].

I-I-1- DEFINITION OF NANOCOMPOSITE MATERIAL

According to the scientific definition proposed recently by the British Standards Institution [2] nanocomposite can be defined as a Multiphase structure with at least one of the Phases on the nanoscale dimension [3,2]; Likewise, the term *nanomaterial* is described as a manufactured or natural material that possesses unbound, aggregated or agglomerated particles where external dimensions are between 1–100 nm size range [4].

I-I-2- CLASSIFICATION OF NANO-COMPOSITE MATERIALS

ACCORDING TO MATRIX :

The nanocomposites materials can be divided in three class according the nature of the matrix :

I-I-2-1-nanocomposite with organic matrix

The nanocomposites with organic matrix represent the most important class of these new types of materials due to the many advantages that these organic matrix bring, such as ease of implementation, their low cost, their resistance to corrosion and, their major asset compared to metal compounds, their low weight. Examples include automotive applications (chassis, bumpers, etc.), aeronautical applications, bridge cables and corrosion protection piping [5].

They are divided into two groups: the thermoplastic polymer and thermosetting polymer.

A thermoplastic resin consists of linear or branched chains with covalent bonds. These chains are linked together by weak Van der Waals and hydrogen links, for example. Thermoplastics can be dissolved in certain solvents and soften with heat, hence the term “thermoplastic” [6].

This group encompass (Polyamide PA, Polyethylene PE, Polypropylene PP, Polystyrene PS, Polycarbonate PC, etc. . . .) they are the most developed due to their commercial importance and the mastery (cost and know-how), many manufacturing processes can only be used in a temperature range not exceeding 200 to 300°C [1].

A thermosetting resin is made up of reticuled linear chains. The chains are linked by strong covalent bounds [6]. Otherwise; Thermosetting resins undergo chemical reactions (curing process) that crosslink the polymer chains and thus connect the entire matrix together in a three-dimensional network. Once cured, they cannot be remelted or reformed. Thermosetting resins tend to have high dimensional stability, high-temperature resistance, and good resistance to solvents because of their three-dimensional cross-linked structure (U.S.

Congress, Office of Technology Assessment, June 1988). The most frequently used thermosetting resins are polyesters, vinyl esters, epoxies, phenolics, polyamides (PA), and bismaleimides (BMI) [7].

I-I-2-2- nanocomposite with metalical matrix

The manufacturing processes of metal matrix composites are inspired by powder metallurgy. Metal matrix composites, called Mmcs have been developed owing to the ease and control of manufacturing processes and their low cost. They can be used up to 600°C [1].

I-I-2-3-nanocomposite with ceramic matrix

The class of materials known as Ceramic matrix composites (CMCs) shows considerable promise for providing fracture toughness values similar to those for metals such as cast iron. Two kinds of damage tolerant ceramic-ceramic composites have been developed. One incorporates a continuous reinforcing phase such as a fiber. The other, a discontinuous reinforcement such as whiskers. The major difference between the two is in their failure behavior [8]. They are used for higher temperature applications up to 1000°C, such as oxides, carbides or nitrides [9]. far more, they have been designed to be used in severe environments. With respect to monolithic ceramics, CMCs are characterized by a non-linear stress/strain mechanical behavior, a high resistance to crack propagation, a noncatastrophic failure and thus an improved reliability [10].

I-I-3- CLASSIFICATION OF NANO-COMPOSITE MATERIALS

ACCORDING TO THE FROME OF NANAOCARGE :

In general, there are three possible classifications of nanocomposites materials according to the geometry of reinforcements (Figure I.I.1). they are classified according to the factor of shape of the incorporated load (ratio of length to thickness or diameter). [11]

Figure I.1.1 represent different types of nanoreinforcements, Surface area/volume relations for different reinforcement geometries is shown in the figure according to the type forme of nanocharge.

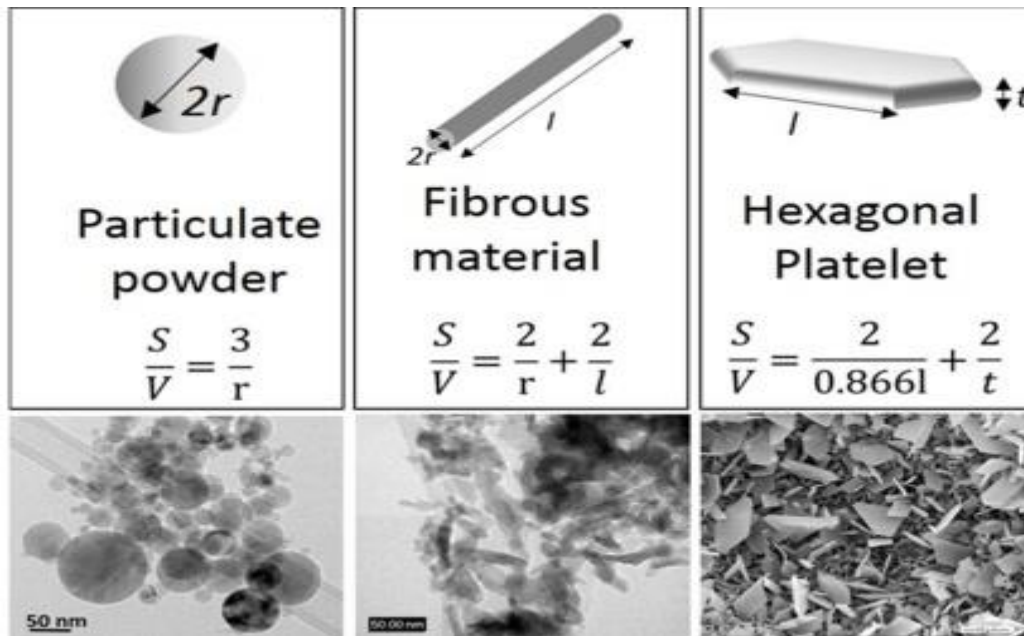


Figure I.1.1 : Schemes and images of different types of nanoreinforcements, redrafted from [9]. Surface area/volume relations for different reinforcement geometries are also displayed [12].

In the first type, Lamellar nanofillers (Plates / lamella / sheets) when a dimension is nanometric like platelet clays (montmorillonite) and graphene [13,14] ; MXene [15,16] in the form of sheets of one to a few nanometer thick and of hundreds to thousands nanometers long are present in polymeric matrices. While, In this case the charges presents in an aspect ratio (length / width) at least equal to 25 [12]. The lamellar structure of this class are designed to improve the mechanical and barrier properties. Clays are generally used at rates below than 10% by mass due to a significant increase in viscosity with the charge percentage in weight. In the second type, two dimensions are in nanometer scale and the third is much larger (> 100 nm), forming an elongated one-dimensional structure, these nanoscale fillers include nanofibers or nanotubes, e.g., carbon nanofibers and nanotubes [17] or halloysite nanotubes [18] , The form factor (length/diameter) is at least 100 [12] this class of reinforcing nanofillers lead to obtain materials with exceptional properties. Especially in term of stiffness. The third type is the nanocomposites containing nanoscale fillers of three dimensions in the order of nanometers. These nanoscale fillers are iso-dimensional low aspect ratio nanoparticles such as spherical silica [19,20]. Due to their very small size, some spherical nanoloads increase the stiffness of the composite while maintaining the transparency of the matrix.

I-I-4- METHODS OF PREPARATION AND SYNTHESIS OF NANOCOMPOSITES POLYMERS

The synthesis of polymer matrix nanocomposites is an integral aspect of polymer nanotechnology [21]. Basically there are four main ways to prepare nanocomposites. They are: solution casting, melt blending and in-situ polymerization, melt compounding [22, 23].

I-I-4-1-In situ polymerization :

In situ synthesis of nanoparticles in a polymer matrix is a simple and effective route to prepare nanocomposites. This method consists, at first step, to mixing the monomer solution and the clay sheets. Polymerization starts either using heat, radiation, initiator diffusion, or by organic initiator or catalyst fixed through cationic exchange [24]. The monomers then polymerize in between the interlayers forming intercalated or exfoliated nanocomposites. The advantage of this approach lies in the better exfoliation achieved compared to melt and exfoliation adsorption methods [25]. Figure I.I.2 illustrates the synthesis of nylon-6/clay nanocomposite via *in situ* polymerization in which clay is dispersed in caprolactam monomer and under polymerization conditions, an exfoliated nanocomposite is formed. Figure I.I.3 illustrates the synthesis of Nylon-6 nanocomposite formed through in situ polymerization with ADA–MMT, an intercalated nanocomposite is formed.

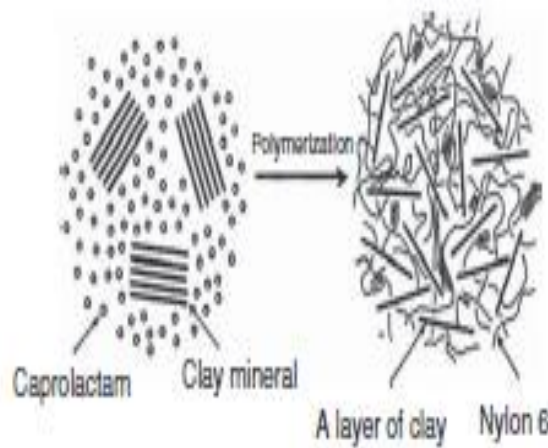


Figure I.I.2 : Schematic example of *in situ* polymerization process involving the synthesis of nylon-6/clay nanocomposite. Reproduced from ref [26]

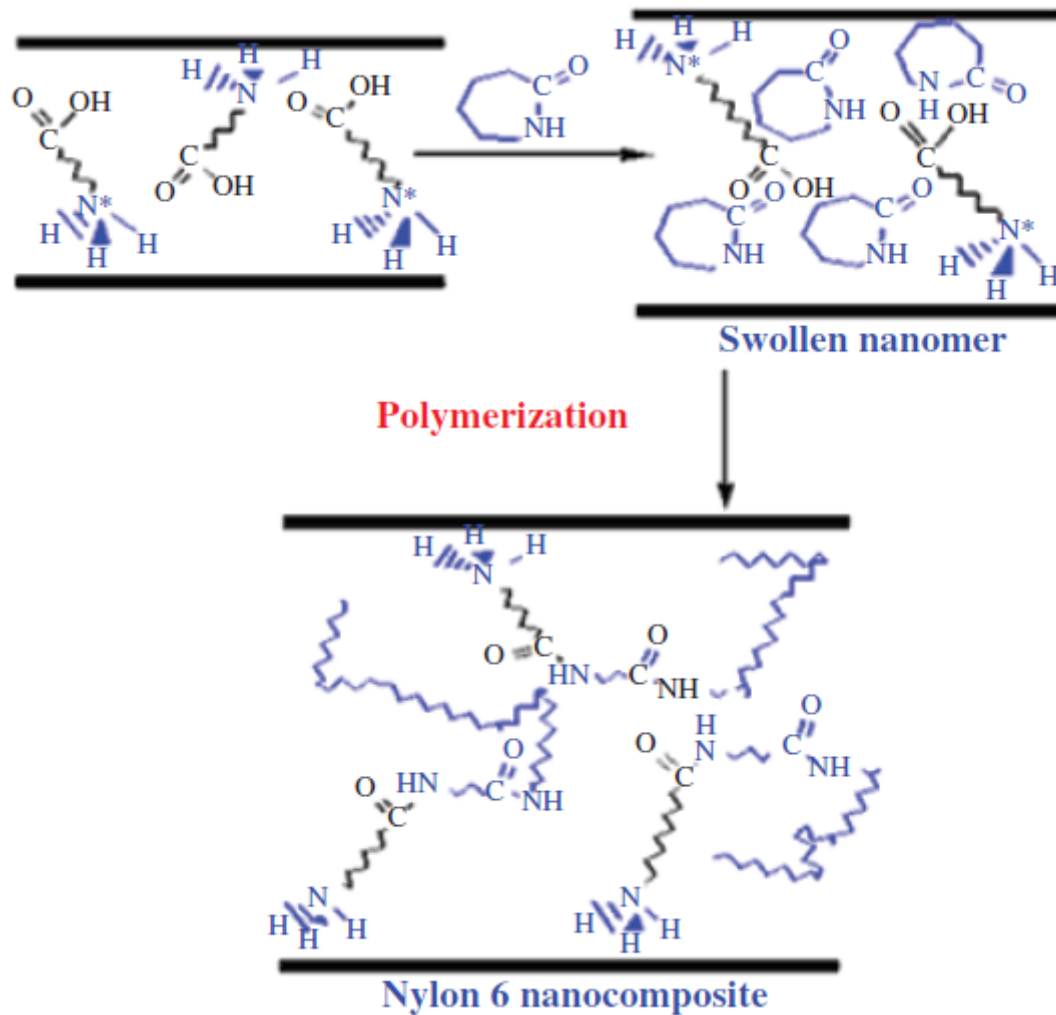


Figure I.1.3 : Nylon-6 nanocomposite formed through in situ polymerization with ADA–MMT [27]

I-I-4-2- solution mixing or blending

Solution mixing is a method based on a solvent system in which the polymer or prepolymer is soluble and the nanofillers are swellable (for layered nanofillers) [28]. In this method, both of the polymer, the solvent and nanoreinforcement are combined and thoroughly mixed by ultrasonication and the solvent is allowed to evaporate leaving behind the nanocomposite typically as a thin film [29]. This is a good method when the solvent used is less toxic (chloroform, acetone, alcohol or water)[30]. While, a different quantities of nanoparticles can be dispersed due to the good interaction with the solvent and polymer. The solvent chosen should completely dissolve the polymer as well as disperse the nanoreinforcement. The solvent used will help in the mobility of the polymer chains which in turn helps in the intercalation of the polymer chains with the layered nanoreinforcement [30].

This is the easiest method to obtain good nanocomposites. Some care must be taken in the manipulation of the solvent since it must be completely eliminated afterward [31, 32, 33, 34].

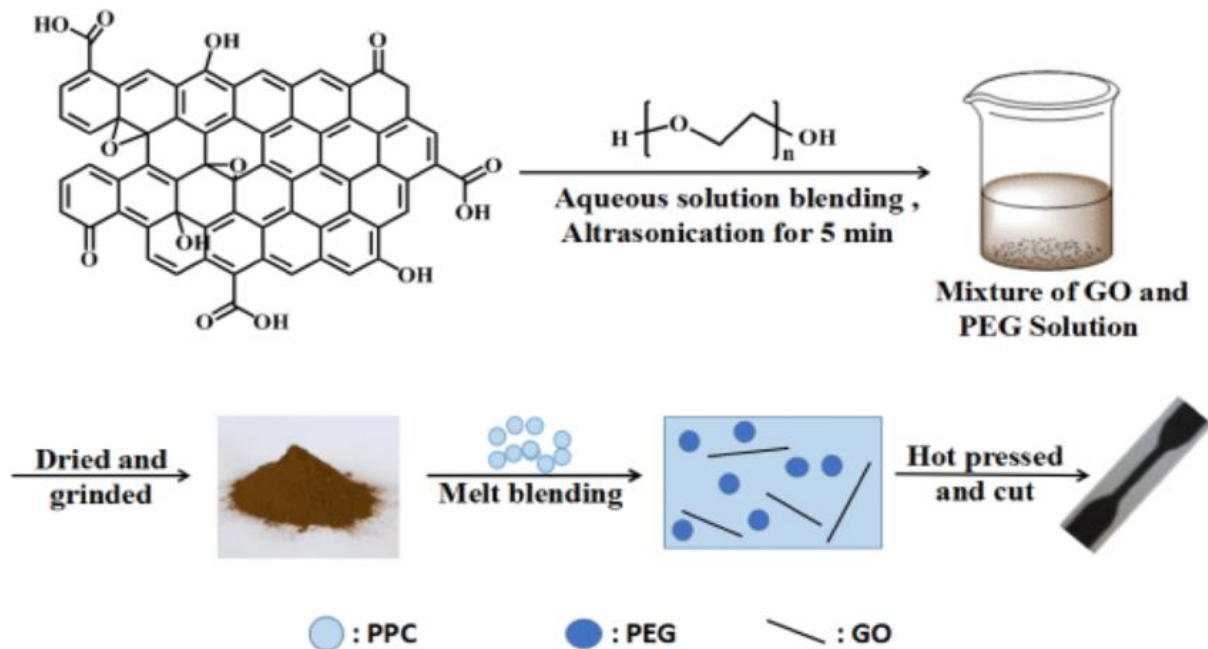


Figure I.I.4 : Schematic preparation of PPC/PEG/GO nanocomposites using solution blending and melt mixing from ref [35].

I-I-4-3-Melt belding

Melt blending is the preferred method for preparing clay/polymer nanocomposites of a thermoplastics and elastomeric polymeric matrix [36] Because of this, this method is found to be environmental friendly, cost-effective, and best for mass production [37]. In this technique, no solvent is required [38,39,40,41] and the nanoreinforcementt is mixed within the polymer matrix in the molten state. A thermoplastic polymer is mechanically mixed by conventional methods such as extrusion and injection molding [42] with organophilic clay at an elevated temperature. The polymer chains are then intercalated or exfoliated to form nanocomposites. This is a popular method for preparing thermoplastic nanocomposites. The polymers, which are not suitable for adsorption or in situ polymerization, can be processed using this technique [43].

Direct mixing of polymer and nanoparticles has many advantages since polymer shaping techniques are well established and controlled [44]. In addition, this method makes possible the synthesis of many types of nanocomposites by simple variations in the nature of the introduced particles and the polymer used.

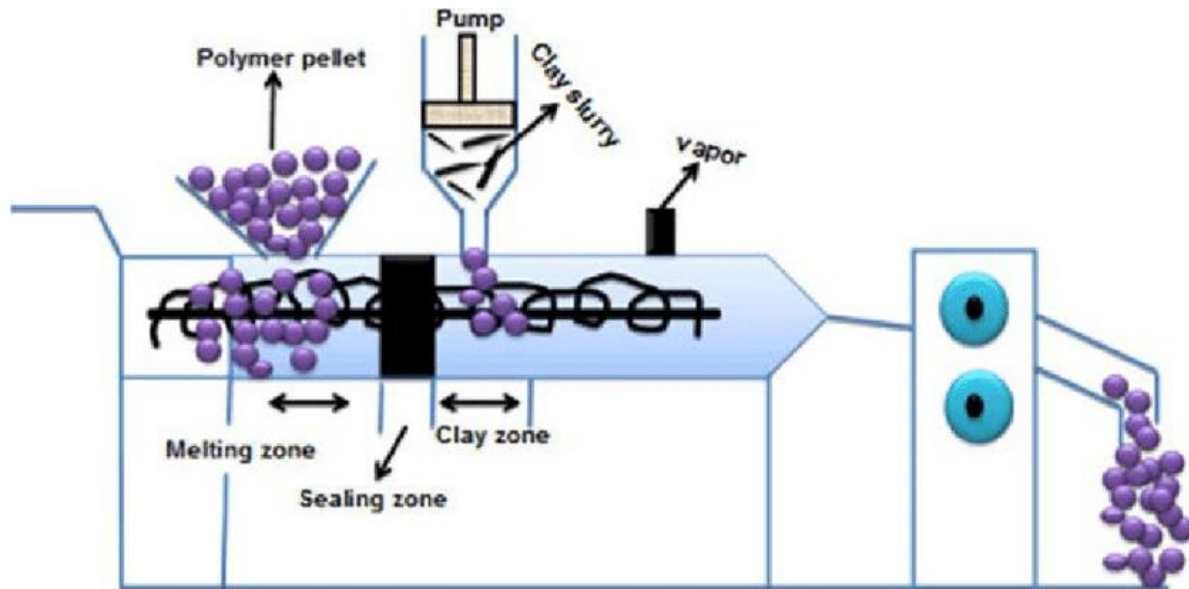


Figure I.I.5: the compounding process for preparing the NCH-CS using the clay slurry from ref [45].

I-I-4-4- Melt Compounding

This method involves nanofibers addition to the polymer above the glass transition temperature. In this kind of method, the shear stress (hydrodynamics force) is induced in the polymer melt by viscous drag, and this shear stress is used to breakdown the nanofiller aggregates and thereby promotes homogeneous and uniform nanofiller dispersion in the polymer matrix [37].

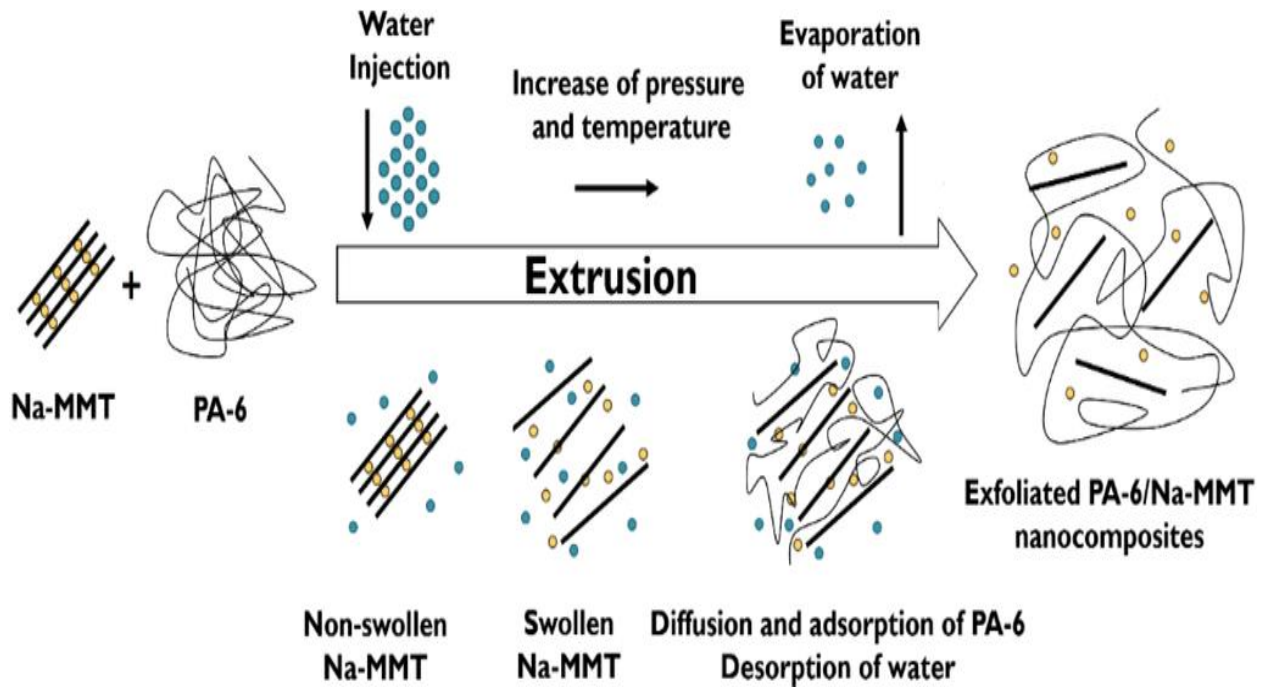


Figure I.I.6 : Montmorillonite (MMT) exfoliation in PA-6 during WA melt compounding schematically. Note: in this case water was injected into the molten PA-6 containing pristine MMT (Na-MMT). [46]

I-I-5 : TYPES OF NANOCOMPOSITES

Nanocomposites can be classified into three types depending on the structure and arrangement of the clay in the polymer matrix. They are (a) intercalated nanocomposites, in which the polymer chains are inserted in the interlayer gallery and the interlayer distance increases, resulting in a well ordered multi-layer morphology built up with alternating polymeric and inorganic layers (b) flocculated nanocomposites which are similar to intercalated nanocomposites where in the clay platelet sizes have been increased by flocculation due to hydroxylated edge-edge interaction and (c) exfoliated or delaminated nanocomposites, where the individual clay layers are separated and uniformly distributed in a continuous polymer matrix [45].

Otherhand , It is widely reported in the bibliography that Principilly there are three kind of nano reinforcement dispersion in the matrix polymer defined by the following paragraphs:

I-I-5-1 Microcomposite polymer

The polymer is not inserted between the silica layers for clay. Phases are separated, not miscible; polymer and clay have incompatibility or very low compatibility; this category has no interesting properties compared to those of the starting polymer.

I-I-5-2 Intercalated nanocomposite

One (sometimes several) polymer chain is inserted between the clay layers. The result is a relatively ordered and dilated structure with an alternation of polymer and inorganic layers.

I-I-5-3 Exfoliated nanocomposite

These are delaminated structures where the clay layers are completely and uniformly distributed across the polymer matrix. Delamination has the effect of maximize polymer/clay interactions significantly increasing the surface of contact and creating the specific properties of this type of nano-composites.

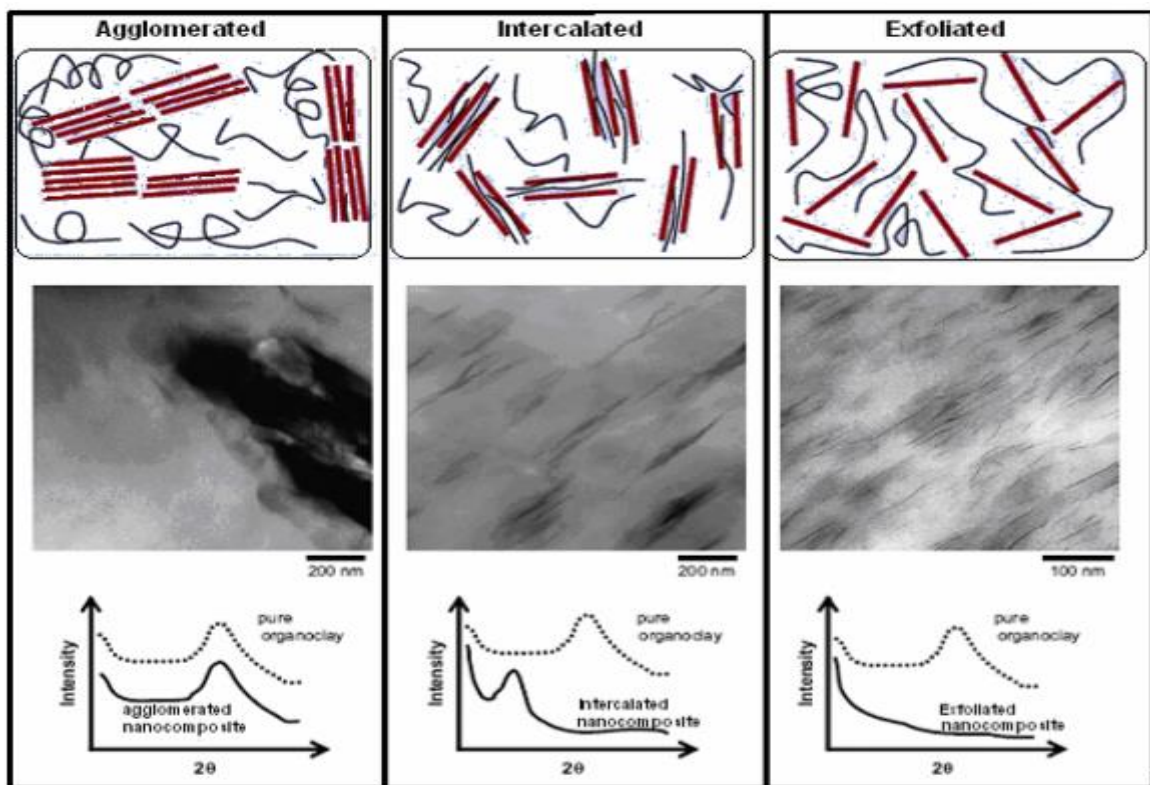


Figure I.1.7 : Structure of clay in nanocomposites with corresponding wide angle X-ray scattering (WAXS) and transmission electron microscopy (TEM) results [47]

References of section I chapter I

- [1] A Illaik, Synthèse et caractérisation de nanocomposites polymères / hydroxydes doubles lamellaires (HDL), doctorat thesis, University Blaise Pascal (U.F.R. de Recherche Scientifique et Technique),(2008).
- [2] J Jeevananda, A Barhoum, Y S. Chan, A Dufresne and M K. Danquah, Review on nanoparticles and nanostructured materials: history, sources, toxicity and regulations, Beilstein J. Nanotechnol ;9:1050–1074 (2018).
- [3] R Sarkhel, P Ganguly, P Das, A Bhowal, A Saha, Industrial dye degradation by different nanocomposite doped material, Elsevier, 2 :377-404 (2021).
- [4] W V Verlag GmbH, C KGaA, Weinheim , in Optimization of Polymer Nanocomposite Properties (ed. V. Mittal) : 1–19 ((2010)
- [5] J M Thomassin, C Jérôme, Les nanocomposites à base de polymères : vers de nouveaux matériaux légers ultraperformants, Bulletin de la Société Royale des Sciences de Liège,82 : 143 – 148 (2013).
- [6] P Weiss, la chimie des polymères, a supported cours, Société Francophone de Biomateriaux Dentaires, Université Médicale Virtuelle Francophone, Date de création du document 2009-2010.
- [7] S Lasmi, Effets des taux de l'agent traitant et de l'agent compatibilisant sur les propriétés des nanocomposites Polypropylène/Silice, magister memory, university setif 1 (2014) .
- [8] H Nguyen, W Zatar, H Mutsushi, Hybrid polymer composite materials properties and characterization/ chap 4 : mechanical properties of hybrid polymer composite, elsevier, all right reserved : 1st ed : 83-113 (2017).
- [9] M Schwartz , materials parts and finish, CRC press : Taylor francois group, New york, 3rd Ed(2016).
- [10] R Naslai, advanced structural and functional materials ; chap thermostructural ceramic matrix composites :an overview, springer berlin heidelberg, 51-91 (1991).
- [11] D M Marquis, E Guillaume, C Chivas-Joly. "Properties of nano-fillers in polymer". In: " Nanocomposites and polymers with analytical methods", 261-284 (2011).
- [12] P Palmero, Structural Ceramic Nanocomposites: A Review of Properties and Powders' Synthesis Methods, Nanomaterials,5 :656-696(2015).
- [13] R J Young, I A Kinloch, L Gong, K S Novoselov, The mechanics of graphene nanocomposites: a review, Compos. Sci. Technol. 72 : 1459–1476 (2012).
- [14] J H Du, H M Cheng, The fabrication, properties, and uses of graphene/polymer composites, Macromol. Chem. Phys. 213 : 1060–1077 (2012).

- [15] X Q Li, C Y Wang, Y Cao, G X Wang, Functional MXene materials: progress of their applications, *Chem. Asian J*, 13 : 2742–2757 (2018).
- [16] S B Tu, Q Jiang, X X Zhang, H N Alshareef, Large dielectric constant enhancement in MXene percolative polymer composites, *ACS Nano* 12 : 3369–3377 (2018).
- [17] P. Calvert, Nanotube composites - a recipe for strength, *Nature* 399 : 210–211 (1999).
- [18] M.X. Liu, Z.X. Jia, D.M. Jia, C.R. Zhou, Recent advance in research on halloysite nanotubes-polymer nanocomposite, *Prog. Polym. Sci.* 39 : 1498–1525(2014).
- [20] J E Mark, Ceramic-reinforced polymers and polymer-modified ceramics, *Polym.Eng. Sci.* 36 : 2905–2920 (1996).
- [19] E Reynaud, C Gauthier, J Perez, Nanophases in polymers, *Rev. Metall.* 96 : 169–176. (1999).
- [21] A Lagashetty , A Venkataraman , Polymer Nanocomposites, *resonance*, 49-60 (2005).
- [22] T Kuilla, S Bhadra D, N H Yao, K S Bose, J H lee, recent advanced in graphene based polymer composites, *prog polym sci*, 35(1) :1350-75 (2010).
- [23] C Nanosci, carbon nanotubes composites processing grafting and mechanical and thermal properties, 6(1) : 12-39 (2010).
- [24] M Alexandre, P Dubois, Polymer-layered silicate nanocomposites: preparation, properties and uses of a new class of materials, *Mater. Sci. Eng.*28 : 1–63 (2000).
- [25] S Abedi, M Abdouss, A review of clay-supported Ziegler-Natta catalysts for production of polyolefin/clay nanocomposites through in situ polymerization., *Appl. Catal. Gen.*, 475 :386–409 (2014).
- [26] S S Ray,M Okamoto, Polymer/layered silicate nanocomposites: a review from preparation to processing, , *Prog. Polym. Sci.*, 25 :1539–1641(2003).
- [27] F Hussain, M Hojjati, Review article: Polymer-matrix Nanocomposites, Processing, Manufacturing, and Application: An Overview, *Journal of composite materials*, 40(17) : 1511-65 (2006)
- [28] A Vasudes Rane, K Kanny, VK Abitha, S Thomas , chap 5 : methods for synthesis of nanoparticles, « synthesis of inorganic nanomaterials advanced and key technologies » , ed : sneha mohan bhagyaraj, oluwatdsi samuek oluwafemi, nandakumar kalarikkal, sabu thomas, micro and nano technologies series, elsevier, 121-139 (2018).
- [29] S Anandhan, S Bandyadhyay, chap 1 : polymer nanocomposites from synthesis to application, « nanocomposites and polymers with analytical methods » , ed : John Cuppoletti, 1-27 (2011).

- [30] M I Bruno Tavares, E Oliveira da Silva, P Rangel Cruz da Silva and L Rodrigues de Menezes, chap: Polymer Nanocomposites , Nanostructured Materials - Fabrication to Applications , ED : Mohindar Singh Seehra, IntechOpen, (2017).
- [31] P S Rangel Cruz da; Tavares, M I Bruno, Solvent Effect on the Morphology of Lamellar Nanocomposites Based on HIPS. SILVA, Materials Research;18(1):191-195 ,(2015).
- [32] S S B M Monteiro, R C Lopes, P C R Neto, M I Bruno, The Structure of Polycaprolactone-Clay Nanocomposites Investigated by ^1H NMR Relaxometry. Journal of Nanoscience and Nanotechnology;12(9):7307-7313 (2012).
- [33] S I Lopes, C J Pereira, L Leandro, S Emerson Oliveira da, S Diego de Holanda Saboya; Tavares, M I Bruno, Evaluation of the Influence of Modified TiO_2 Particles on Polypropylene Composites, Journal of Nanoscience and Nanotechnology, Journal of Nanoscience and Nanotechnology , 15(8): 5723-5732 (2015).
- [34] A Cunha, M I Bruno, T Oliveira Silva, S Zaioncz, The Effect of Montmorillonite Clay on the Crystallinity of Poly(vinyl alcohol) Nanocomposites Obtained by Solution Intercalation and In Situ Polymerization. Journal of Nanoscience and Nanotechnology, 15(4):2814-2820 (2015).
- [35] G Jiang, N Zhao, S Zhang, X Zhang, Thermal, Mechanical Properties and Rheological Behavior of Poly(Propylene Carbonate)/Poly(Ethylene Glycol)/Graphene Oxide Nanocomposites, Journal of Polymers and the Environment, 27 :2201–2212 (2019) .
- [36] A V Rane, K Kanny, V K Abitha, S S Patil, ed : Kh Jlassi, M Chehimi, S Thoma, Clay-Polymer Nanocomposites , Chap 4: Clay–Polymer Composites: Design of Clay Polymer Nanocomposite by Mixing,, elsevier, 4 : 113-144 (2017) .
- [37] D Verma, Kh Limgoh, chap 11 : Functionalized Graphene-Based Nanocomposites for Energy Applications, « functionalized graphene nanocomposite and their derivatives », , ed : Mohammad jawaid, Rachid bouhid and Abou el kacem qaiss, 11 :219-243 (2019).
- [38] H R Dennis, D Hunter, D Chang, S Kim, D R Paul, Effect of Melt Processing Condition on the Extent of Exfoliation in Organoclay-based Nanocomposites, Polymer, 42: 9513–9522 (2001).
- [39] R A Vaia , K D Jant, E J Kramer, E P Giannelis, Microstructural Evaluation of Melt-intercalated Polymer-Organically Modified Layered Silicate Nanocomposites, Chem.Mater., 8: 2628–2635 (1996).
- [40] A Rehab, N Salahuddin, Nanocomposite Materials Based on Polyurethane Intercalated into Montmorillonite Clay, Materials Science and Engineering A, 399: 368–376 (2005).

- [41] S D Burnside, E P Giannelis, Synthesis and Properties of New Poly(dimethylsiloxane) Nanocomposites, *Chem. Mater*, 67(1995)
- [42] X Kornmann, H Linderberg, L A Bergund, Synthesis of Epoxy–Clay Nanocomposites: Influence of the Nature of the Curing Agent on Structure, *Polymer*, 42: 4493–4499 (2001).
- [43] S S Ray, M Okamoto, M Prog, Polymer/layered Silicate Nanocomposite: A Review from Preparation to Processing, *Polymer Sci*, 28: 1539–1641. (2003)
- [44] W S Khan, N N Hamadneh, W A Khan, Science and applications of Tailored Nanostructures, chap 4 : Polymer nanocomposites – synthesis techniques, classification and properties, 50-68 (2011).
- [45] R Grande, LA.Pessan, A J F Carvalho, Ternary melt blends of poly(lactic acid)/poly(vinyl alcohol)-chitosan, *Industrial Crops and Products*, 72 : 159-165, (2015).
- [46] J Karger-Kocsis, A Kmetty, L Lendvai, S X. Drakopoulos, T Bárány, Water-Assisted Production of Thermoplastic Nanocomposites: A Review, *Materials* 8(1): 72-95 (2015).
- [47] SS Ray, M Okamoto, Polymer/layered silicate nanocomposites: a review from preparation to processing, *Prog Polym Sci*, 28:1539-1641 (2003).

I-II MINERALS CLAY

I-II-1 DEFINITION OF MINERALS CLAY

The term "clay" is applied both to materials having a particle size of less than 2 micrometers (25,400 micrometers = 1 inch) and to the family of minerals that has similar chemical compositions and common crystal structural characteristics (Velde, 1995) described in the next section. Clay minerals have a wide range of particle sizes from 10's of angstroms to millimeters. Thus, clays may be composed of mixtures of finer grained clay minerals and clay-sized crystals of other minerals such as quartz, carbonate, and metal oxides [1]. They include some minerals such as bentonite and kaolinite have different molecular structures and are used in different purposes. These materials can be found in the nature from different sources and can also be synthesized in the laboratory [2]. Mineral clay is one part of a class of silicate minerals; phyllosilicates [2]. In cool, dry, or temperate climates, clay minerals are fairly stable and are an important component of soil [3]. Clay minerals act as "chemical sponges" which hold water and dissolved plant nutrients weathered from other minerals. This results from the presence of unbalanced electrical charges on the surface of clay grains, such that some surfaces are positively charged (and thus attract negatively charged ions), while other surfaces are negatively charged (attract positively charged ions). Clay minerals also have the ability to attract water molecules. Because this attraction is a surface phenomenon, it is called **adsorption** (which is different from *absorption* because the ions and water are not attracted deep inside the clay grains) [3]. Clay minerals resemble the micas in chemical composition, except they are very fine grained, usually microscopic.

I-II-2 MINERALS CLAY CLASSIFICATION

The atomic structure of the clay minerals consists of two basic units, an octahedral sheet and a tetrahedral sheet. The octahedral sheet is comprised of closely packed oxygen and hydroxyls in which aluminium, iron and magnesium atoms are arranged in octahedral coordination (Figure. I.II.1). When aluminium with a positive valence of three is the cation present in the octahedral sheet, only two-thirds of the possible positions are filled in order to balance the charges. When only two-third of the positions are filled, the mineral is termed as di-octahedral. When magnesium with a positive charge of two is present, all three positions are filled to balance the structure and the mineral is termed tri-octahedral. [4]

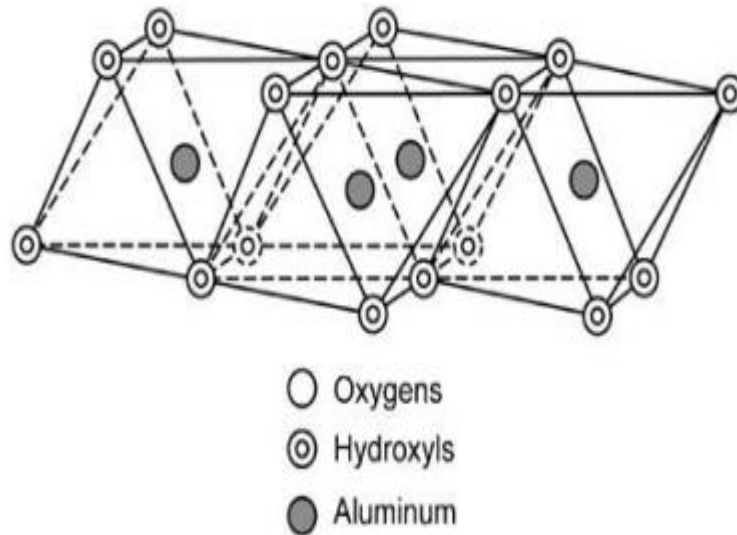


Figure I.II.1 : Octahedral Sheet of Clay [5,6]

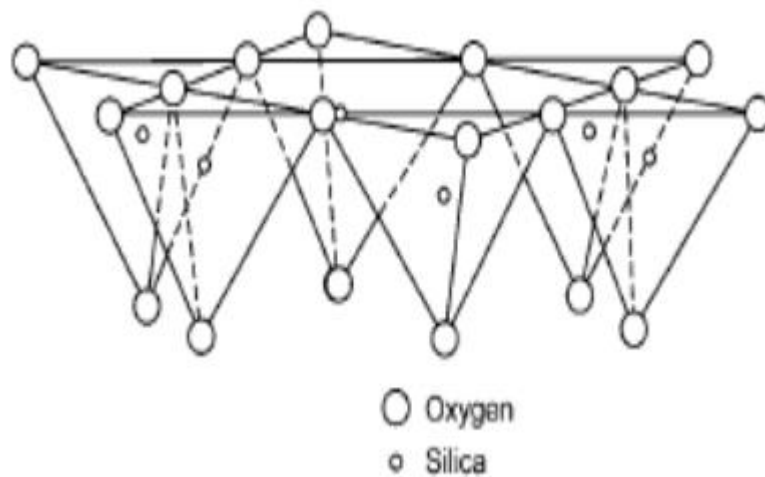


Figure I.II.2 : Tetrahedral sheet of Clay [5,6].

The second structural unit is the silica tetrahedral layer in which the silicon atom is equidistant from four oxygen atoms or possibly hydroxyls arranged in the form of a tetrahedron with the silicon atom in the centre. These tetrahedra are arranged to form a hexagonal network repeated infinitely in two horizontal directions to form silica tetrahedral sheet shown in Figure. I.II.1.

Clay minerals are generally classified into three layer types based upon the number and arrangement of tetrahedral and octahedral sheets in their basic structure.

These are further separated into five groups that differ with respect to their net charge (Table I.II.1) [7].

Table I.II.1 : Properties of clay mineral group [8]

Group	Layer type	Net negative charge (c mol kg ⁻¹)	Surface area (mV)	Basal spacing (nm)
Kaolinite	1:1	2-5	10-30	0.7
Fine-grained mica	2:1	15-40	70-100	1.0
Smectite	2:1	80-120	600-800	1.0-2.0
Vermiculite	2:1	100-180	550-700	1.0-1.5
Chlorite	2:1:1	15-40	70-100	1.4

✓ **Type 1/1(or T-O) minerals**: The sheet consists of an octahedral layer and a tetrahedral layer, the characteristic equidistance is about 7 Å, to this type corresponds the kaolinite group. [9 ,10]

✓ **Type 2/1 minerals (or T-O-T)**: The sheet consists of an octahedral layer framed by two tetrahedral layers with the second tetrahedral layer being inverted in relation to the first, these three layers are bound together by oxygen atoms. The characteristic equidistance varies from 9.4 to 15 Å depending on the content of the interface. To this type correspond the groups of talc, smectites, illites, vermiculites and micas, [9 , 10] these clays can be found in three different situations:

- No isomorphic substitution.
- Octahedral substitutions.
- Tetrahedral substitutions.

- In the first situation, all octahedral sites are occupied by Mg²⁺, not isomorphic substitution. As a result, there is no load deficit on the surface. The sheets are then electrically neutral and have a large stability vis-à-vis water, exactly as in the case of T-O clays.

- If there is isomorphic substitution, there is a load deficit (often negative) on the surface of the sheets, which is naturally compensated by In the case of isomorphic substitution, there is a load deficit (often negative) on the sheet surface, which is naturally compensated by the compensating cations. The resulting burden deficit is offset in the space interfolias by potassium

ions K^+ which ensure strong bonds between the sheets is compensated by the introduction into the space interfoliar.

✓ **Minerals type 2/1/1(or T-O-T-O):** The sheet consists of alternating T-O-T sheets and Interfoliar octahedral layer, this layer neutralizes the loads carried by the T-O-T sheets. The characteristic equidistance is then about 14 Å, to this type corresponds the chlorite group. [9, 10]

I-II-2-1 Kaolinite group :

Kaolinite group which includes clay minerals like kaolinite, hallosite, nacrite and dickite, is a 1:1 type clay mineral. It is composed of one layer of silica and one layer of alumina, which is formed under acidic conditions through advanced weathering processes or hydrothermal changes of feldspars and other aluminosilicates (Miranda-Trevino, 2003). The chemical formula of kaolinite is $Al_2O_3 \cdot 2SiO_2 \cdot 2H_2O$ (39% Al_2O_3 , 46.5% SiO_2 and 14.0% H_2O) and its structure possesses strong binding forces between the layers which resists expansion when wetted (Miranda-Trevino, 2003; Trickova, 2004). The cation exchange capacity (CEC) of kaolinite is less than that of montmorillonite due to its low surface area and low isomorphous substitution that result from its high molecular stability (Aroke, 2013; Murray, 1999) and this contributes to its low plasticity, cohesion, shrinkage and swelling. However, the material can adsorb small molecular substances such as lecithin, quinolone, paraquat, diaquat polyacrylonitrile, some proteins, bacteria and viruses (Williams and Environmental, 2005) [11].

Typical wet chemical analyses of kaolin minerals frequently include small amounts of Fe, Ti, K, and Mg (Deer et al., 1976), generally due to the presence of impurities such as Fe- and Tioxides and mica. Improvement in instrumentation, especially in electron microscopy associated to energy dispersive analyses (EDX) has shown that, in most cases, K present in kaolinite analyses is due to interlayering with other clay minerals (e.g. Lee et al., 1975), whereas some other cations, such as Fe, Ti or Cr frequently substitutes in minor amounts in the structure (e.g. Brookins, 1973; Herbillon et al. 1976; Maksinovic et al., 1981; Mestdag et al. 1980). Maxima amounts of ionic substitutions (Fe =0.44 apfu; Cr=0.56 apfu - atoms per formula unit for $O_5(OH)_4$) have been described in halloysites (Newman and Brown, 1987). It appears that the type of foreign cations present in the kaolinite structure mainly depends on the bulk-rock composition, whereas the amount of substitution appears to be controlled by the structure, the disordered varieties accepting higher amounts of substitutions (Brindley et al., 1986). The physical and chemical conditions under which the kaolin minerals form are

relatively low pressures and temperatures. These minerals are typical of three main environments: 1) weathering profiles; 2) hydrothermal alterations; and 3) sedimentary rocks. The most common parent minerals from which kaolin minerals develop are feldspars and muscovite. The transformation of potassium feldspar into kaolin minerals occurs according to the equation:

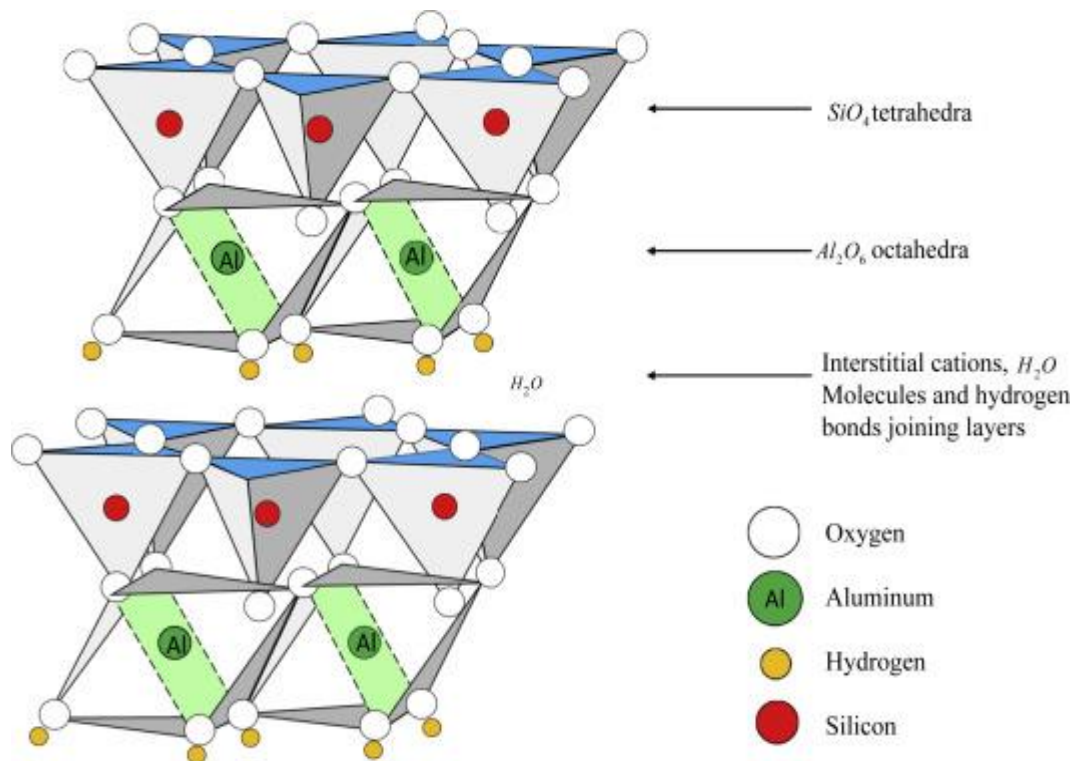
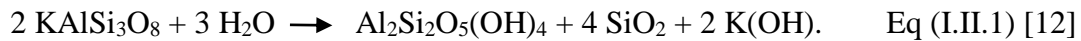


Figure I.II.3 : structure of kaolinite group [13]

I-II-2-2 Mica group

Mica minerals have a basic structural unit of the 2:1 layer type like pyrophyllite and talc, but some of the silicon atoms (ideally one-fourth) are always replaced by those of aluminum. This results in a charge deficiency that is balanced by potassium ions between the unit layers. The sheet thickness (basal spacing or dimension along the direction normal to the basal plane) is fixed at about 10 Å. Typical examples are muscovite, $\text{KAl}_2(\text{Si}_3\text{Al})\text{O}_{10}(\text{OH})_2$, for dioctahedral species, and phlogopite, $\text{KMg}_3(\text{Si}_3\text{Al})\text{O}_{10}(\text{OH})_2$, and biotite, $\text{K}(\text{Mg, Fe})_3(\text{Si}_3\text{Al})\text{O}_{10}(\text{OH})_2$, for trioctahedral species. (Formulas rendered may vary slightly due to possible substitution within certain structural sites.) Various polytypes of the micas are known to occur. Among them, one-layer monoclinic (1M), two-layer monoclinic (2M, including 2M_1 and 2M_2), and three-layer trigonal (3T) polytypes are most common. The majority of clay-size micas are dioctahedral aluminous species; those similar to muscovite are called illite and generally

occur in sediments. The illites are different from muscovite in that the amount of substitution of aluminum for silicon is less; sometimes only one-sixth of the silicon ions are replaced. This reduces a net unbalanced-charge deficiency from 1 to about 0.65 per unit chemical formula. As a result, the illites have a lower potassium content than the muscovites. To some extent, octahedral aluminum ions are replaced by magnesium (Mg^{2+}) and iron ions (Fe^{2+} , Fe^{3+}). In the illites, stacking disorders of the layers are common, but their polytypes are often unidentifiable [14].

Celadonite and glaucosite are ferric iron-rich species of dioctahedral micas. The ideal composition of celadonite may be expressed by $K(Mg, Fe^{3+})(Si_{4-x}Al_x)O_{10}(OH)_2$, where $x = 0-0.2$. Glaucosite is a dioctahedral mica species with tetrahedral Al substitution greater than 0.2 and octahedral Fe^{3+} or R^{3+} (total trivalent cations) greater than 1.2. Unlike illite, a layer charge deficiency of celadonite and glaucosite arises largely from the unbalanced charge due to ionic substitution in the octahedral sheets [14].

Studies have shown that there are over 30 members of mica group, but six forms that are found in nature and commonly used in microscopy and other analytical applications consist of muscovite, biotite, phlogopite, lepidolite, fuchsite and zinnwaldite (Orlando, 2002). Three members (illite group) which includes illite, glaucosite and muscovite are referred to as clay minerals because they exhibit characteristic properties of clay, with illite mineral being the most common. Illite is formed from weathering of potassium and aluminum rich rocks like muscovite and feldspar under alkaline conditions. Illite group is a 2:1 layer silicate clay mineral which is non expansive because the space between the crystals of individual clay particles is filled by poorly hydrated potassium cations or calcium and magnesium ions which hinder water molecules from entering the clay structure. The cation exchange capacity of Illite ranges between 20-40 meq per 100 g. The colour of the minerals ranges from grey white, silvery white to greenish grey. The illites find application in structural clay industry and in agro minerals due to high potassium content (Njoka et al., 2015; Van, 2002). Mica clay ores contain a variety of impurities which includes quartz, feldspar, kaolin and pyroxene (Capedri et al., 2004). Presence of these minerals in mica ores will impact upon the industrial value of these deposits and the processing complexity thus reducing or increasing its value depending on the applications (Gaafar, 2014). [11]

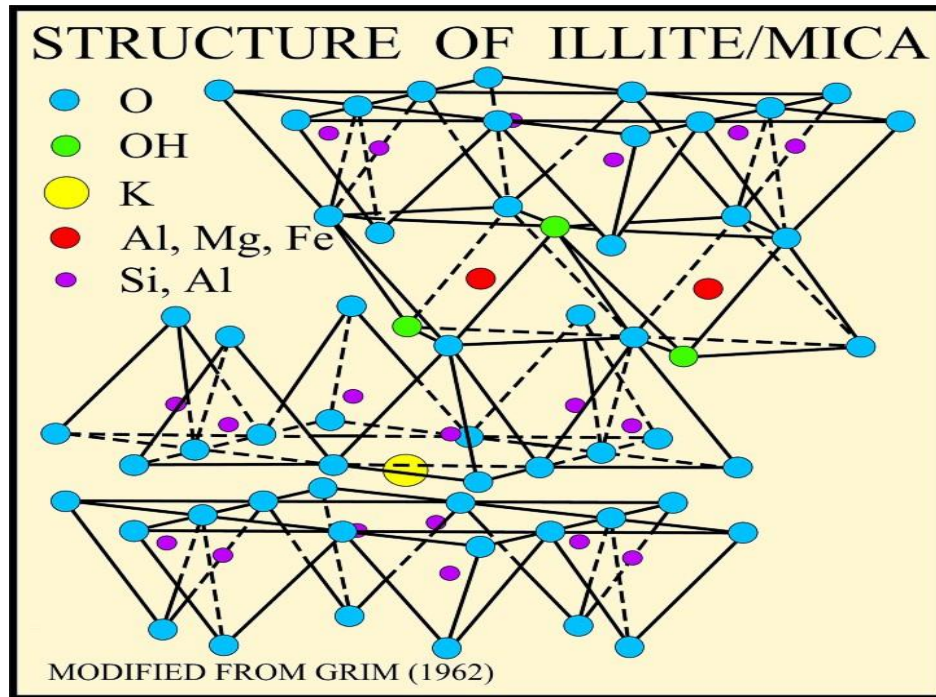


Figure I.II.4 : structure of illite Mica [15].

I-II-2-3 Smectite group

Smectite is the name used for a group of phyllosilicate mineral species, the most important of which are montmorillonite, beidellite, nontronite, saponite and hectorite [16]. Smectite, are 2:1 layer clay minerals formed from the weathering of soils, rocks (mainly bentonite) or volcanic ash and belongs to a group of hydroxyl aluminosilicate (Erdogan, 2015). The variation of physical and chemical properties of bentonites within and between deposits is caused by differences in the degree of chemical substitution within the smectite structure, the nature of the exchangeable cations present, type and the amount of impurities present (Christidis and Warren, 2009). Minerals associated with smectites include quartz, cristobalite, feldspars, zeolites, calcite, volcanic glass and other clay minerals such as kaolinite (Abdou, 2013). The groups of smectite clays are distinguished by differences in the chemical composition pertaining to substitutions of Al^{3+} or Fe^{3+} for Si^{4+} in the tetrahedral cation sites and Fe^{2+} , Mg^{2+} or Mn^{2+} for Al^{3+} in the octahedral cation sites. Smectites have very thin layers and small particle sizes which contribute to high surface area and hence a high degree of absorbency of many materials such as oil, water and other chemicals (Marek, 2010; Amel, 2013). Additionally, smectites have higher cation exchange capacities, swelling and shrinkage properties than other clays which contribute to high surface area and hence a high degree of absorbency of many materials such as oil, water and other chemicals (Marek, 2010; Amel, 2013). otherwise, Smectite clays have a variable net negative charge, which is balanced by

Na, Ca, Mg and, or, H adsorbed externally on interlamellar surfaces [11]. The structure, chemical composition, exchangeable ion type and small crystal size of smectite clays are responsible for several unique properties, including a large chemically active surface area, a high cation exchange capacity, interlamellar surfaces having unusual hydration characteristics, and sometimes the ability to modify strongly the flow behaviour of liquids. In terms of major industrial and chemical uses, natural smectite clays can be divided into three categories, Na smectites, Ca—Mg smectites and Fuller’s or acid earths. Large volumes of Na smectites and Na-exchanged Ca-M g smectites and Fuller’s earth are directly used in the foundry, oil well drilling, wine, and iron ore and feed pelletizing industries, and are also used in civil engineering to impede water movement. Significant volumes of Na smectites are used for various purposes in the manufacturing of many industrial, chemical and consumer products. Large quantities of Ca-M g smectites are used directly in iron foundries, in agricultural industries and for filtering and decolorizing various types of oils. A significant fraction of the Ca-M g smectites used for decolorizing has been acid treated. Large volumes of Fuller’s or acid earths are commercially used for preparing animal litter trays and oil and grease absorbents, as carriers for insecticides, and for decolorizing of oils and fats. Natural Na smectites occur in commercial quantities in only a few places, but Ca-M g smectite and Fuller’s earth deposits of considerable size occur on almost every continent [16].

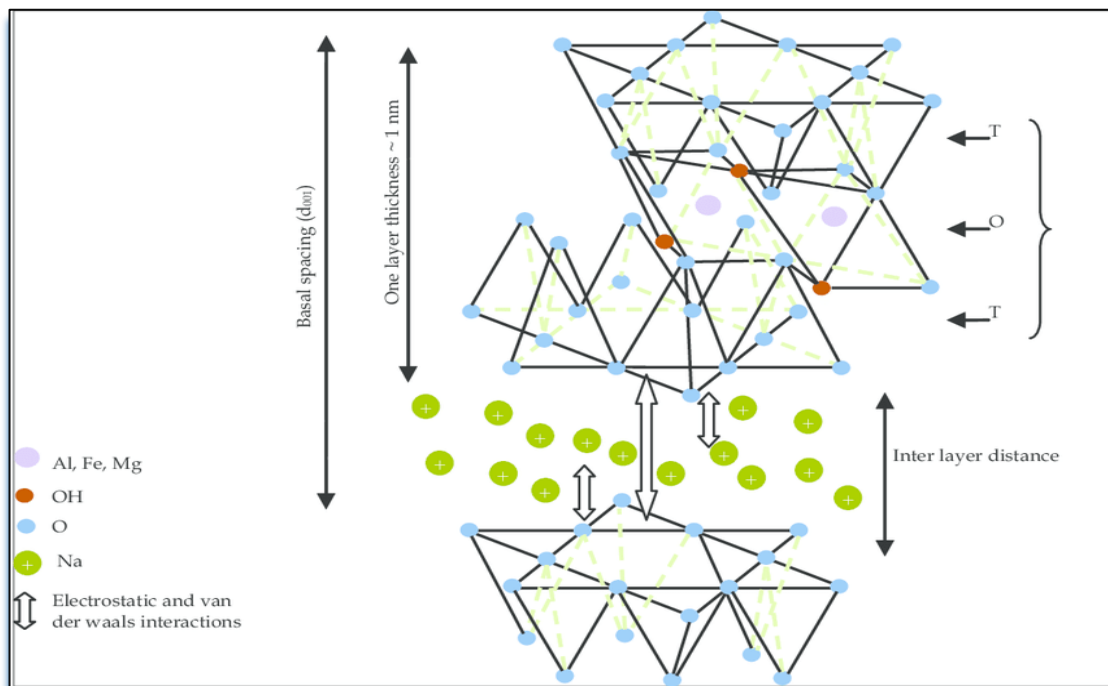


Figure I.II.5 : structure of smectite [17].

I-II-2-4 Vermiculite

The vermiculite unit structure consists of sheets of trioctahedral mica or talc separated by layers of water molecules; these layers occupy a space about two water molecules thick (approximately 4.8 Å). Substitutions of aluminum cations (Al^{3+}) for silicon cations (Si^{4+}) constitute the chief imbalance, but the net charge deficiency may be partially balanced by other substitutions within the mica layer; there is always a residual net charge deficiency commonly in the range from 0.6 to 0.8 per $\text{O}_{10}(\text{OH})_2$. This charge deficiency is satisfied with interlayer cations that are closely associated with the water molecules between the mica layers. In the natural mineral, the balancing cation is magnesium (Mg^{2+}). The interlayer cation, however, is readily replaced by other inorganic and organic cations. A number of water molecules are related to the hydration state of cations located at the interlayer sites. Therefore, the basal spacing of vermiculite changes from about 10.5 to 15.7 Å, depending on relative humidity and the kind of interlayer cation. Heating vermiculite to temperatures (depending on its crystal size) as high as 500° C drives the water out from between the mica layers, but the mineral quickly rehydrates at room temperature to maintain its normal basal spacing of approximately 14 to 15 Å if potassium or ammonium ions are not present in the interlayer sites. It has been reported that some dioctahedral analogues of vermiculite occur in soils [14].

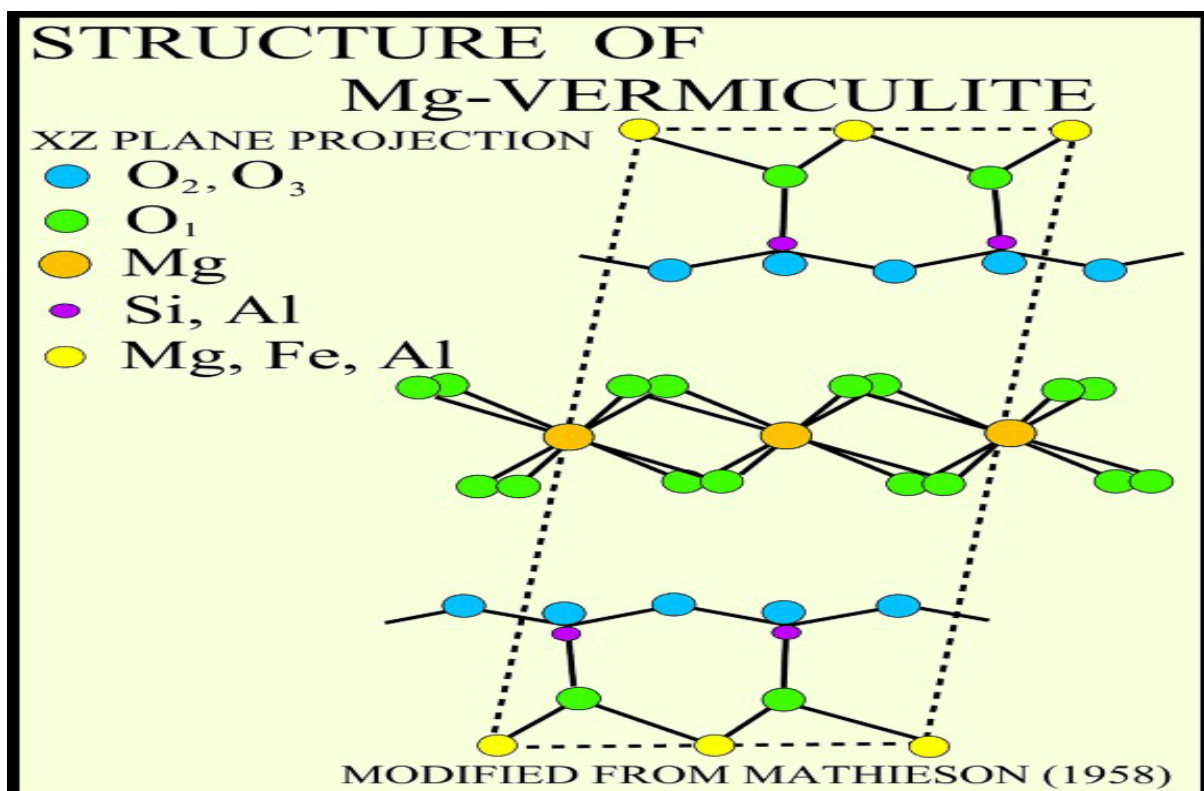


Figure I.II.6 : structure of Mg vermiculite [18]

I-II-2-5 Chlorites group

Chlorites are hydrous aluminosilicates that are arranged in a 2:1 structure with an interlayer (Wiewiora, 1990). They incorporate primarily Mg, Al and Fe cations and to a less extent Cr, Ni, Mn, V, Cu and Li cations in the octahedral sheet within the 2:1 layer and in the interlayer hydroxide sheet. They also exhibit a large substitution of Si by Al cations in the tetrahedral sheet (Ako, 2015). The colour of chlorites varies from white to almost black or brown with a tint of green where these optical properties are coupled to the chemical composition of chlorite (Saggerson, 1982) [11]. The structure of the chlorite minerals consists of alternate micalike layers and brucitelike hydroxide sheets about 14 Å thick. Structural formulas of most trioctahedral chlorites may be expressed by four end-member compositions:

$(\text{Mg}_5\text{Al})(\text{Si}_3\text{Al})\text{O}_{10}(\text{OH})_8$	(clinochlore)
$(\text{Fe}_{5^{2+}}\text{Al})(\text{Si}_3\text{Al})\text{O}_{10}(\text{OH})_8$	(chamosite)
$(\text{Mn}_5\text{Al})(\text{Si}_3\text{Al})\text{O}_{10}(\text{OH})_8$	(pennantite)
$(\text{Ni}_5\text{Al})(\text{Si}_3\text{Al})\text{O}_{10}(\text{OH})_8$	(nimite)

The unbalanced charge of the micalike layer is compensated by an excess charge of the hydroxide sheet that is caused by the substitution of trivalent cations (Al^{3+} , Fe^{3+} , etc.) for divalent cations (Mg^{2+} , Fe^{2+} , etc.). Chlorites with a muscovite-like silicate layer and an aluminum hydroxide sheet are called donbassite and have the ideal formula of $\text{Al}_{4.33}(\text{Si}_3\text{Al})\text{O}_{10}(\text{OH})_8$ as an end-member for the dioctahedral chlorite. In many cases, the octahedral aluminum ions are partially replaced by magnesium, as in magnesium-rich aluminum dioctahedral chlorites called sudoite. Cookeite is another type of dioctahedral chlorite, in which lithium substitutes for aluminum in the octahedral sheets [14].

Chlorite structures are relatively thermally stable compared to kaolinite, vermiculite, and smectite minerals and are thus resistant to high temperatures. Because of this, after heat treatment at 500°–700° C, the presence of a characteristic X-ray diffraction peak at 14 Å is widely used to identify chlorite minerals [14].

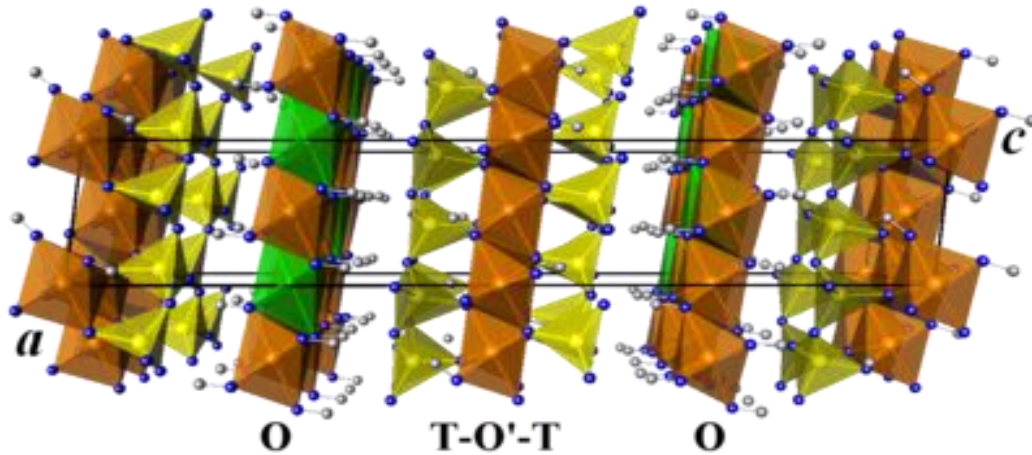


Figure I.II.7 : Crystal structure of cookeite $\text{LiAl}_4(\text{Si}_3\text{Al})\text{O}_{10}(\text{OH})_8$, space group Cc , projected along the b direction with perspective viewing [19].

(Yellow: silicon, orange: aluminum, green: lithium, blue: oxygen, gray: hydrogen. All the octahedra in the layers containing lithium have in fact a mixed occupancy of lithium and aluminum, the green octahedron being the only one with above 50% lithium. The octahedra layer sandwiched by SiO_4 tetrahedra contain only aluminum).

I- II-3 MULTI-SCALE STRUCTURE OF MONTMORILLONITE CLAY

Depending on the scale of observation, montmorillonites have different levels of organization. Figure I. II. 8 summarizes the various possible structures.

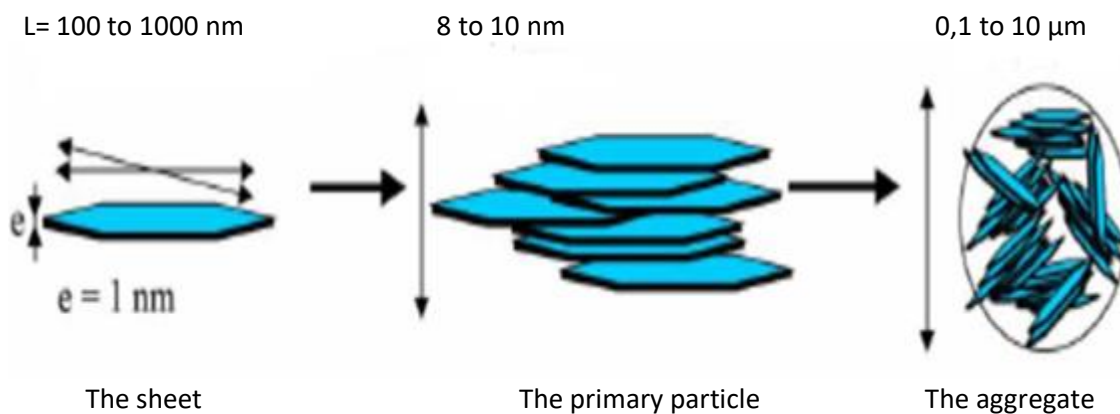


Figure I.II.8 : Multi-scale structure of montmorillonite clay [6]

I-II.3.1. The sheet :

The sheet can be assimilated to a disk or plate having lateral dimensions of about one tenth of a micron and a thickness of about one nanometer. Studies have shown that the sheets are relatively flexible and deformable [20].

I-II.3.2. The primary particle or tactoid

The primary particle consists of 5 to 10 sheets stacked on top of each other and held together by attractive electrostatic forces of the Van Der Waals type. The thickness of the primary particle varies, generally, from 8 to 10 micrometers [21].

I-II.3.3. The aggregate

The aggregate is a grouping of primary particles oriented in all directions. The aggregate size ranges from 0.1 to 10 microns [21].

Using the data from Oberlin and Mering (1962) and Van Olphen (1964) on expandable minerals as a reference, Tessier (1975) proposed a nomenclature to name the different modes of particle

association [22]: edge to edge and face to face. The aggregate of several primary particles has been called a morphological unit. Figure I-14 shows the different assumed modes of associations forming the aggregate [23].

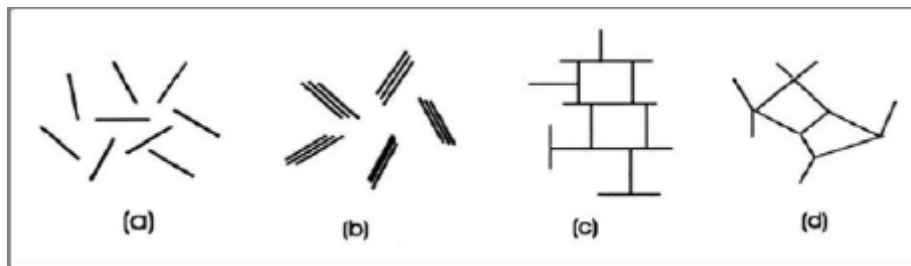


Figure I.II.9: Patterns of associations assumed for suspended montmorillonite strips: (a) dispersion, (b) face-to-face aggregation, (c) edge-to-face association, (d) edge-to-edge association (from Van Olphen, 1964) [22, 23].

When considering the main mineralogical species, three main types of stacking are to be considered (Figure I.II.10) [23]:

- i) Ordered stacking: In this case the sheets are stacked on top of each other in a perfect order. This is the case of phyllosilicates whose interfoliar space is empty or anhydrous (kaolinites or illites).
- ii) Semi-ordered stacking (or translational disorder): Successive sheets have

«semi-definite» translations. The sheets are separated by a few water molecules, the particle thickness is variable and depends on the degree of hydration. They can slide sideways on top of each other.

iii) Disorderly stacking (or turbostratic disorder): In this case of stacking, successive sheets present any translations and/or rotations throughout the building. The sheets are separated by a film of water allowing a free rotation around an axis perpendicular to the plane of the particle.

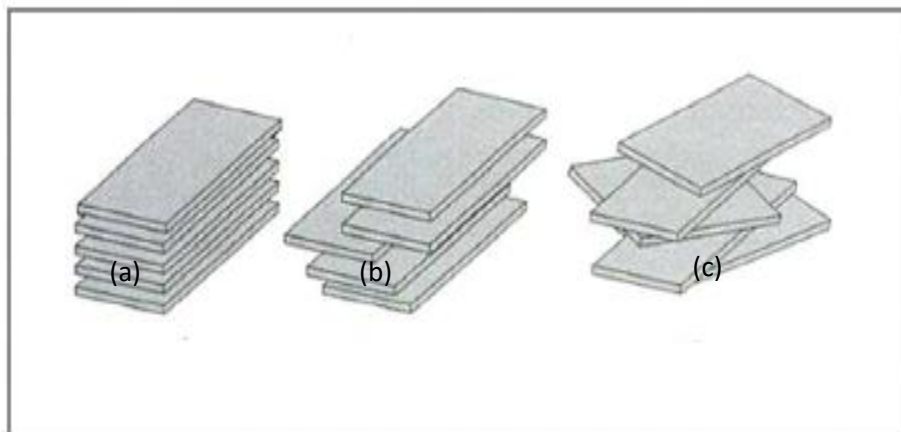


Figure I.II.10: The different types of stacking in the clays

Ordered stacking (a) Semi-ordered stacking (b) Disorderly stacking [23]

In the literature, researcher is often found that bentonites is formed by non-homogeneous minerals known as "interstate" [24,25, 26]. These clay particles are consisting of the superposition of sheets which are:

- (i) of a different nature (illite-smectite, vermiculite-smectite, etc.),
- (ii) of the same nature but different in their interfoliar fillings as the case of hydrated montmorillonite where the interfoliar space can contain one, two, three or four layers of water,
- (iii) or by nature and interfoliar filling at the same time, as the case of illite smectite with smectite sheets in varying states of hydration [27, 28].

Among these minerals, illite/smectite interstratified minerals are the most studied. They are found in bentonites commonly used in drilling sludge [25,28, 29].

In the case of interstated minerals, stacking is essentially characterized by the succession of leaves of a different nature according to the normal plan. Thus, if we consider an interstate

mineral containing two types of sheet A and B, we can consider essentially three types of interstate (Figure I.II.11) [26]:

Segregated: a given particle has AAABBB sequences (Figure I.II.11.a). The diffraction diagram X is the superposition of the diagrams produced by each of the components.

Regular: a given particle then contains ABABAB... AB sequences (Figure I.II.11.b). A period of over structure perpendicular to the plane of the sheets equal to the sum of the thicknesses of the two sheets appears ($d_T = d_A + d_B$). The diffraction diagram X then contains basal over structure reflections corresponding to d_T .

Random: that is, all intermediate cases between the two described above (Figure I.II.11.c). In this case, the diffraction diagrams X present irrational reflections (001), and their interpretation is very delicate.

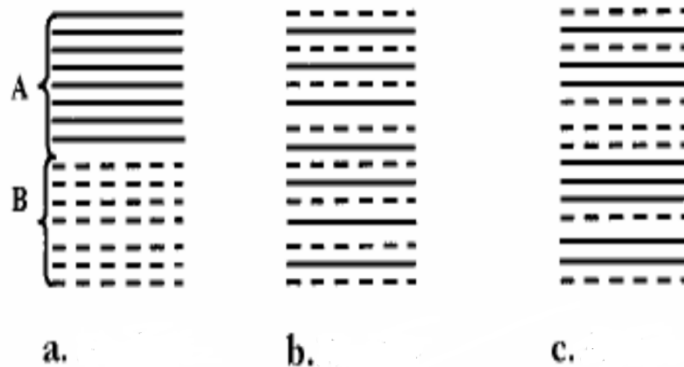


Figure I.II.11 : Different modes of succession of sheets within an inter-stratified unit

I-II-4 STRUCTURE OF BENTONITE

Bentonite is a geological term for soil materials with a high content of a swelling mineral, which usually is montmorillonite [30]. There are a few types of bentonite and their names depend on the dominant elements, such as K, Na, Ca, and Al. With characteristic of this bentonite, bentonite is interesting to use as a catalyst [31] and adsorbents in the form of nanoclay [32,33].

As is cited in the definition of bentonite the most important in this mineral clay is montmorillonite. The montmorillonite belongs to the smectite group, in which all members have an articulated layer structure. The thickness of an individual mineral layer is around 1 nm (Figure I.II.12) and the extension in the two other directions is often several hundred nanometers. Each layer is composed of a central sheet of octahedrally coordinated cations,

which on both sides is linked through shared oxygens to sheets of tetrahedrally coordinated cations. Clay minerals of this type are often referred to as 2:1 layer structures. By definition, the following applies for the mineral montmorillonite. The octahedral sheet has aluminum as central ion, which is partly substituted principally by Mg. The tetrahedral sheet has silicon as central ion, which partly may be substituted by principally aluminum. The substitutions result in a net negative charge of the montmorillonite layer in the range of 0.4 to 1.2 unit charges per $O_{20}(OH)_4$ -unit, and the octahedral charge is larger than the tetrahedral. The mineral is termed beidellite if the tetrahedral charge dominates. The induced negative layer charge is balanced by cations (c) located between the individual layers (interlayer space). A variable number (n) of water molecules may be intercalated between the individual mineral [34].

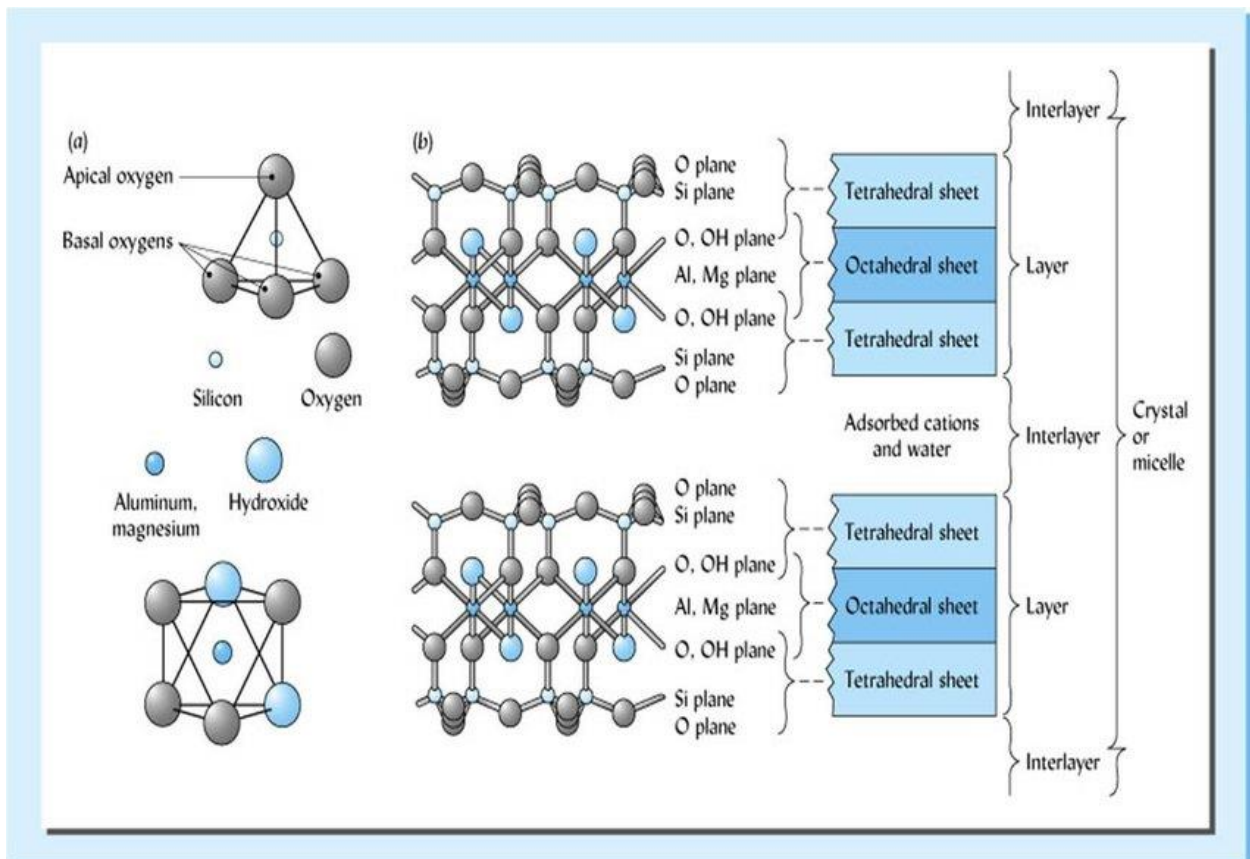


Figure I.II.12 : structure of bentonite

I-II-5 : TYPES OF BENTONITE

I-II-5-1-Calcium bentonites

They constitute the largest share of mined deposits in the world. They contain mainly ions (Ca²⁺) in the interfoliar position. These clays have a swelling rate 3 to 7 times the initial volume.

I-II-5-2-Sodium bentonites.

These are rare clays. Their interfoliar or exchangeable ion is Na. They have a very high swelling capacity (12 to 18 times) (BOUGDAH, 2007) [35].

I-II-5-3- activated Bentonites:

In order to improve the adsorption properties of calcium bentonites, those are the most often activated by sodium carbonate and then dried and crushed; bentonites are obtained activated calcium with properties equal to or greater than those of sodium bentonites. The properties of these activated or permeated bentonites are less stable over time (3 to 18 months) and depend on the activation and the levels of magnesium, calcium and sodium. These different types of bentonites are in the form of spherical or cylindrical powder or granules. They have very variables ranging from white for the purest products to grey, beige or green for the others.

I-II-6-PROPRIETIES OF BENTONITE:

The most important properties of bentonite for which it is employed in many different industries are the following:

➤ Water absorption and swelling

A fundamental property of bentonite is to absorb water and expand. However, not all bentonites have the same absorption capacity. Its level of hydration and swelling depends on the type of exchangeable ions contained, with different hydrophilic and solvating power. Swelling is mainly due to two factors: 1) water absorption at platelet surface level, and 2) osmotic repulsive forces, forcing platelets to detach and open up like a “stack of cards”. Sodium bentonite, with sodium cation prevalence (Na^+) allows water to penetrate through the platelets, forcing them apart, thus leading to swelling. Conversely, calcium bentonite, with calcium cation prevalence (Ca^{2+}), while getting hydrated in much the same way, due to its strong positive charge, has lower absorption properties, not permitting water to penetrate through the platelets. In this latter case, platelets flake off rather than swell.

➤ Viscosity and thixotropy of aqueous suspensions

when bentonite is dispersed in water, highly stable colloidal suspensions are formed with high viscosity and thixotropy. At high enough concentrations, these suspensions begin to take on the characteristics of a gel. Suspensions are formed when water molecules penetrate into platelet interlayers. Here, hydrogen bridge bonds are formed by the hydrogen atoms contained in the water molecules. Platelets become isolated from each other, while bonded through interposition water. When left still, a mesh is formed which, by incorporating water, jellifies. Conversely, under mechanical stress, these bonds partially break, thus allowing platelets to

move more freely. Viscosity under these conditions is lower than at rest. This reversible sol-gel-sol process is known as thixotropy. These properties shown by bentonite aqueous suspensions are mainly exploited in drilling slurries.

➤ *Colloidal and waterproofing properties*

when water is absorbed by bentonite, a semisolid gel is formed with strong hydrostatic pressure resistance. A montmorillonite platelet can be figured out as a thin packet of negatively charged layers. Due to their negative charge, they repel each other while letting water through. In this way, while the packet swells, a stable shell is formed around the platelet. When saturated, this shell will repel water, even under pressure. For all these properties, bentonite is employed in ponds and docks, to seal off soil infiltrations, and line the base of landfills.

➤ *Binding property*

This bentonite property is mainly exploited to produce green molding sand. In this application, bentonite with a suitable moisture content covers quartz sand grains and acts as a connective tissue to the entire mass. Under this homogenous coating, even at maximum compression, water will remain in a highly “rigid” state, binding the sand grains and lending maximum resistance to the sand mould. Bentonite vitrification temperature is higher than other clays. Therefore, when used as an additive, it makes green sand more durable, and, in particular, more resistant to heat stress.

➤ *Surface properties (coagulation– absorption – adsorption)*

Bentonite absorption – adsorption properties are determined by the high specific surface and free charges present on each micelle. Coagulation occurs through the adsorption of ions of opposite charge to that of colloidal particles.

I-II-6-1 Physical and chemical properties of bentonite :

Bentonite feels greasy and soap-like to the touch (Bates & Jackson, 1987). Freshly exposed bentonite is white to pale green or blue and, with exposure, darkens in time to yellow, red, or brown (Parker, 1988). The special properties of bentonite are an ability to form thixotropic gels with water, an ability to absorb large quantities of water with an accompanying increase in volume of as much as 12– 15 times its dry bulk, and a high cation exchange capacity[36].

➤ **Cation exchange capacity (CEC)**

The specific cation exchange capacity (CEC) of a bentonite depends on the number of cation exchangers in the clay and the specific cation exchange capacity of the smectite it self in terms of charge per gram. If the CEC of the smectite is known, the bulk CEC of a bentonite is a good measure of the smectite content, as long as no other cation exchangers are present. The

CEC can be determined in several ways. One method is to extract the cations with an NH_4Cl (or NH_4OAc) solution. Analysis of the extract gives information regarding the type and number of the cations present. One disadvantage with this method is that dissolvable phases (e.g. gypsum) also contribute to the result. This can however be minimized with an 80% ethanol solution instead of water (Belyayeva, 1967). Another method is to exchange with a Cu^{2+} - triethylenetetramine complex (Meier and Kahr, 1999). As the Cu-tri complex has a very strong blue color this reaction can be rapidly quantified by using spectrophotometry. The exchange reaction is fast and is normally completed in 15- to 30 minutes (Figure I.II.13).

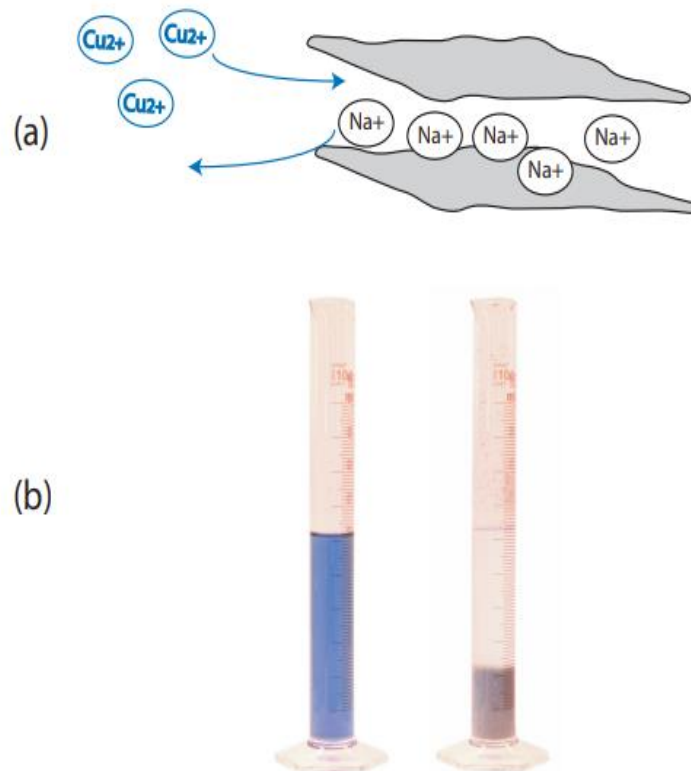


Figure I.II.13 : (a) Schematic illustration of the cation exchange reaction of Na^+ to Cu^{2+} in montmorillonite (b) The cylinder to the left contains a pure solution of a Cu^{2+} complex. In the cylinder to the right, sodium dominated bentonite (MX-80) has been added and mixed with the solution. Decoloring of the solution finished in approximately ten minutes |[37].

➤ **Acidic activation of bentonite**

Acidic activation involves the treatment of clay with a solution of mineral acid (HCl , H_2SO_4), in order to increase the specific surface area, porosity and acidity of the surface [38]. It increases the specific surface of clay from $40 \text{ m}^2 \text{ g}^{-1}$ to $500 \text{ m}^2 \text{ g}^{-1}$ by disintegrating the

clay particles, removing several mineral impurities, and removing the cations from the octahedral layer [39]. The acid activation process destroys part of the clay structure, removing iron, aluminum and magnesium from the octahedral layer (Figure I.II.14). The exchangeable cations are replaced mainly by the cations of Al^3 and H [39].

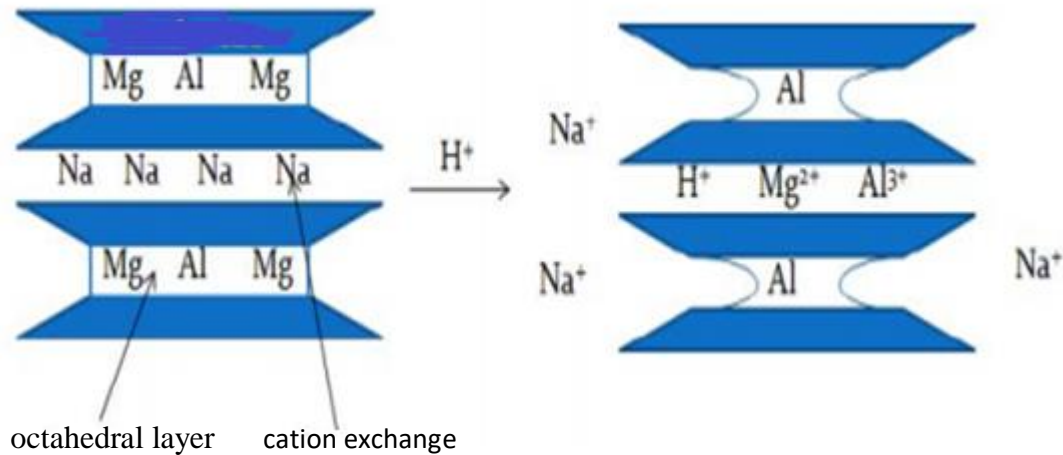


Figure I.II. 14 : acidic activation process of bentonite [40]

The destruction of the octahedral leaf increases not only with the increase of the concentration of acid, temperature and contact time, but also with magnesium percentage in the octahedral layer. According to the study J.Ravichandran et al [41] where they treated bentonite by HCl with different concentrations, they showed that the specific surface increases with increasing the concentration to 1M. For concentrations above 1M the specific surface begins to decrease. Another work carried out by B. Tyagi et al [42] where they treated the bentonite with H_2SO_4 with different concentrations, they showed that the destruction of the octahedral layer at low concentration. More than 3M the tetrahedral layer begins to destroy itself.

I-II-6-2 ; Chemical composition and some physical properties of maghnia bentonite performed in subsequent research studies.

Table I.II.2 : Chemical composition of bentonite (maghnia) reported from three different references. [35,43,44]

ref oxydes	B BENT	S BENT	N Bent (ENOF 1993)	N Bent (SIDAM 1994)	N Bent (Ramdani N et al 2016)
SiO ₂	61.0	62.4	60.2	59.89	65.19
Al ₂ O ₃	16.10	17.33	18.5	17.37	17.26
Fe ₂ O ₃	2.80	1.20	3.45	3.32	2.11
MgO	3.53	2.56	4.14	3.37	3.08
CaO	3.15	0.81	1.07	1.06	1.21
Na ₂ O	1.50	1.59	0.94	1.32	2.13
K ₂ O	1.60	1.50	1.50	1.30	0.58
MnO	0.04	0.04	0.06	0.07	Ni
TiO ₂	0.22	0.20	0.28	0.28	0.19
H ₂ O ⁺	10.16	12.37	9.86	4.46	Ni
H ₂ O ⁻	Ni	nI	Ni	8.26	Ni
LOI				8.2 3	
So ₃	Ni	nI	Ni	0.68	Ni

Table I.II.3 : Trace elements of bentonite [43]

Elements	Ba	Sr	Cu	Pb	Zn	S	SO ₄
%	210	60	20	35	70	270	810

Table I.II.4 : Cationic Echange of bentonite With Differents Cation [43]

Sample	CEC meq/100g	Na meq/100g	Ca meq/100g	Mg meq/100g	Total
Bent roussel	67.5	21.3	12.5	15.5	49.3

Table I.II.5 : Specific surface of bentonite-Na [43]

Element	Naturel bent (m ² / g)	Bent Na ⁺ (m ² / g)
Specific surface	47.20	88.88

Table I.II.6 : Particle size analysis of bentoite of maghnia (rousseau) [35]

Dimension (μm)	70	60	50	40	30	20	10	5	3	2
percentage	100	100	100	97	91	78	50	26	17	11

Table I.II.7 : Physico-chemical and rheological properties of natural bentonite [43]

Parameters	viscosity	Humidity	I of swelling	Ph	coloidality
Bent rousseau	4	18.10	10	7.23	67

Table I.II.8 : The important physico-chemical properties of bentonit (maghnia) reported from ref [45]

Chemical composition % mass			Physical characteristics	
Elements	SEM	EDS		
SiO ₂	57.96	52.51	Loss on ignition (%)	12.19
Al ₂ O ₃	22.05	21.25	Density	1
Fe ₂ O ₃	2.83	2.25	Granulometry (μm)	2 to 1
CaO	8.49	15.0	Capacity swelling Cg	8.27
Cl ₂ O	1.138	1.25	pH for 10 g/L	10.7
MgO	2.37	2.37	Conductance (μS) for 0.5 g/L	66.4
Na ₂ O	1.91	1.25	CEC (meq/g)	0.90
K ₂ O	2.84	1.25		
TiO ₂	0.12	2.50		

In table I.II.8 the SiO₂/Al₂O₃ ratio equal 2.63 indicated that the major mineral was the montmorillonite.

I-II-7: USE AND APPLICATION OF BENTONITE

The versatile character of bentonites have been described by many authors in the past, including Grim (1962), Hartwell (1965), Grimshaw (1971), Highley (1972), Hofstadt & Fahn (1976), Grim & Güven (1978), Patterson & Murrey (1983) Odom (1984), Clarke (1985), Robertson (1986) and O'Driscoll (1988). They all presented the fields where the bentonites find applications. Generally speaking, the applications can be divided into those which use large tonnages of bentonites and those where bentonites are used in small quantities (Odom, 1984, O'Driscoll, 1988) [46]. Because of the above mentioned bentonite properties, they have a wide range of applications: In the petroleum industry, particularly in the catalysis field [47]: Acid-treated bentonite is used in many reactions such as dimerization of unsaturated fatty acids to dicarboxylic acids and alkylation of phenols. The bentonites exchanged by the cations are also effective catalysts, we give for example: the bentonites exchanged by Al and Cr are used in lactonization reactions, noting also the bentonite exchanged by the Fe and the Co which serve for the protonation of several organic species. Sodium Bentonite exchanged by cations with a high charge density such as Al, Cu, Fe and Cr are effective and selective catalysts for the production of ethyl acetate from ethylene and acetic acid. In drilling as a drilling fluid. In the field of depollution, Bentonite has a wide field of application aimed either at the degradation of polluting organic compounds or their transformation into less harmful products [48, 49].

The most Important uses of bentonites are resumed in the following points [35, 50].

In addition to the industrial applications listed above, Bentonites are used as:

- Abrasives, for example, arc stabilizer, forming slag, such as extrusion aid, etc.
- Absorbents, for example in pet beds as a desiccant.
- Carriers for pesticides and other biocides

Also:

- In agriculture, Bentonites are used to improve the properties of sandy and acidic soils. They are also used for coating certain types of seeds to increase their size for both easier mechanical distribution and also improved germination.
- In ceramic applications, they are used in applications such as glass suspending agents and plasticizers
- In welding, they are used as a component of arc electrodes, and as stabilizers, welding group protectors, casting agents and modifiers of slag
- In the paper industry, Bentonites are used for fading recycled paper and controlling pitch, as well as wastewater clarification, auxiliary retention, coverage, carbonless copy paper, etc.

- In paintings, Bentonites are used in waterproofing or thixotropic paints
- In electrical porcelain, Bentonite is used as a plasticizer that increases the dry and fired strength and reduces absorption
- To develop the color in the colorants in carbonless paper, acid-activated Bentonite is used.
- For the manufacture of paints, greases, lubricants, plastics, and cosmetics, organophilic clays are used because of their ability to swell and disperse in organic solvents. Therefore, Bentonites are found in gelling agents, thixotropic agents and emulsifiers.
- For pesticides and other biocides, they are widely used as dry and diluent carriers.
- For plastic, Bentonite reduces the gas permeability of plastic films.

References of chapter I section II

- [1] N K Foley: Environmental Characteristics of Clays and Clay Mineral Deposits; U.S. Geological Survey; Eastern Publications Web Team; 04-01(2009).
- [2] M Sirait, N Bukit, N Siregar, Preparation and characterization of natural bentonite in to nanoparticles by coprecipitation method, AIP Conference Proceedings 1801, 020006 (2017).
- [3] W K Tong . Introduction to clay Minerals and soils, (2000).
- [4] H Murray, Chapter 2 Structure and Composition of the Clay Minerals and their Physical and Chemical Properties ; Developments in Clay Science, 2 :7-31 (2006).
- [5] R G McLaren, K C Cameron, Soil Science, Sustainable production and environmental protection. Oxford University Press (1996).
- [6] A Mathieu, Investigation of cement substitution by blends of calcined clays and limestone : doctorat thesis, EPFL suisse (2013).
- [7] CD. Barton ; A.D. Karathanasis, CLAY MINERALS, Encyclopedia of Soil Science by Marcel Dekker, Inc. AH rights reserved , 187-192 (2002).
- [8] N Brady, Soil Colloids: Their Nature and Practical Significance. The Nature and Properties of Soils, 10th Ed.; Macmillan Publishing Co.: New York, 177-212 (1990).
- [9] O M'Bodj, N K. Ariguib, M T Ayadi , A Magnin, Plastic and elastic properties of the systems interstratified clay-water-electrolyte-xantha J. Colloid Interface Sci. 273 :675-684 (2004).
- [10] G Derafa, Synthèse et caractérisation de montmorillonite : modifiée : Application à l'adsorption des colorants cationiques, magister memory, university ferhat abbas- Setif-1 ; (2014).
- [11] O Ombaka, Characterization and classification of clay minerals for potential applications in Rugi Ward, Kenya, African Journal of Environmental Science and technologie, 10(11) : 415-431, (2016).
- [12] M D Ruiz Cruz, Genesis and evolution of the kaolin-group minerals during the diagenesis and the beginning of metamorphism, Departamento de Química Inorgánica, Cristalografía y Mineralogía. Facultad de Ciencias. Universidad de Málaga. 29071 Málaga (Spain).
- [13] R Valapa,S Loganathan,G Pugazhenthii,S Thomas,T Varghese,Chapter 2 - An Overview of Polymer–Clay Nanocomposites, 29-81 (2017).
- [14] H Kodama, R E. Grim, clay mineral rock, Encyclopædia Britannica,(2014)
- [15] N Güven, Mica Structure and fibrous growth of illite, Clays and Clay Minerals 49 (3): 189–196 (2001).

- [16] I E Odom , Smectite clay minerals: properties and uses Philosophical Transactions of the Royal Society of London. Series A, Mathematical and Physical Sciences 311 :391–409 (1984).
- [17] A Olad, Advances in Diverse Industrial Applications of Nanocomposites Chap: Polymer/Clay Nanocomposites, March (2011).
- [18] T Al Ani, O Sarapaa, Clay and clay mineralogy, Geological Survey of Finland, Report, (2008).
- [19] H Zheng, S W Bailey, Refinement of the cookeite structure, American Mineralogist 82(9-10): 1007-1013 (1997).
- [22] X chen, Y peng, Managing clay minerals in froth flotation—A critical review Mineral Processing and Extractive Metallurgy Review , 39(5) :289-307 (2018).
- [23] A Elhachimi, Argile et minéraux argileux: propriétés physico-chimiques et propriétés et propriétés colloïdes, Université Abdelmalek Essaadi - Master fondamentale Chimie (2013).
- [24] S Caillère, S Hénin, M Rautureau, "Minéralogie des argiles" Masson, Tomes 1 et 2, 184-189 (1982).
- [25] S Laribi, J M Fleureau, JM., J L Grossiord, Effect of pH on the rheological behavior of pure and interstratified smectite clays. Clays Clay Miner, 54 :29–37 (2006).
- [26] A Mansri, Composites à base de copolymères et de bentonite pour la rétention des polluants et pour l'inhibition de la corrosion, University Usto Oran, (2016).
- [27] H Ben Rhaiem, D Tessier, C H Pons, Clay Minerals, 21 :9-29 (1986).
- [28] N. Jozja, Etude de matériaux argileux albanais : caractérisation multi-échelle d'une bentonite magnésienne : impact de l'interaction avec le nitrate de plomb sur la perméabilité, Orléans (2003).
- [29] O M'bodj, N K Ariguib, MT Ayadi, A Magnin, Plastic and elastic properties of the systems interstratified clay-water-electrolyte-xanthan. Journal of Colloid and Interface Science . 273, 675-684 (2004).
- [30] O Karnland, S Olsson, U Nilsson, Mineralogy and sealing properties of various bentonites and smectite-rich clay materials, Technical Report, TR-06-30 (2006).
- [31] X Gao, H Zhong, Yao, W Guo, F.Jin, Hydrothermal conversion of glucose into organic acids with bentonite as solid base catalyst, Catalyst today, 247 : 1-6(2016)
- [32] C Y Cao, L K Meng, Y H Zhao, Adsorption of Phenol From Wastewater by Organo bentonite, Desalination and Water Treatment, 52 :3504–3509(2013)
- [33] Z T Le, L Shi, The effect of Copper Chloride on the Surface of Bentonite in Adsorption of Propylmercaptan, Energy Sources, Part A, 34:1231–1237 (2012).

- [34] O Karnland, S Olsson, U Nilsson, Mineralogy and sealing properties of various bentonites and smectite-rich clay materials, Technical Report TR-06-30, 12 (2006).
- [35] A Melki, Etude analytique des caractères physico-chimiques et hydriques de deux types de bentonite (exemple de la bentonite de Maghnia et de la bentonite de Mostaganem), UABB Tlemcen, (2012).
- [36] S Bilal, M Dabo, Determination of morphological features and molecular interactions of nigerian bentonitic clays using scanning electron microscope (SEM), Bayero Journal of Pure and Applied Sciences, 9(2): 279 – 285 (2016).
- [37] S Daniel. The Bentonite Barrier Swelling Properties, Redox Chemistry and Mineral Evolution, Centre for Analysis and Synthesis, 184(2015).
- [38] Hand book of clay science. Édition EL SEVIER. 1 (2006).
- [39] F Wypych, G K Satyanarayana, Clay Surfaces Fundamentals and Applications. Édition ELSEVIER (2004).
- [40] M A Zenasni, Synthèse et caractérisation des nanocomposites biodégradables élaborés par trois procédés (intercalation en solution, polymérisation in situ et par voie fondue), University of lorraine fr (2018).
- [41] J Ravichandran, B Sivasankar, clays and clays minerals. 45 (6) : 854-858(1997).
- [42] B Tyagi , C D Chudasama, R V Jasra. Spectrochimica Acta Part A. 64 (2006) 273.
- [43] I Belbachir, Modification de la Bentonite de Maghnia et Applications dans l'adsorption de colorants textiles et de métaux lourds, doctorat thesis, university of abou bekr belkaid tlemcen, university abou bekr belkaid, 09(2018)
- [44] N Ramdani, Préparation des Copolymères Poly(4-vinylpyridine)(s) Greffés par des Groupes Alkyles. Application à la Modification des Argiles et à la Rétention des Molécules Organiques. University abou bekr belkaid, 05(2015).
- [45] Z Meçabih, R Jérôme, D Borschneck, Urban Wastewater Treatment by Adsorption of Organic Matters on Modified Bentonite by (Iron-Aluminum) , Journal of Encapsulation and Adsorption Sciences,(4) : 71-79, (2014).
- [46] H H Murray, Chapter 6 Bentonite Applications, Developments in Clay Science,(2) : 111-130, (2006).
- [47] H H Murray, Applied clay mineralogy: Occurrences, Processing and Application of Kaolins, Bentonites, Palygorskite-Sepiolite, and Common Clays, Chapter 6, Elsevier. Edition (2007).

- [48] Y H Shen, Removal of butylated hydroxyanisole with enzyme based polymerization using organo-clays, *Water Research*. 36 :1107(2002).
- [49] J Ojiang, C Cooper, S Ouki, Urban wastewater treatment by adsorption of organic matters on modified Bentonite by (Iron-Aluminium), *Chemosphère*. 47: 711(2002).
- [50] D M Baebieria, B L Robert, J Dykec, H ch Penxiang, Z Shazim et al, Calcium bentonite and sodium bentonite as stabilizers for roads unbound, *cleaner engineering and technology* , 6 : 100-372 (2022).

I-III POLYACRYLAMIDES

Polyacrylamide belongs to a highly versatile group of polymers that can find use in a wide range of applications including wastewater treatment, oil recovery [1], soil conditioning, agriculture, biochemistry, and biomedical applications [1,2,3] and even as a subdermal filler for aesthetic surgical procedures[1,4]. The toxicity of these polymers has also attracted considerable attention as some of the aforementioned applications include direct contact with either humans or animal livestock. The concentration of the residual monomer in particular has to be in ppm levels (500 ppm), and hence polymerization reactions that can afford quantitative monomer conversion are highly desired. Free radical polymerization has been utilized for the synthesis of AM homopolymers and statistical block copolymers. However, the need for enhanced control over the MWDs and sophisticated architectures facilitated the employment of controlled radical polymerization methods (CRP) [1, 5,6].

I-III-1 : DEFINITION OF THE POLYACRYLAMIDE

Polyacrylamide (PAAm) is obtained by radical polymerization of acrylamide (AAm) ($\text{CH}_2 = \text{CHCONH}_2$). This monomer (M.P. = 71 g / mol) is a crystalline, white solid, soluble in water, with good thermal stability. It is known to be carcinogenic.

Once polymerized, it loses these characteristics, but still remains water-soluble. It is polymerized by a number of techniques [7, 8]: gamma radiation, ultrasound and photopolymerization. In some situations, it can still be achieved by X-ray initiation and photosensitization with the help of hydrogen peroxide. Nevertheless, the most used technique is that of a redox type reaction, the most used initiator being ammonium persulfate (PSA) $[(\text{NH}_4)_2\text{S}_2\text{O}_8]$ with tetramethylethylenediamine (TEMED). The polyacrylamide thus produced is commonly used in fundamental studies on solutions of macromolecules [7,9] and in applied experimental studies on the adsorption of polyelectrolytes [7,10,11]. It is also used in studies of diffusion of solutes: W Masinghe et al. [12] used the polyacrylamide to induce elasticity in corn syrup solutions; they observed that this increases the diffusivity of KCl in these solutions by 55%. Polyacrylamides have a double interest: industrial and fundamental. High molecular weights can be obtained by radical polymerization, they find their most important applications as thickeners, flocculants for water treatment [13-14], soil treatment agents [15-16], and in many biomedical applications [17-18]. In particular, gels and membranes made from polyacrylamides have been used extensively in recent years for protein separations [19-20].

From a fundamental point of view, they belong to the family of vinyl polymers (backbone identical to that of polystyrene) and their amide groups give them solubility in water. There are many methods of synthesizing polyacrylamide [21,22], but the polymerization of acrylamide under adiabatic conditions remains the most suitable method for preparing polymers of large molecular masses.

The adiabatic polymerization of acrylamide has been progressively developed in order to improve the properties of the resulting polymers. This method makes it possible to carry out the polymerization of concentrated acrylamide solutions and to have high molecular weight polyacrylamides, but the optimization of this technique and of this reaction is always essential. The study of Zitouni et al were devoted to the improvement of some parameters, such as the duration of the polymerization, the mass of the polymers obtained and even the ease of setting up the reaction [23].

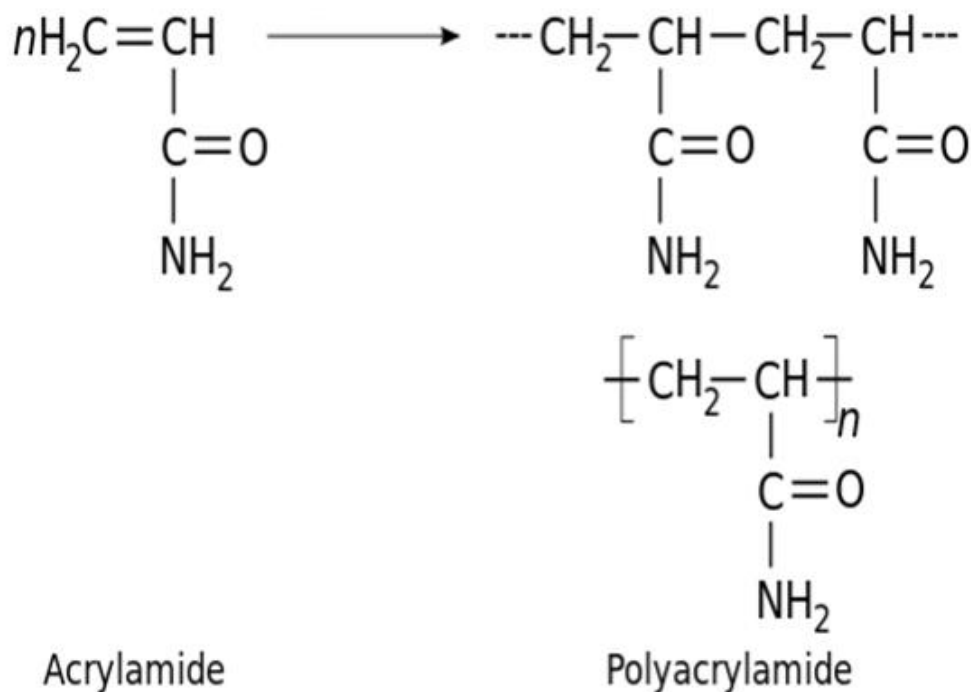


Figure I.III.1 : radicalar polymerization of polyacrylamide

I-III-2 : EFFECT OF INITIATOR QUANTITIES AND CONDITION OF SYNTHESIS IN THE WEIGHT MOLAR OF POLYACRYLAMIDE

Rh mi vachon and al were synthesized the polyacrylamide by uncontrolled radical polymerization with a pair of redox initiators (Figure I.III.2).

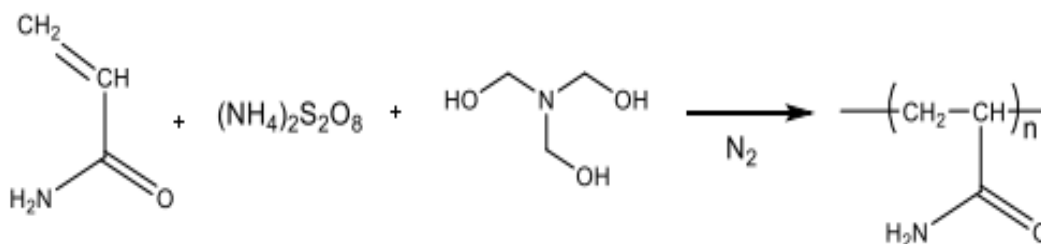


Figure I.III.2 : radicalar polymerization of polyacrylamide with a pair of redox initiator ammonium persulfate and triethanolamine [24].

For PAM-5 shown in table I.III.1, rh mi vachon et al were prepared a solution of acrylamide (50.0 g, 0.7 mol), ammonium persulfate (20.0 mg, 87.7 μ mol) and triethanolamine (80.0 mg, 0.5 mmol) in distilled water (500 mL) bubbled with a nitrogen jet for 15 minutes and stirred under a nitrogen atmosphere for 24 hours. The gel formed is subsequently diluted with distilled water (200 mL), then precipitated in methanol. The polymer is recovered and dried under vacuum at room temperature for 48 hours. A white solid is recovered. $^1\text{H NMR}$ (400 MHz, D_2O , ppm): 2.41-2.14 (m, 1H,CH), 1.85-1.46 (m, 2H, CH₂)

Tableau I.III.1 : Synthesis conditions of polyacrylamide and the weight molar [24] .

Copolymere	[M] (M)	[A] Persulfate D'ammonium (M)	[A] Triethanolamine (M)	M_n (g/mol)	M_w (g/mol)	ID
PAM-1	1,41	$2,6 \times 10^{-2}$	$1,6 \times 10^{-1}$	130 100	243 100	1,87
PAM-2	1,41	$4,3 \times 10^{-3}$	$3,0 \times 10^{-2}$	569 100	917 600	1,61
PAM-3	1,41	$1,2 \times 10^{-3}$	$1,2 \times 10^{-3}$	1 865 000	2604 300	1,40
PAM-4	1,41	$5,3 \times 10^{-3}$	$3,2 \times 10^{-3}$	4 528 300	4 932 300	1,09
PAM-5	1,41	$1,8 \times 10^{-4}$	$1,1 \times 10^{-3}$	6 762 000	6 976 700	1,03
PAM-6	1,41	$1,8 \times 10^{-4}$	$1,3 \times 10^{-3}$	8 392 700	8 958 300	1,07

I-III-3 : THERMO-PHYSICAL PROPERTIES OF POLYACRYLAMIDES : EXPERIMENTAL / LITERATURE DATA [25]

Table I.III .2 : Thermo-Physical Properties Of Polyacrylamides : Experimental / Literature Data

Property	Unit	Value range
Molar volume	ml mol ⁻¹	54.6
Density	G mol ⁻¹	1.30
Glass transition Tg	K	426-461
Index of refraction	None	1.45

I-III-4 : THERMO-PHYSICAL PROPERTIES OF POLYACRYLAMIDES : CALCULATED DATA [25]

Table I.III.3 : thermo-physical properties of Polyacrylamides : calculatd data.

Property	Unit	Value range	Prefered
Molecular weight of repeat unit	g mol ⁻¹	71 .08	
VAN der waals volume V _{vw}	ml mol ⁻¹	38.60	
Molar volume V _m	ml mol ⁻¹	59.40	
Density	g mol ⁻¹	1.2	
Solubility parameter	Mpa ^½	24.0-27.8	25.9
Molar cohesive energie	J mol ⁻¹	34100-45900	39800
Glass transition	K	436	
Molar heat capacity Cp	J (mol.K)-1	90-104	96
Index of refraction (n)	None	1 .49	14000

I-III-5 CHEMICAL PROPERTIES OF POLYACRYLAMIDES

Polyacrylamide is relatively stable to heat with its solid only being softened at 220~230 °C and its solution subjecting to significant degradation only at above 110 °C. Polyacrylamide is insoluble in benzene, toluene, xylene, gasoline, kerosene, diesel fuel, but soluble in water. Polyacrylamide can react with alkaline with partial hydrolysis of polyacrylamide. It will have imidization reaction in strongly acidic ($\text{pH} \leq 2.5$) which will reduce its solubility in water. It can be cross-linked by the poly-nuclear olation complex ion formed between aldehyde (such as formaldehyde) and high metal (such as aluminum, chromium, zirconium, etc.) and is easy to be degraded by the action of the mechanical and (or) oxygen. In oil exploitation, it is mainly used as oil displacement agent, water blocking agent, profile control agent, thickener, drag-reducing agent, water treatment agent.

I-III-6 : PHYSICAL PROPERTIES OF POLYACRYLAMIDES

Solubility in water:

Upon rapid mechanical stirring, polyacrylamide is easily soluble in cold water form a transparent adhesive solution. Increasing the temperature does not affect its solubility and only affects its dissolution when the concentration is increased to a high viscosity.

Solubility in Other Solvents:

Polyacrylamide has a over 1% solubility in solvents such as glycerol, ethylene glycol, formaldehyde, acetic acid and lactic acid (these materials may be used as the plasticizer for laminating polyacrylamide).

However, it can only be swelled without being dissolved in solvents such as propionic acid, propylene glycol; it is also not soluble in solvent such as acetone and hexane.

Stability:

Polyacrylamide has a moderate hygroscopic property, if not exposed to position of high temperatures, the powdered polyacrylamide can subject to long-term storage. For liquid polyacrylamide, when its concentration is greater than 17%, it can be stored for more than one year with no significant change in the solution viscosity. In the pH range of 3 to 9, it can maintain a good degree of stability; at high pH, the viscosity will be increased gradually.

Miscibility:

In generally used concentration, polyacrylamide has miscibility with most water-soluble natural or synthetic resins, latex systems, and most of the salts. Polyacrylamide can also quickly miscible with non-ionic, cationic and anionic surfactants, though with certain surfactants affecting the viscosity.

Viscosity:

The viscosity of polyacrylamide solution has a linear correlation with its molecular weight; in addition, the higher the temperature, the lower the viscosity.

Intrinsic viscosity:

The increase of the molecular weight of polyacrylamide will cause increased intrinsic viscosity.

Ion property:

The carboxyl group in long-chain yields anionic polyacrylamide; the amino group yields cationic version. Because of the existence of amino group or carboxyl group in the long-chain of polyacrylamide, it is easy for flocculation when encountering aluminum ions.

Retention property:

The retention trend of polyacrylamide is similar with that of rosin soap with the former one having a high retention rate.

Toxicity:

Polyacrylamide itself is non-toxic, but if it contains polymerized monomers (a double bond), it would be toxic to humans. For this reason, upon the completion of its preparation, a certain amount of sodium bicarbonate should be added to remove residual monomers. The above information is edited by the chemicalbook of Dai Xiongfen.[26]

I-III-7 : TYPES OF POLYACRYLAMIDES :

Polyacrylamide could be made to four series,e.g.,non-ion polyacrylamide,zwitterionic polyacrylamide, cationic polyacrylamide CPAM, and anionic polyacrylamide APAM.

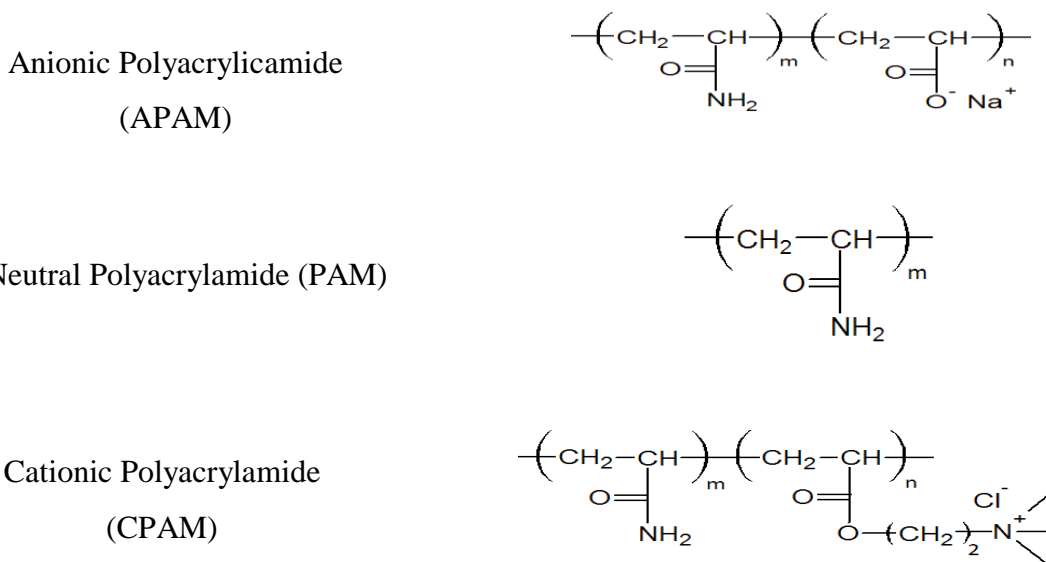


Figure I.III.3: different kind of polyacrylamde [26]

Anionic polyacrylamide (APAM) is a kind of polyacrylamide (PAM) and shows electronegative which contains functional groups of sulfonic acid, phosphoric acid or carboxylic acid 1 . Due to more charge, the molecular chain of polymer can be more stretching in the water which will increase the capacity of adsorption and bridge for suspended particles removal 2,3 . The main interaction between APAM and suspended particles is static electricity, hydrogen bonding or covalent bond 4-6 . Anionic polyacrylamide with high molecular weight and good solubility property can be an important kind of flocculants. And it has been widely used in water treatment because of good flocculation performance 7 . Generally, molecular weight of polysaccharide polymer is determined by intrinsic viscosity 8 . Accordingly, how to improve the intrinsic viscosity and solubility property of APAM is the most critical point in the polymerization [27].

Synthesis technology progress of APAM: The earliest in 1893, Moureu prepared polyacrylamide by using acryloyl chloride and ammonia in the low temperature. And in 1954, America takes the lead in realizing the industrialization production of polyacrylamide. However, in the 1960s, APAM was firstly developed through alkaline hydrolysis process in the world. Up to now, synthesis technology of APAM has experienced a lot of improvements, the basic reaction of polymerization usually expressed as Figure. I.III.4 . According to the APAM synthesis development history of these years, successively appeared the following six different synthesis technologies: Homopolymerization posthydrolysis process, homopolymerization cohydrolysis process, copolymerization approach, inverse emulsion polymerization, precipitation polymerization and radiation polymerization [27].

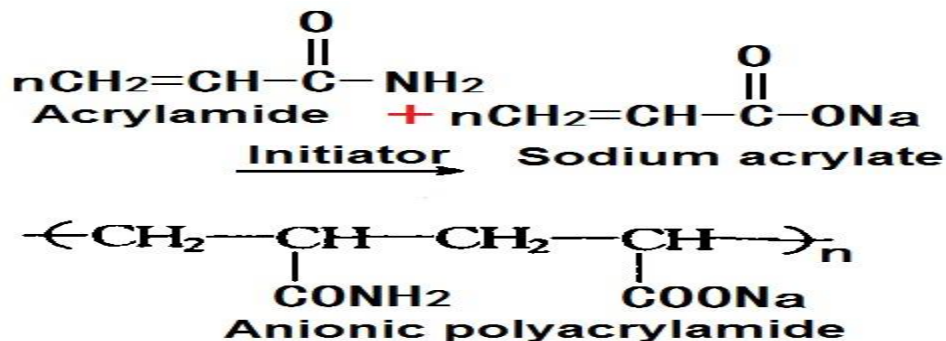


Figure. I.III.4 : The synthetic route of Anionic polyacrylamid [26]

Cationic polyacrylamides (CPAM) are a kind of important cationic polyelectrolyte and extensively used as flocculants for liquid/solid separation, retention and drainage aids in papermaking, flotation aids and demulsifiers for oil/water clarification, as soil improvers and drainage aids, etc. [28]. Various types of methods for producing CPAM have been developed,

such as homogeneous aqueous solution polymerization, inverse emulsion polymerization, inverse suspension polymerization and dispersion polymerization, and so on [28].

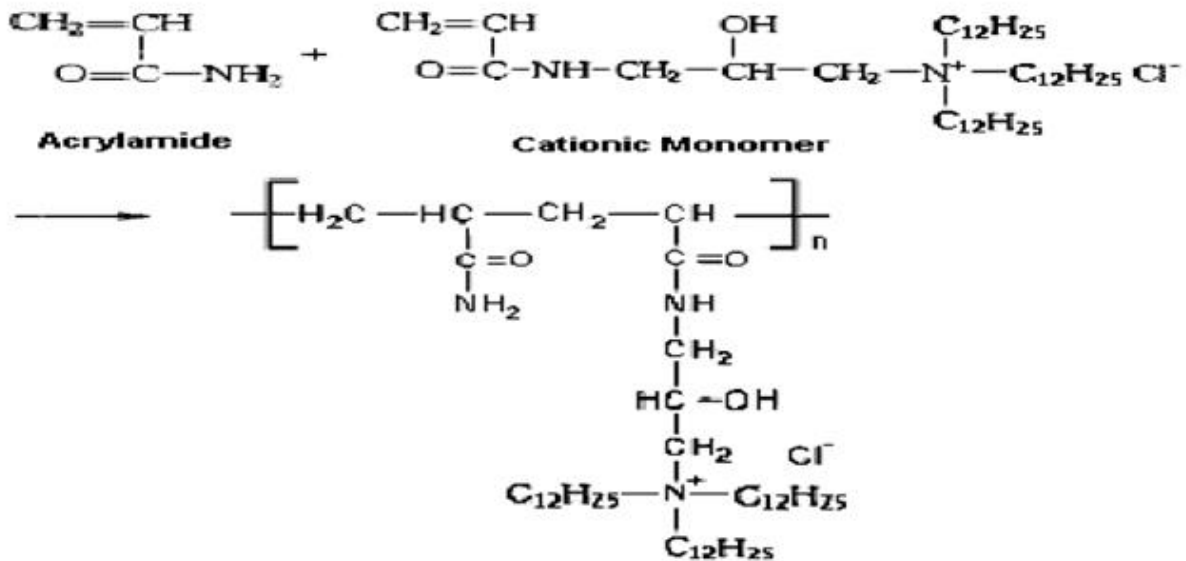


Figure I.III.5 : hydrophobically modified cationic acrylamide copolymer [29]

Partially hydrolyzed polyacrylamides are used in secondary petroleum recovery processes as a thickening agent, to lower the mobility of the aqueous phase relative to the oily phase. One can thus increase the production of a well by recovering part of the oil inaccessible by conventional methods [30]. Nevertheless, their viscosity and their stability are very sensitive to the nature and to the salt concentration of the deposits and their efficiency is, in fact, very variable. Being also used in various other industrial processes (flocculation, etc....) the study of their properties has been the object of numerous works [31] especially as they constitute interesting models of flexible polyelectrolytes with variable density dump.

References of chapter I section III.

- [1] R Glen Jones, Z Li, A Anastasaki, D J Lloyd, P Wilson, Z Qiang , Rapid Synthesis of Well-Defined Polyacrylamide by Aqueous, *Macromolecules* , 49(2) : 483–489, (2016) .
- [2] S Hassan, J Kim, Z Suo, Polyacrylamide hydrogels. IV. Near-perfect elasticity and rate-dependent toughness, *Journal of the Mechanics and physics of solids*,158 : 104-675(2022).
- [3] J J Zhue, recent patents on materials science , 11(2) :1874-4656 (2018).
- [4] F Zhi, Y Jiang, M Guo, W Jin et al, Effect of polyacrylamide on the carbonation behavior of cement paste,156: 106-756 (2022).
- [5] M J Caulfield, G G Qiao, D H Solomon, Some aspects of the properties and degradation of polyacrylamides, *Chem. Rev*, 102 (9) : 3067– 3084, (2002).
- [6] A Shipp, G Lawrence, R Gentry, T McDonald, H Bartow, J Bounds et al, Acrylamide: Review of Toxicity Data and Dose-Response Analyses for Cancer and Noncancer Effects . *Critical . Reviews in. Toxicology*, 36 (6–7) : 481–608, (2006).
- [7] P J Do Amaral Sobral, diffusivite de l'eau dans le gel polyacrylamide-eau autour de la transition vitreuse, *Institut national polytechnique de lorraine*,(1992).
- [8] J P Riggs, F Rodriguez,"Persulfate-initiated polymerization of acrylamide.", *Journal of Pol ymer Science: Part A-1*, 5: 3151-3165 (1967).
- [9] F A Bovey, G V D Tiers, *Polymer NMR spectroscopy. IX. Polyacrylamide and polymethacrylamide in aqueous solution*,*Journal of Polymer Science*, 1 :849-861(1963).
- [10] J Meadows, P A Williams, M J Garvey, R Harrop. G O Philips, Characterization of the adsorption-desorption behavior of hydrolyzed polyacrylamide, *Journal of Colloid and Interface Science*, 132 (2) :319-328, (1989).
- [11] D D RA Vetkar, V D Ambeskar et R A Mashelkar, Diffusion-adsorption problems in macromolecular systems : New techniques for parameter estimation.",*Journal of Applied Polymer Science*, 39 : 769-783 (1990).
- [12] S R Wickramasinghe, D V Boger , R C Pratt, G W Stevens, Diffusion in elastic fluids,*Chemical Engineering Science*, 46 (2) : 641-650 (1991).
- [13] W F Barvenik, Polyacrylamide characteristics related to soil applications, 158(4) : 235-243 (1994).
- [14] X Hao, Degradation on polyacrylamides. Part I. Linear polyacrylamid,polymer, 44(5):1331-1337(2003).
- [15] C A Seybold, Polyacrylamide review: Soil conditioning and environmental fate, *communications in Soil Science and Plant Analysis*, 25:2171-2185 (1994).

- [16] A Rai, Agricultural polymers polyacrylamide preparation, application and prospects in soil conditioning, *Commun Soil Sci Plant Anal*; 11(8):767 (1980)
- [17] P Chabreck, DLohmann. In Process for coating a material surface, *Eur. Pat. Appl.*; 2001.
- [18] T Marshall, KM Williams, The simplified technique of high resolution two-dimensional polyacrylamide gel electrophoresis: biomedical applications in health and disease. *Electrophoresis*. 12:461-71(1991).
- [19] G Patras, GG Qiao, DH Solomon, Characterization of the pore structure of aqueous three-dimensional polyacrylamide gels with a novel cross-linker *Electrophoresis*, 21:38-43 (2000).
- [20] M J Caulfield, H H Purss, D H Solomon. Degradation on polyacrylamides. Part I. Linear polyacrylamide, *Electrophoresis*, 22:4297 (2001).
- [21] L L Gur'eva, A I Tkachuk, Ya I Estrin, B A Komarov, Et al, Synthesis and free-radical polymerization of water-soluble acrylamide monomers, *Polymer Science*, Vol. 50, No. 3, pp. 283–290 (2008).
- [22] B Grassl, G Clisson, A Khoukh, L Billon, Nitroxide-mediated radical polymerization of acrylamide in water solution, *European Polymer Journal* 44 : 50–58 (2008).
- [23] B Bouras , Nouveaux Copolymè Respoly(acrylamide-co-4-vinylpyridine)-proprietes Et Applications, UABB Tlemcen, (2014).
- [24] G R Jonest, L Zzidong, A Anastasaki, Rapid Synthesis of Well-Defined Polyacrylamide by Aqueous Cu(0)-Mediated Reversible-Deactivation Radical Polymerization, *Macromolecule*, 49 :483–489 (2016).
- [25] polymer properties data base, Free Polymer Information Source.
- [26] Polyacrylamide Basic information, chemical book,
- [27] H Zheng, J Ma , F JI , X Tang , W Chen , J Zhu , et al, Synthesis and Application of Anionic Polyacrylamide in Water Treatment, *Asian Journal of Chemistry*, 25(13) : 7071-7074 (2013).
- [28] J. Xu, W. P. Zhao, C. X. Wang, Y. M. Wu, Preparation of cationic polyacrylamide by aqueous two-phase polymerization, *express Polymer Letters* Vol.4(5) : 275–283, (2010).
- [29] K E Lee , B T Poh, M Norhashimah, T.T Teng, Synthesis and Characterization of Hydrophobically Modified Cationic Acrylamide Copolymer, *international journal of polymer analysis and characterization*, 13(2) :95-107 (2008).

[30] A Mansri, L Tennouga, Neutralization degree effect on viscosimetric behaviour of hydrolyzed polyacrylamide-poly(4-vinylpyridine) [AD37-P4VP] mixture in aqueous solution J Desbrières. *Polymer Bulletin* 61, 771–777 (2008)

[31] M Mandel, T Odijk , dielectric properties of polyelectrolyte solution, *Ann Rev Phys Chem* ,35 :75 (1984).

chapter II

Experimental techniques

Our study focuses on the preparation of nanocomposites based on polyacrylamide and bentonite in aqueous suspension. The suspension was obtained by mixing bentonite and acrylamide in double-distilled water. Followed by radical polymerization with ammonium persulfate as initiator was carried out by adiabatic processes. Our samples obtained is characterized by different techniques DRX, SEM, DSC, EDS, M Ind , N ind, instrumentation and method used are described and detailed in this chapter.

II-1 X-RAY DIFFRACTION :

II-1-1 Definition of XRD

X-ray diffraction is a powerful nondestructive technique for characterizing crystalline materials. It provides information on structure, phases, preferred crystal orientations (texture), and other structural parameters, such as average grain size, crystallinity, strain, and crystal defects [1].

It has been used extensively to measure lattice constant of a variety of crystalline materials [2].

XRD peaks are produced by constructive interference of a monochromatic beam of X-rays scattered at specific angles from each set of lattice planes in a sample. The peak intensities are determined by the atomic positions within the lattice planes. Consequently, the XRD pattern is the fingerprint of periodic atomic arrangements in a given material. An online search of a standard database for X-ray powder diffraction patterns enables quick phase identification for a large variety of crystalline samples [1].

II-1-2 : Bragg's law :

X-ray diffraction is based on Bragg's law :

$$n\lambda = 2d.\sin\theta. \quad (\text{II-1})$$

A monochromatic beam of X-rays is allowed to incident on a sample, and reflected X-rays are detected by a detector. X-ray diffraction pattern is a characteristic of the substance under investigation [3]. Otherwise, When a crystal is bombarded with X-rays of a fixed wavelength (similar to spacing of the atomic-scale crystal lattice planes) and at certain incident angles, intense reflected X-rays are produced when the wavelengths of the scattered X-rays interfere constructively. In order for the waves to interfere constructively, the differences in the travel path must be equal to integer multiples of the wavelength. When this constructive interference occurs, a diffracted beam of X-rays will leave the crystal at an angle equal to that of the incident beam [4].

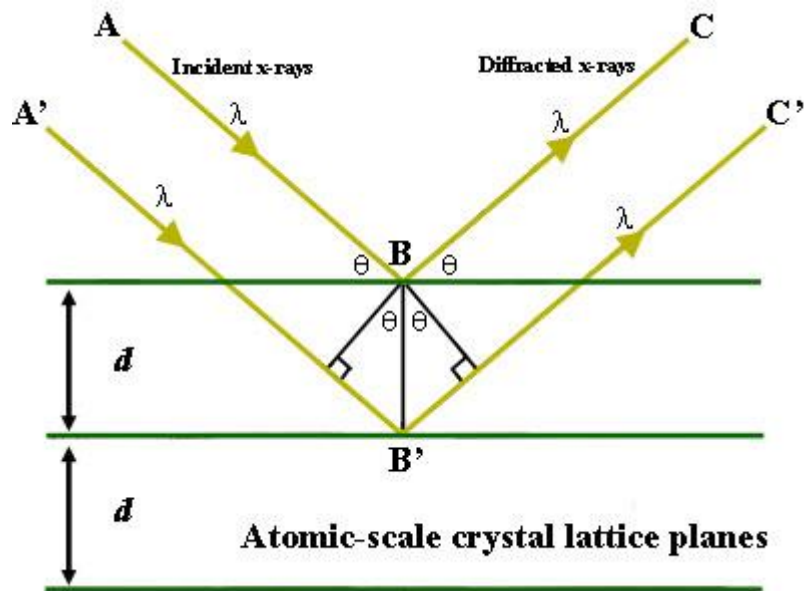


Figure II.1. Bragg's Law reflection. The diffracted X-rays exhibit constructive interference when the distance between paths ABC and A'B'C' differs by an integer number of wavelengths (λ).

X-ray diffraction technique is useful in determining the percent crystallinity in the natural fibers before and after physical or chemical treatment. Generally, X-ray diffractogram of the sample is recorded on an X-ray diffractometer operating at known voltages and current using a Cu K α X-rays ($\lambda = 0.15406$ nm) over the 2θ range from 10 to 100 degrees in the steps of 0.01 degree at room temperature in open quartz sample holders. Amorphous regions of the samples produce broad peak, whereas crystalline regions produce sharp peaks. The degree of crystallinity (X_c) can be determined by determining the intensities of the crystalline (I_c) and amorphous (I_a) contents in the sample [3]:

$$X_c = \frac{I_c}{I_c + I_a} \quad (\text{II-2})$$

II.2. SCANNING ELECTRON MICROSCOPE SEM « MEB »

(SEM) is one of the most widely used instrumental methods for the examination of microstructure, morphology of the materials [5]. This instrument may also be used in conjunction with other related techniques of energy-dispersive X-ray microanalysis (EDX, EDS, EDAX), for the determination of the composition or orientation of individual crystals or features [6].

II-2-1 SEM principle

An electron source also referred to as an electron gun emits electrons that get accelerated by an applied voltage. Magnetic lenses converge the stream of electrons into a focused beam, which then hits the sample surface in a fine, precise spot. The electron beam then scans the surface of the specimen in a rectangular raster. The user can increase the magnification by reducing the size of the scanned area on the specimen. Detectors collect the backscattered and secondary electrons (SE). The corresponding signals are measured and the values are mapped as variations in brightness on the image display. The secondary electrons are more frequently used as read-out signal. They highlight the topography of the sample surface: bright areas represent edges while dark regions represent recesses. light microscopes [7]. In a scanning electron microscope (Benchtop SEM- JCM 6000 - Jeol, Leica DM Inverted Research Metallurgical Microscope, Kruss - MSZ 5600, Kruss - MMB 2300, Zeiss - Axio Scope A1), the image is obtained sequentially point by point by moving the primary electron beam on the surface of sample. Microstructure and macrostructure imaging of a sample in mode transmission or reflection provides valuable information about the samples metallurgical, biological and geological. Samples can grow up to 1000imes. Processing in optical analyzer and application of polarization of light also provide respected data on the performance of microscopes optics. Scanning electron microscopy (Jeol SEM tray) is capable of to enlarge a sample to 60,000 [8].



Figure II .2 : Benchtop SEM- JCM 6000 - Jeol, Leica DM Inverted Research Metallurgical Microscope, Kruss - MSZ 5600, Kruss - MMB 2300, Zeiss-Axio Scope A1 [9]

II-3 DIFFERENTIAL SCANNING CALORIMETRY DSC

II-3-1: DSC definition

Calorimeters are used frequently in chemistry, biochemistry, cell biology, biotechnology, pharmacology, and recently, in nanoscience to measure thermodynamic properties of the biomolecules and nano-sized materials. Amongst various types of calorimeters, differential scanning calorimeter (DSC) is a popular one [10], Differential scanning calorimetry is a thermoanalytical technique used to study and quantify the thermal phenomena (endothermic or exothermic) which accompany a change in physical state such as a structural change or chemical reaction. Cast iron of a crystalline polymer or the glass transition [11, 12,8]. The instrument used in our work is shown in figure I-10.



Figure II.3: DSC instrument Pyris 6 de Perkin Elmer [9]

II-3-2- Detection of phase transitions

The basic principle underlying this technique is that, when the sample undergoes a physical transformation such as phase transitions, more or less heat will need to flow to it than the reference to maintain both at the same temperature. Whether less or more heat must flow to the sample depends on whether the process is exothermic or endothermic. For example, as a solid sample melts to a liquid it will require more heat flowing to the sample to increase its temperature at the same rate as the reference. This is due to the absorption of heat by the sample as it undergoes the endothermic phase transition from solid to liquid. Likewise, as the sample undergoes exothermic processes (such as crystallization) less heat is required to raise the sample temperature. By observing the difference in heat flow between the sample and reference, differential scanning calorimeters are able to measure the amount of heat absorbed

or released during such transitions. DSC may also be used to observe more subtle phase changes, such as glass transitions. It is widely used in industrial settings as a quality control instrument due to its applicability in evaluating sample purity and for studying polymer curing [13].

II -3-3 DSC curves

The result of a DSC experiment is a curve of heat flux versus temperature or versus time. This curve can be used to calculate enthalpies of transitions. This is done by integrating the peak corresponding to a given transition. It can be shown that the enthalpy of transition can be expressed using the following equation:

$$\Delta H = KA \quad (II-3)$$

where ΔH is the enthalpy of transition, K is the calorimetric constant, and A is the area under the curve. The calorimetric constant will vary from instrument to instrument, and can be determined by analyzing a well-characterized sample with known enthalpies of transition [13].

Interpretation of Dsc curves

The computer traces the difference between the heats of the two containers according to the temperature, ie the heat absorbed by the polymer as a function of the temperature. The curve is that given below, figure II.4.

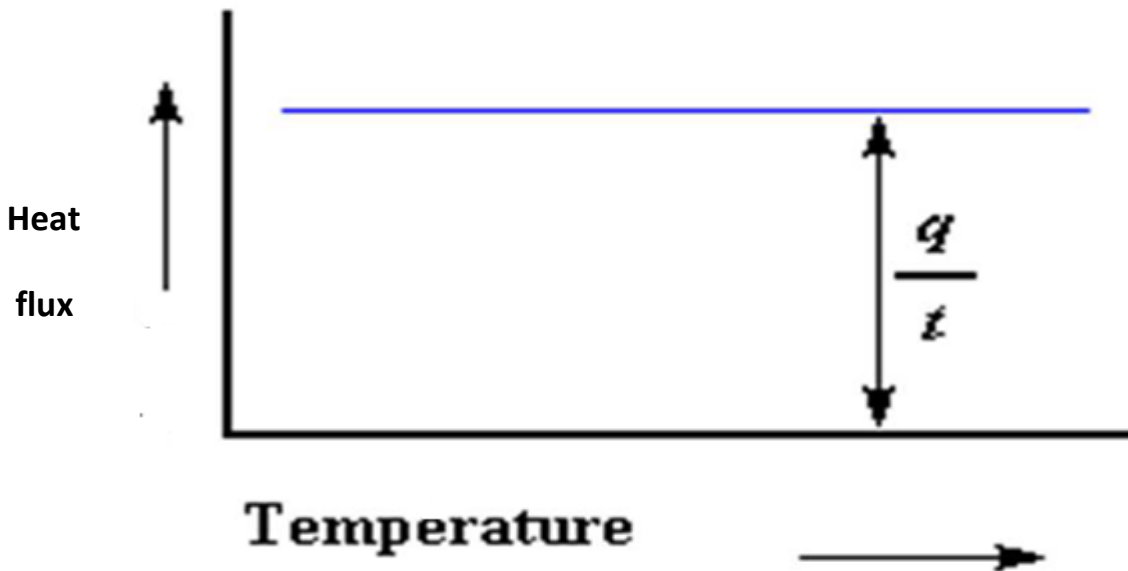


Figure II .4: Heat flux as a function of temperature

The heat flux is given in units of heat q per unit of time t . The speed of heating is the increase T in temperature per unit of time t [8].

$$\frac{\text{heat}}{\text{time}} = \frac{q}{t} = \text{heatflux} \quad (\text{II-4})$$

$$\frac{\Delta T}{t} = \text{heatingspped} \quad (\text{II-5})$$

By dividing the heat flow q / t by the heating rate $\Delta T / t$, we obtain the quantity of heat defined as the heat capacity C_p found in the DSC curve.

$$\frac{\frac{q}{t}}{\frac{\Delta T}{t}} = \frac{q}{\Delta T} = C_p = \text{heatcapacity} \quad (\text{II-6})$$

The melting of a polymer is detected by the presence of an endothermic peak on the thermogram, Figure II.5.a (curve of the calorimetric analysis as a function of temperature). Crystallization leads to the reverse process, namely the formation of a exothermic zone [8]. , Figure II.5.b.

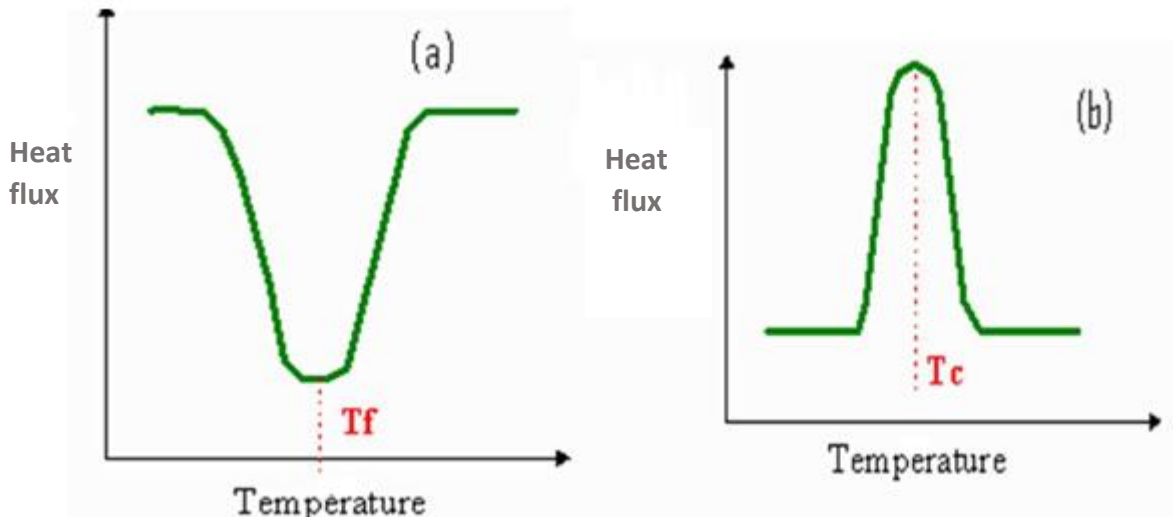


Figure II.5 : Thermogram (a) of endothermic transformation and (b) of exothermic transformation.

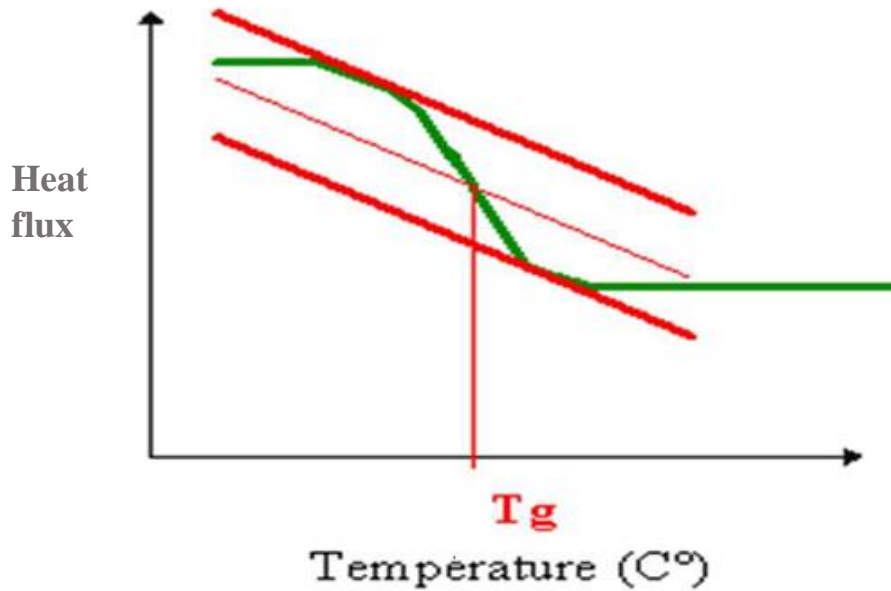


Figure II.6 : thermogram of glass transition

The DSC curve provide other information on the polymer such as glass transition (T_g) Figure II-13. The glass transition temperature, denoted T_g , is conventionally defined as the temperature at the inflection point of the setback presented by the thermogram; this setback is interpreted as a specific heat jump, that is to say a variation of the heat capacity C_p [11-12].

II.4. ADIABATIC PROCESS

II-4-1. Adiabatic process definition

In thermodynamics, an **adiabatic process** is a type of thermodynamic process which occurs without transferring heat or mass between the system and its surroundings. Unlike an isothermal process, an adiabatic process transfers energy to the surroundings only as work [14 ;15].

Kinetic laws of the adiabatic polymerization of acrylamide have been established by obeying the following assumptions [16]:

- Monomer and polymer have the same heat capacities ($0.5 \text{ cal / mol. } ^\circ \text{C}$).
- No loss of water by evaporation.
- Any heat produced is the result of increasing the temperature of the mixture.

The temperature rises rapidly under these conditions due to the heat of the polymerization which remains in the interior environment without heat exchange with the environment outside [16].

II-4-2-The adiabatic reactor

A reactor operates in adiabatic mode when it does not exchange heat with $\Delta Q = 0$. It results from it that the heat of the external environment. The thermal transfer is null: absorbed or given off by the reaction is taken or given up to the reaction medium itself, which cools or heats up in proportion to the progress of the reaction.

The acrylamide was polymerized in an adiabatic reactor, which consists of a receive aluminum with a very thin internal organic coating layer [17]. It is equipped with a heating element to increase the temperature of the contents above the initial temperature (30 ° C), coated with a thick layer of polyurethane foam, its outer surface is covered by aluminum.

Figure I.5 shows a model of an adiabatic reactor. The adiabatic reactor (A) contains stainless steel walls and a stirring blade. Compartment (B) is provided an internal heating element to control the temperature of the contents.

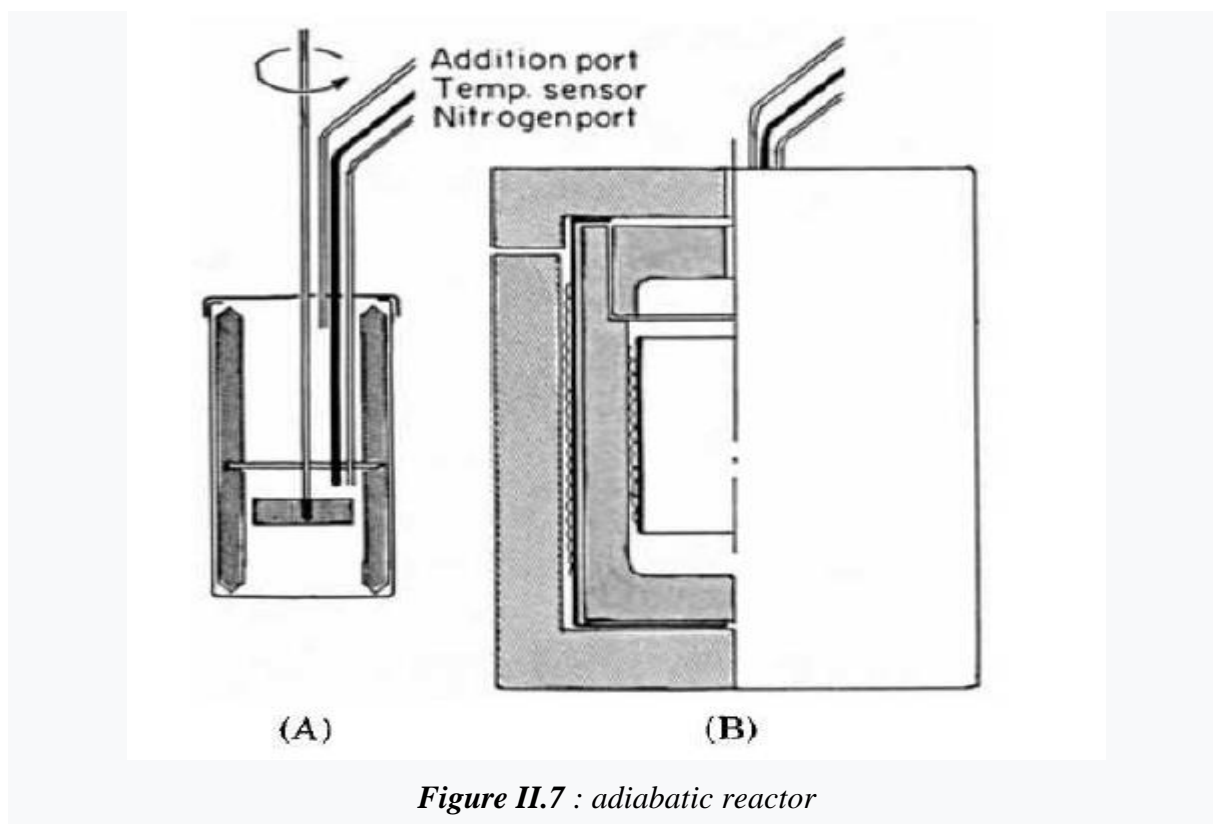


Figure II.7 : adiabatic reactor

II-4-3 Adiabatic polymerization

The Potential risks associated with thermal behavior of chemicals processes require a stability study, which must be performed before performing the reaction, to ensure process safety.

An uncontrolled self-heating process during a chemical reaction can cause a thermal explosion. In general, the majority of accidents that occur during a reaction are due to human error or lack of security measures. In addition, it is known that polymerization reactions are characterized by high exothermicity and a self-accelerating kinetics, which makes the system studied in a situation difficult to control. Several types of monomers such as acrylamide, acrylate and methacrylate are, in general, highly reactive and give off great heat which leads to sudden increase in pressure during their polymerization. Therefore, a reaction polymerization can cause considerable damage if the measurements are not taken of security. After analyzes and developments of some accidents caused by exothermic reactions, it has been found that most of the mistakes made by the experimenter are due to the poor understanding of the chemistry of the reaction studied and the poor structure of the reactors used [18].

For better protection and to avoid damage caused by reactions exothermic, it is advisable to use an adiabatic reactor which serves to conserve the reaction mixture in an isolated environment from the outside.

Adiabatic calorimetry is a technique that was introduced as a measurement important to avoid the risk of an exothermic chemical reaction [19].

Polymerization of acrylamide is often carried out under conditions adiabatic. Several theoretical and experimental studies have been devoted to studying the kinetics of this reaction [20].

Adiabatic polymerizations are carried out in order to prepare polymers of high molecular weight. In the case of concentrated acrylamide solutions, there is a sudden increase in viscosity which leads to the formation of insoluble products in water because of intermolecular interactions, which poses enormous problems. This phenomenon is known as: Trommsdorf effect or gel effect. All of these complications can be largely avoided by carrying out the polymerization in a diet

adiabatic where the temperature rises remarkably because of the heat of the polymerization and the process is characterized by low viscosity, which increases the flexibility of macromolecules, reduce intermolecular interactions and make the polymerization of concentrated solutions of acrylamide possible.

Adiabatic polymerization usually takes place in a special reactor called "Dewar", it is equipped with an agitator, an inert gas stream and a thermometer.

A. Mansri et al., [21] studied the adiabatic radical copolymerization in aqueous solution of acrylamide (AM) and 4-vinylpyridine (4VP). Measurement by conductimetry has shown that the acrylamide copolymerization exhibits functions hydrolyzed and that the variation of the surface tension of copolymers in solutions aqueous solutions revealed a surfactant behavior of the copolymer. The result obtained was compared to that of a model surfactant which is N-dodecyl-pyridinium chloride (DPC).

Ferdinand et al. [22] studied the adiabatic photopolymerization of acrylamide. They used a redox couple as an initiation system, and UV light to initiate the reaction. This method makes it possible to produce polymers of large molecular masses, but the disadvantages of this method lie in the difficulty of carrying out the assembly reaction and the unsatisfactory purity of the polymers obtained.

The adiabatic polymerization technique was used by Bruno et al. [23] for prepare the hydrophobic associative polyacrylamides, they made a copolymerization micellar acrylamide and N-octadecylacrylamide. The duration of this reaction is long, it lasts 8 hours when the temperature increases from 14 to 85 ° C.

In our case, we will try to carry out the adiabatic polymerization of acrylamide with BC at different percentage in weight.

II- 5 INDENTATION TECHNIQUES:

II-5-1 Micro indentation techniques

II-5-1-1 Micro indenter test

The micro-indenter is an instrument that determines parameters related to the compression modulus of a material.

The measurement is non-destructive, fast and carried out at room temperature on flat materials such as polymers and metals, or on coatings such as varnishes, paints and metallic deposits

The Micro Indenter can be used for measurement of:

- Micro-indentation, micro-hardness
- Micro-impact and fatigue
- Micro scratch and wear

These tests can be done at high temperature (max 800°C) or in inert environments. While, an optical microscope is associated to the micro tester, it can be used for precise positioning of indentations [24].

II-5-1-2 Micro indentation working principles

Micro hardness testing still employs indentation to probe the surface of a sample and measure the resulting impression. The principles vary from test-to-test, but – typically – a sample is placed on a piezo-driven stage and positioned below a diamond-tipped indenter and a calibrated optical microscope with built-in imaging. Once in position, the indenter is pressed into the surface up to a pre-defined load where it dwells for a pre-defined period. Various material characteristics can be extrapolated from the subsequent impression made in the surface. The microhardness can be determined using directly the indentation imagery registered in the microscope. Otherwise, indentations on the samples are marked in the Ordinator in order to calculate the hardness values [25].

II-5-1-3 Micro hardness

Hardness H is an essential mechanical property that basically defined as a measure of the resistance of materials to contact load applied. H is obtained by dividing the peak contact load P and the projected area of impression A [26,27].

This impression, A, is often, of the order of 10-100 squared microns. That's why, the experimental values of H are commonly referred to as ‘microhardness’[28]

Micro indentation tests are the most widely used in determining materials microhardness [29]. This method is easy, quick, and requires only a tiny area of specimen surface for testing [29]. Because of its simplicity, it has become a common technique to explain the micromechanical behavior of polymers composites and its correlation with microstructure. [30] This technique involves the formation of permanent impression, with a diamond indenter ((a Knoop or a Vickers) after loading the surface of the material for a certain period of time [31]. After load removal, diagonals of the indentation can be measured with an optical microscope. Then the Knoop or Vickers hardness of materials is calculated using these equations:

$$HK = 14230 (P/d^2) \quad (II-7) \quad \text{for Knoop microhardness}$$

Or

$$HV = 1854 (P/d^2) \quad (II-8) \quad \text{for Vickers microhardness}$$

The constant value of each equation is calculated from the specific geometry of the indenter; P represents the indentation load (g), and d the diagonal of the indentation (μm).

Generally, 10 imprints should be taken in order to calculate H value and the error for the H-values could be estimated by means of

$$\delta H = \frac{2\Delta d}{d} [32,33] \quad (\text{II-9})$$

- parallel H values ($H_{//}$) and perpendicular (H_{\perp}) to the indented surface sample is measured using equation 1. The indentation anisotropy (ΔH) was calculated from the relation (2):

$$\Delta H = 1 - (H_{\perp} / H_{//})^2 \quad (\text{II-10})$$

II-5-1-4 Instrumentation used

Micro-indentation tests were performed with a Leica VMHT MOT tester with a square diamond base, indenter speed $45 \mu\text{m/s}$, indentation time fixed at 6s, 20, 99 s and load 250 mN. Ten measurements were taken in order to calculate the micro-hardness.



Figure II.8 : Leica VMHT MOT micro indenter

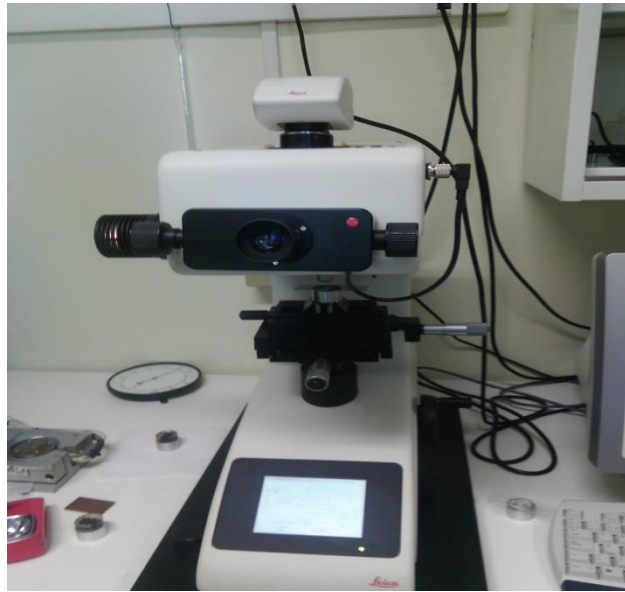


Figure II.9 : microscope associated to the micro indenter.

II-5-2 Nano indentation techniques

II-5-2-1 Definition of nanoindentation technique

Nano indentation has emerged as a critical technique for the evaluation of the mechanical response of small material volumes and thin films or layers to applied loading [34, 35]. It is generally called as, the depth sensing indentation or the instrumented indentation, this technique allows the measurement of the depth of an indenter with known geometry on the surface materials [36,37]. It's meaning that, the profundity of penetration into the specimen surface is measured and combined with the identified geometry form of the indenter to calculate the contact area. The load and unload curves during the indentation practice were described by Ciprari and Van Landingham [38, 39].

II-5-2-2 Nanoindenter Working Principles

At the heart of a nanoindenter is a small probe loaded with a calibrated indenter tip, which may be pyramidal, flat, spherical, wedged, or some other shape. This is used to interrogate the surface of a material and measure the subsequent force-displacement data.

Conventional nanoindenters are typically load-controlled instruments where the tip is brought into contact with the surface under a pre-defined load. Once the nanoindenter has contacted the sample, the load is increased and the tip indents into the material. The area of contact between the tip and the sample, the applied force of the nanoindenter, and the depth of displacement are subsequently used to determine the material's mechanical properties. The disadvantages of a load-controlled system become obvious when doing compression tests on small structures (e.g., micropillars, 3D structures, etc.) where the load feedback loop cannot

cope with sudden displacement excursions. In such cases, nanoindentation measurements using displacement control are far superior.

Traditionally, the size and depth of the residual indentation imprint is taken to calculate the material hardness. This is characterized according to one of several indentation hardness scales, including the Vickers and Brinell scales. Nanoindenters have proven valuable for microhardness testing where samples are small or thin, and they have also demonstrated unique performance for measurements where the microstructural properties of a sample are complex or are non-homogenous [40].

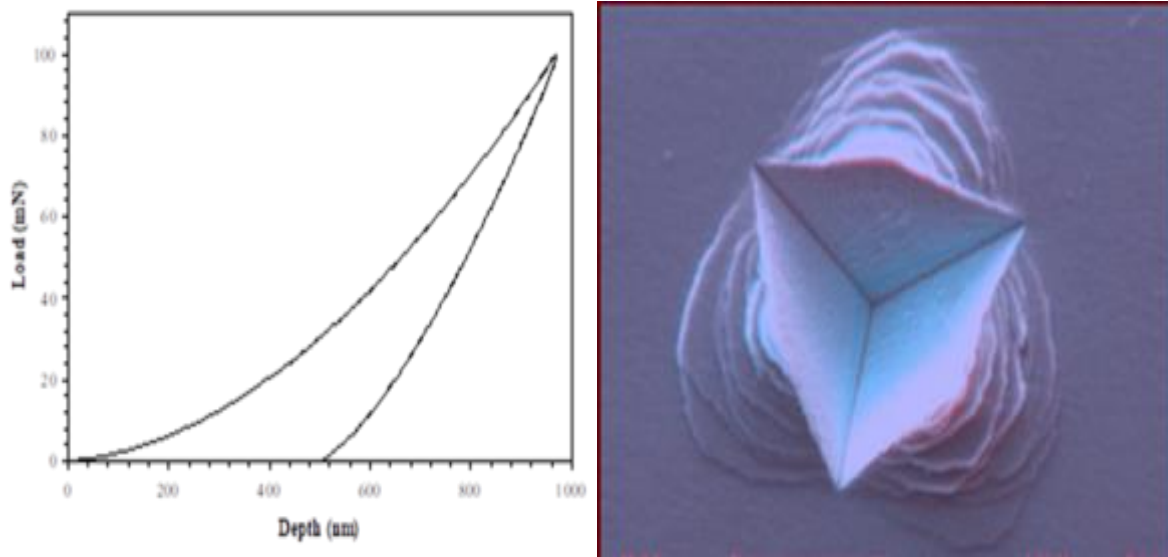


Figure II.10 : Typical example of a nanoindentation load-depth curve (left) and corresponding residual indent (right) Nano hardness [40]

II-5-2-3 Nanohardness test

The hardness and elastic modulus can be resulting via the method developed by (Loubet et al. 1984, Doerner and Nix 1986, Oliver and Pharr 1992) [41-42-43]. The basic equations to determine the hardness, H and modulus, E are:

$$H = \frac{P_{max}}{A} \quad (II-11)$$

Where P_{max} is the peak indentation load and A is the projected contact area at maximum load,

$$E_r = \frac{1}{2} \frac{dp}{dh} \sqrt{\frac{\pi}{A}} \quad (II-12)$$

Where E_r is the reduced elastic modulus.

$$\frac{1}{E_r} = \frac{(1-\nu_s)^2}{E_s} + \frac{(1-\nu_i)^2}{E_i} \quad (II-13)$$

Where, E_r is the reduced modulus, ν_s the Poisson's ratio for the sample (The estimated value of semi crystalline polymeric materials is 0.35 [44, 45]), ν_i the Poisson's ratio for the indenter (for diamond 0.07), E_s the elastic modulus for the sample and E_i the elastic modulus for the indenter

(1141 GPa are often used for a diamond) [46]. By rearranging Eq. (II-13), we obtained elastic modulus (young's modulus) of the sample expression (4):

$$E_s = \frac{1 - \nu_s^2}{\frac{1}{E_r} - \left(1 + \frac{\nu_i^2}{E_i}\right)} \quad (\text{II-14})$$

Polymers and polymers nano-composites are often employed in products because of their ability to both store and damp energy. The complex modulus (E^*) is a phase vector which incorporates both of these capacities [47-49]:

$$E = E' + iE'' \quad (\text{II-15})$$

The real part (E') of the complex modulus is called the storage modulus because it quantifies the material's ability to store energy elastically. In materials with insignificant damping, the storage modulus is equivalent to Young's modulus. The imaginary part of the complex modulus (E'') is called the loss modulus, because it quantifies the material's ability to damp out energy. The tangent of the vector angle, $\tan\delta$, is the ratio of the imaginary part (E'') to the real part (E') [47]. This quantity is called the "loss factor" (LF):

$$LF \equiv \tan\delta = \frac{E''}{E'} \quad (\text{II-16})$$

II-5-2-4 Instrumentation used

A Keysight G200 nano indenter was used to obtain nano hardness and storage modulus data. Maximum indentation depth was 5 μm , surface approach velocity was 10 nm/s, strain rate target 0,05 s^{-1} , frequency 45-50Hz and temperature 25-26°C.



Figure II.11 : Keysight G200 nano indenter

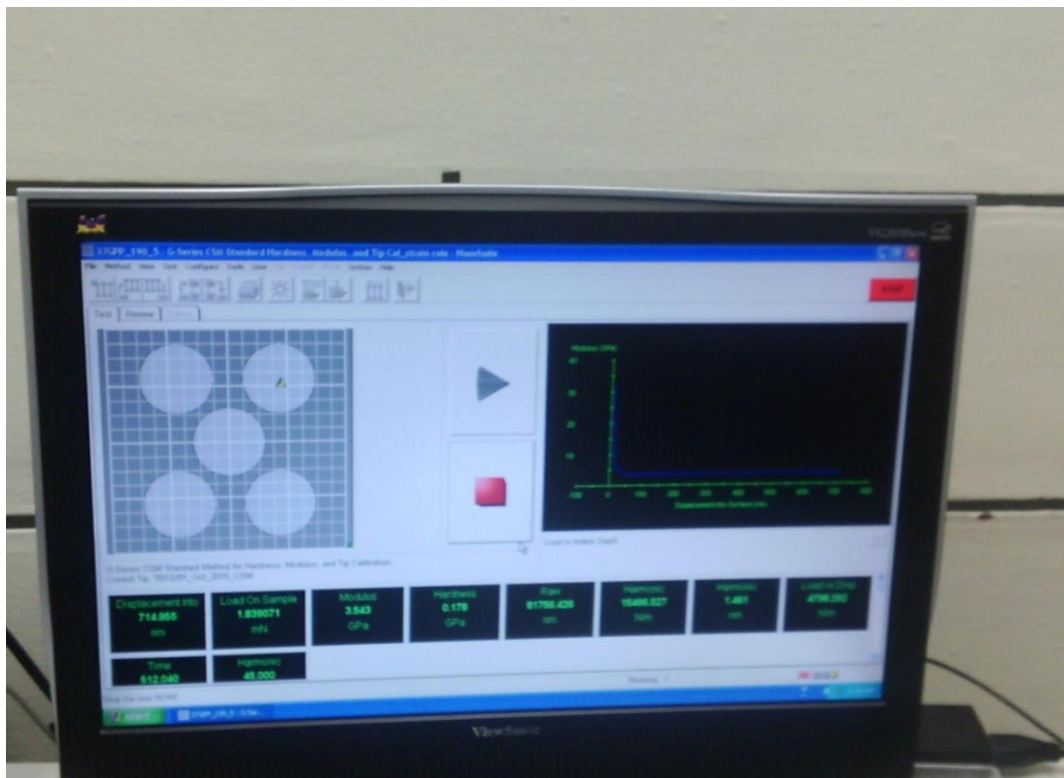


Figure II.12 : capture of indeter calculation during test

References

- [1] E Rajiv Kohli, K L Mittal, Chapter 3 - Methods for Assessing Surface Cleanliness, Methods for Assessment and Verification of Cleanliness of Surfaces and Characterization of Surface Contaminants, 12 : 23-105(2019).
- [2] M Belyansky, Chapter 8 - Thin Film Deposition for Front End of Line: The Effect of the Semiconductor Scaling, Strain Engineering and Pattern Effects, 4 ED : 231-268(2018).
- [3] J P Patel, P H Parsania, Characterization, testing, and reinforcing materials of biodegradable composites, in : Biodegradable and Biocompatible Polymer Composites, 1: 55-79 (2018).
- [4] G N Eby, Principles of Environmental Geochemistry. Brooks/Cole-Thomson Learning, 1 :212-214 (2004).
- [5] M Omid, D Vashae, Characterization of biomaterials, in : Biomaterials for Oral and Dental Tissue Engineering , 1: 97-115 (2017).
- [6] N Raval,R Maheshwari , Chapter 10 - Importance of Physicochemical Characterization of Nanoparticles in Pharmaceutical Product Development, 1 :369-400 (2019).
- [7] F Fernandez, Université de Montpellier, Microscopie Électronique et analytique.
- [8] A Mansri, Composites à base de copolymères et de bentonite pour la rétention des polluants et pour l'inhibition de la corrosion, University Usto Oran, (2016).
- [9] W Bensalah,Gels à base d'acrylamide et de 4-VP -Application à la libération contrôlée des molécules organiques, UABB Tlemcen,(2019).
- [10] P Gill, T Tohidi Moghadam, BRanjbar, J Biomol, Differential Scanning Calorimetry Techniques: Applications in Biology and Nanoscience, 21(4): 167–193, (2010).
- [11] F Dergal, A Mansri, L Billon, Chemical Engineering Transactions. 32 : 2131-2136, (2013).
- [12] G Schwedt, dans Atlas de poche des méthodes d'analyse, Medecine-Sciences, Edition Flammarion, (1993).
- [13] DSC literature.
- [14] C Caratheodory, Untersuchungen über die Grundlagen der Thermodynamik, Mathematische Annalen. 67 (3): 355–386. (1909). .
- Tr : J Kestin, The Second Law of Thermodynamics. Stroudsburg, PA: Dowden, Hutchinson & Ross, (1976).
- [15] M Bailyn, A Survey of Thermodynamics. New York, NY: American Institute of Physics Press, 21(1994).

- [16] B Bouras , Nouveaux Copolymère Respoly(acrylamide-co-4-vinylpyridine)-propriétés Et Applications, UABB Tlemcen, (2014).
- [17] A K Theresa, R. Ferdinand, Polymerization of acrylamide using the hydrogen peroxide–hydroxylamine couple, *Journal of applied Polymer Science*, 28: 633, (1983).
- [18] G Maschio, J A Feliu, J Ligthart, I Ferrara et al, The Use of Adiabatic Calorimetry for the Process Analysis and Safety Evaluation in Free Radical Polymerization, 14: 233, (1987).
- [19] A K Nandi, V B Sutar, et al . Thermal hazards evaluation for sym-TCB nitration reaction using thermal screening unit (TSU). *Journal of Thermal Analysis and Calorimetry* 76, 895–901 (2004).
- [20] A M Ross, K O Chin, M. R. Christine, M. H. John, *Makromol. Chem.*, 184: 1885, (1983).
- [21] A Mansri, B Bouras ,B., T Hocine, *Moroccan Journal of Chemistry*, 5(1):24-34, (2017).
- [22] R. Ferdinand, H. C. Connie, K. C. Wayne, A. R. Mary, *Journal of Applied Polymer Science*, 30: 1629(1985).
- [23] B. Grassl, Z. Zhu, O. Jian, S. Paillet, J. Desbrières, *Eur. Polym. J.*, 43: 824, (2007).
- [24] *Micro Hardness Testing: Principles & Applications*, july (2020).
- [25] <https://alemnis.com/what-is-a-nanoindenter/july> (2019)
- [26] L A Shreiner, the hardness of brittle solids, (ogiz, Leningrad-moscow, (1949) .
- [27] D Tabor, the hardness of metals ,oxford c press, new York (1951).
- [28] F j balta calleja, D s sanditov, V P Privalko, Review: the microhardness of non crystalline materials,, *journal of material science* 37:4507-4516, (2002).
- [29] C Chuenarrom; P Benjakul, P Daosodsai, Effect of indentation load and time on knoop and vickers microhardness tests for enamel and dentin *Mat. Res*,12 :.4 (2009).
- [30] S Fakirov, F J Balta Calleja , M Krumova, On the relationship between microhardness and glass transition temperature of some amorphous polymers, *journal of polymer science part B polymer physics*, 37:1413-1419 (1999).
- [31] F J Balta calleja and H G Kilian, Microhardness of semicrystalline polymers.
- [32] M.F. Mina, G.H. Michler, F.J. Baltá-Calleja, *Journal of Bangladesh Academy of Sciences* , 33:15 (2009)
- [33] F Ania, G. Broza, M.F. Mina, K. Schulte, Z. Roslaniec, F.J. Baltá-Calleja, *Composite Interfaces*, 13: 33 (2006)

- [34] DA Lucca, K Herrmann , MJ Klopstein, *Nanoindentation: Measuring methods and applications*. *Cirp Annals* 59: 803-819 (2010).
- [35] JB Vella, I S Adihetty, K Junker, AA Volinsky , *Mechanical properties and fracture toughness of organo-silicate glass (OSG) low- k dielectric thin films for microelectronic applications*. *International Journal of Fracture* 120: 487-499, (2003).
- [36] D Kyung Kim, *Korea Advanced Institute of Science and Technology*, 2007.
- [37] A R Franco Jr, G. Pintaúde, A. Sinatora, C.E. Pinedo, A.P. Tschitschin, *Materials Research*, 7, 483 (2004).
- [38] X Zhi-Hui, *Doctoral Dissertation, Department of Materials Science and Engineering Royal Institute of Technology Stockholm, Sweden* (2004).
- [39] D L. Ciprari, *Master of Science in Materials Science and Engineering, Georgia Institute of Technology, November* (2004).
- [40] M.R Van Landingham, *J. Res. Natl. Inst. Stand. Technol.* 108-249 (2003).
- [41] J L Loubet, J. M. Georges, O. Marchesini, G. Meille, *Journal of Tribology*, 43: 106 (1984).
- [42] M F Doerner, W.D. Nix, *Journal of materials research*, 1: 601 (1986).
- [43] G M Pharr, W.C. Oliver, *Journal of materials research*, 7: 1565 (1992).
- [44] M Krumova, A. Flores, F.J. Balta Calleja, S. Fakirov, *Colloid and polymer science*, 280-591 (2002).
- [45] Y. Hu, L. Shen, H. Yang, M. Wang, T. Liu, T. Liang, J. Zhang, *Polymer testing*, 25:492 (2006).
- [46] H.N. Dhakal, Z.Y. Zhang, *Polymer Testing*, 25:846 (2006).
- [47] J. Hay, E. Herbert, *Experimental Techniques*, 37:556 (2013).
- [48] J M Antunes, L F Menezes, J.V Fernandes, *International Journal of Solids and Structures*, 44:2732 (2007).
- [49] S. Peter, E. Woldeesenbet, *Materials Science and Engineering*, A 494:179–187 (2008).



party II:

Experimental Studies

chapter III
nano structure and morphology
effect on the PAM/BC properties

III-1 : INTRODUCTION

To the best of our knowledge, we believe that the exfoliation of the system PAM/BC where the content of bleaching clay is under the amount of 1, 3, 5 wt% has not been investigated before.

The choice of lows BC content (1%, 3%, 5%) was taken place in order to study the influence of nano- structure and morphology of the composite in the mechanical and thermal properties of PAM/BC nanocomposite under percentage in weight of 5% BC . While, we have already shown, if we exceed this value, the comporment and properties of our material was completely changed with load in weight of BC, this section, it is discuded in the chapter 4.

III-2 ELABORATION AND SYNTHESIS OF PAM/BC

In the present study, a new adiabatic process for the polymerization of acrylamide under neutral state is used. This technique can produce polymers under ultra-rapid kinetics and without exchanging energy with the external area. In this way, we expect to obtain exfoliated bentonite with new and unknown properties. It must be mentioned, however, that several theoretical and experimental studies have been devoted to study the kinetics of this reaction (adiabatic conditions) [1]. Ferdinard et al.studied the adiabatic photo polymerization of AM, a method used to produce high molecular weight materials.

We describe in this paper the polymerization method of PAM/BC, synthesized by adiabatic radical polymerization in an aqueous solution [2].

Furthermore and in order to examine the correlation between the morphology and the nano-structure with the mechanical properties of our materials, indentation tests at the micro- and the nano-scale have been performed. Accordingly, we investigated the variation of hardness and storage modulus of the nanocomposites with bentonite content. The prepared materials contain three different ratios in weight percent: PAM 99/BC 1, PAM 97/BC 3 and PAM95/BC 5.

III-2-1 Materials used

A sample of bentonite (BC) was supplied by a local company (ENOF), it was obtained from industrial treatment of natural clay issued from the field of Hammam Bougherara-Maghnia, Algeria, it is composed essentially of montomorillonite. The chemical composition of bentonite is shown in table III.1 [3].

Table III.1: Chemical composition of bentonite BC

Species	SiO ₂	Al ₂ O ₃	Fe ₂ O ₃	CaO	MgO	Na ₂ O	K ₂ O	TiO ₂	LOI
%(w/w)	65.2	17.25	2.10	1.20	3.10	2.15	0.60	0.20	8.20

III-2-2 Reagents

The acrylamide monomer compound was provided by Merck; ammonium persulfate (APS) was provided by Aldrich and was used without further purification.

III-2-3 Operator mode of polyacrylamide bentonite nanocomposites

Bentonite/acrylamide nanocomposites were obtained using an adiabatic process of radical polymerization (in-situ) in aqueous solution. The samples were prepared in the ratio of (1-5%:99-95%) in weight of bentonite/acrylamide and ammonium persulfate (APS) was used to propagate polymerization. The diameter of spherical bentonite particles was in the range between the micrometer and the nanometer scale.

At first x% of the bentonite suspension was stirred under a nitrogen atmosphere for 30 min, APS (0.2%) was stirred for 5 min, y % of AM dissolved in bi-distilled water was also stirred for 30-35 min after a fast heating. The AM and APS suspensions were added to the bentonite suspension and stirred for 20min.

The polymer obtained was dispersed in ethanol, filtered and dried under vacuum for 48h.

NB: The quantity of aps in percentage weight was fixed according the results found by bouras brahim in her work in doctorat thesis (table III.2 page 80) [3], in order to btain a maximum conversion rate of PAM/BC system.

Tableau III.2: quantities used in the preparation of PAM/BC nanocomposites.

Reactifs	AM (acrylamide)	BC	H ₂ O	(NH ₄) ₂ S ₂ O ₈
Percentage	95%	1%		0,2%
Percentage	50%		50%	
Quantities used	12,5 g	0,125 g	15ml	0.025

III-3 INSTRUMENTS AND CONDITIONS USED DURING TESTS

A JSM 6610 LA SEM instrument (Japan) was used to examine the morphology of our materials prepared with different percentage.

A differential scanning calorimetry (DSC) Perkin-Elmer DSC-7 was employed to measure the glass transition temperature T_g of the samples (calibration with indium, heating speed in the range of 10°C/ min to 20° C/min, samples mass fixed at 1 mg) [4].

A x-ray diffractometer, Cu α radiation ($\lambda = 1,541 \text{ \AA}$), was used in the continuous scan mode with scan step size of 0,0167 degrees and time per step 4,84 s [5].

Micro-indentation tests were performed with a Leica VMHT MOT tester with a square diamond base, indenter speed 45 $\mu\text{m/s}$, indentation time and load were respectively fixed at 6s and 500 mN. Ten measurements were taken for each sample in order to calculate the micro-hardness.

III-4. RESULTS AND DISCUSSION

III-4-1. SEM of polymer nanocomposites at different ratios of BC/AM

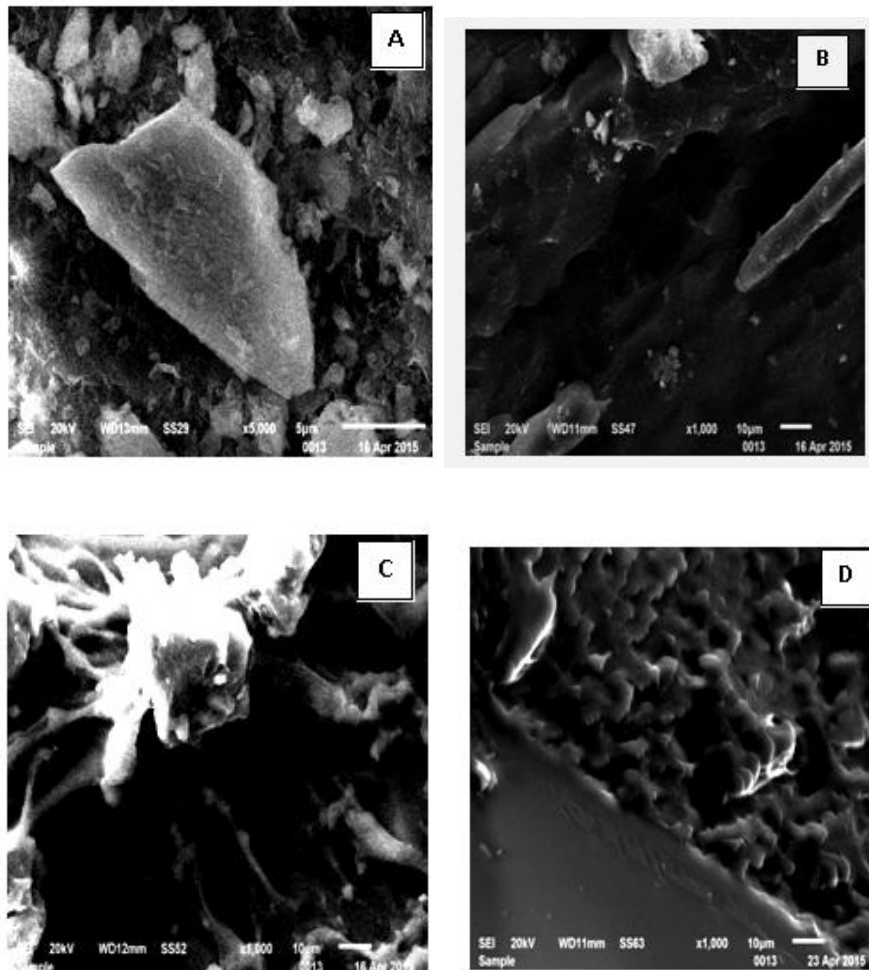


Figure III.1: SEM micrographs of (A): pure bentonite (magnification x5000)(B): PAM/BC 1% (x1000) (C): PAM/BC 3% (x1000) and (D): PAM/BC 5% (x1000)

Figure III.1 (A) shows the SEM micrograph of pure BC without polymer (5 μm scale bar) and using a voltage of 20kV.

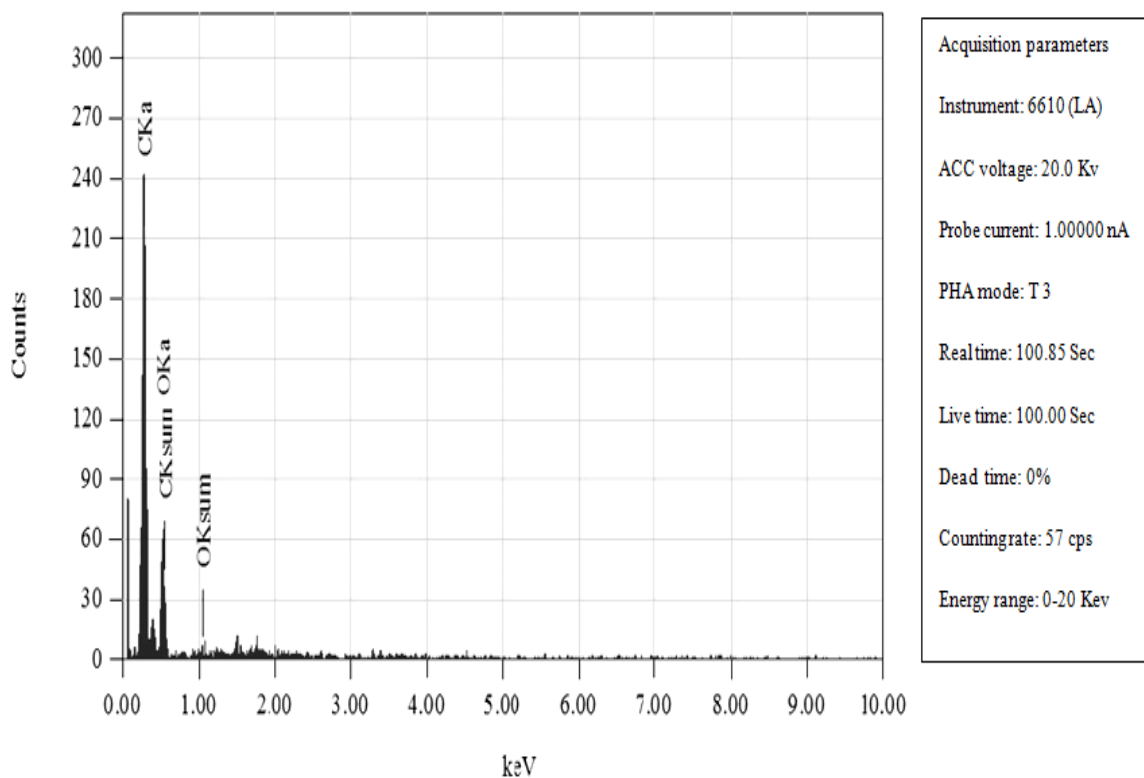
Figure III.1 (B) corresponds to the SEM micrograph of PAM99/BC1 (10 μm scale bar) and the same voltage as before. In the latter figure, it is noteworthy the existence of the clay aggregates and intercalated layers. Therefore, the morphology is heterogeneous, which reveals an intercalated/exfoliated structure (BC was partially exfoliated in this system). This kind of nano-structure has been confirmed by XRD analysis. The heterogeneity of this arrangement was related to the amount of BC and to a worse stirring.

Figure III.1 (C) represents the SEM image of PAM97/BC3 (10 μm scale bar), taken at a voltage of 20kV. In this figure, we clearly observed that the polymer is cross-linked with BC aggregates, which proves that the polyacrylamide PAM was not intercalated in BC gallery.

Figure III. 1 (D) shows a SEM image of PAM95/BC 5 (10 μm scale bar, voltage fixed at 20kV). A stacked BC layers on the matrix was observed in this structure.

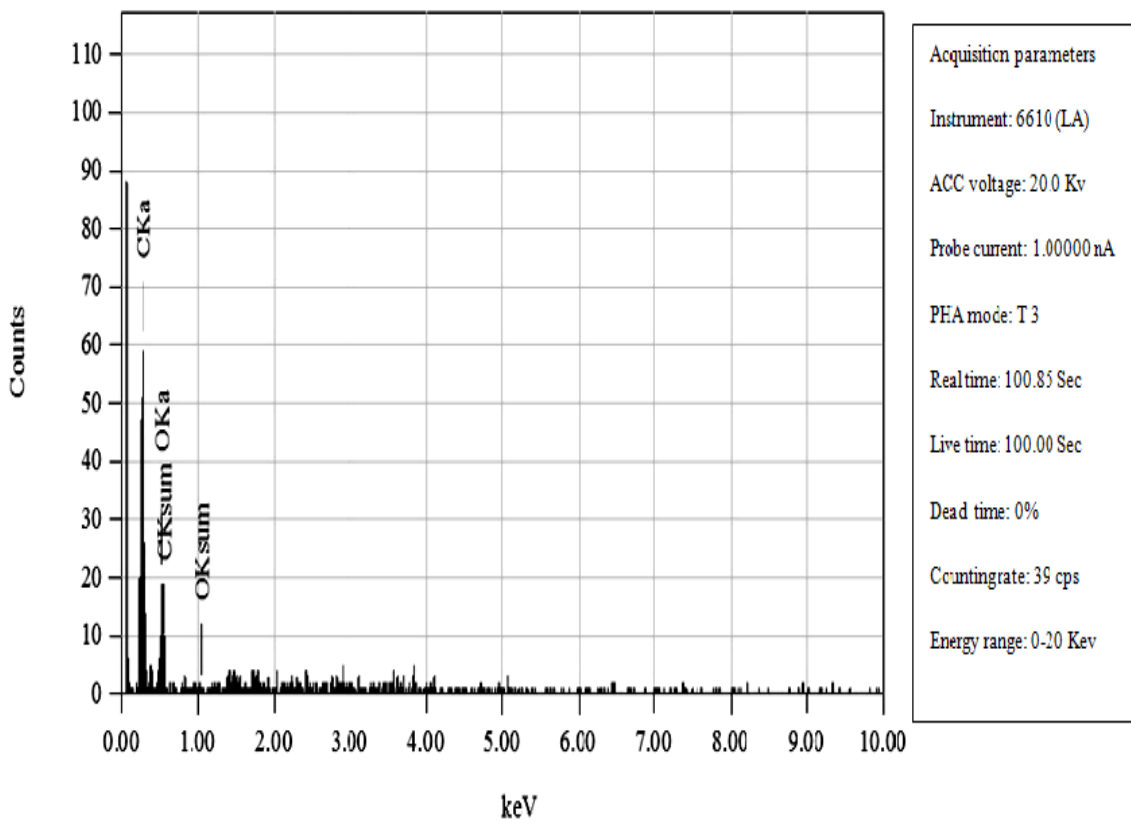
Energy Dispersive X-ray Spectroscopy (EDS) results, providing the elemental percent composition in each polymer nanocomposite, are collected in the following three table

Table III.3: EDS spectrum and elemental percent composition for the polymer composite prepared with 1% of BC.



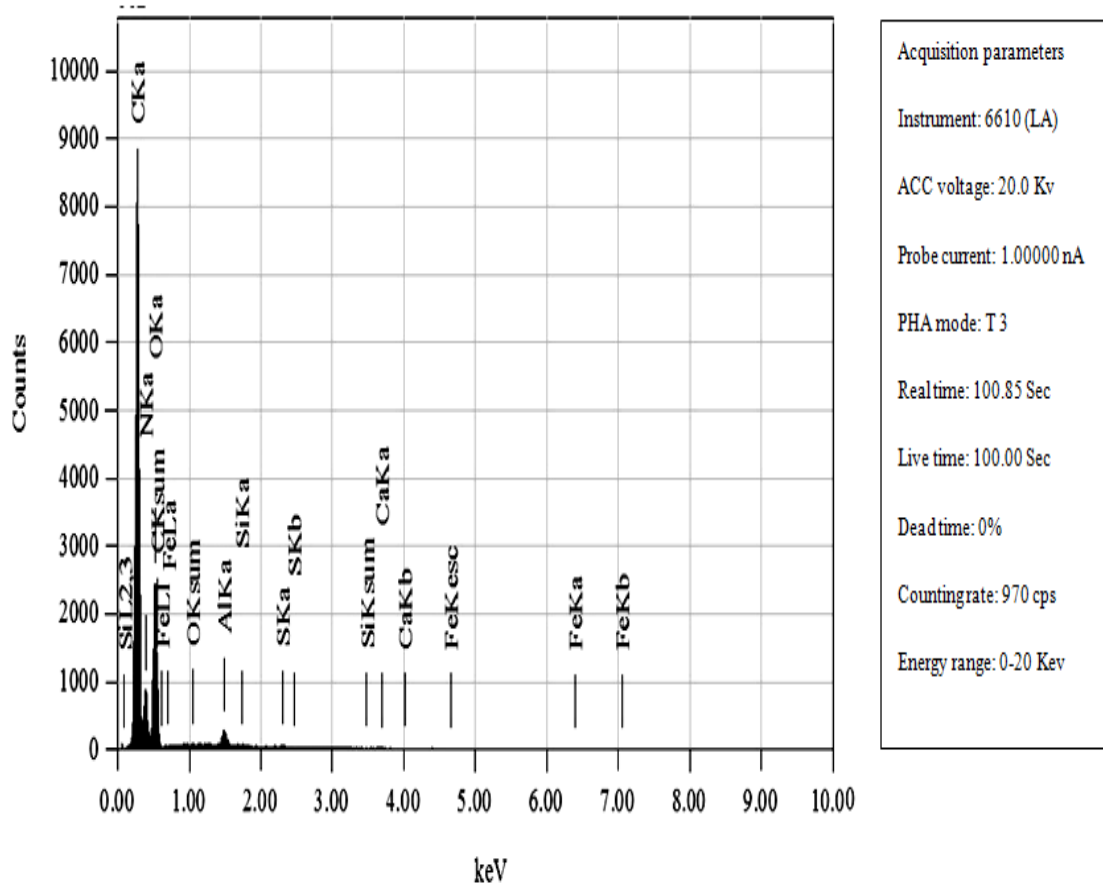
ZAF method standarless quantitative analysis					
Fitting coefficient: 0.4486					
Element	(Kev)	Mass (%)	Sigma	Atom (%)	K
O K	0.525	35.48	1.45	29.22	24.4330
C K	0.277	64.52	0.75	70.78	75.5670
Total		100		100	

Table III.4: EDS spectrum and elemental percent composition for the polymer composite prepared with 3% of BC.



ZAF method standarless quantitative analysis					
Fitting coefficient: 0.732					
Element	(Kev)	Mass (%)	Sigma	Atom (%)	K
O K	0.525	35.48	2.98	29.22	24.9940
C K	0.277	64.52	1.54	70.78	75.006
Total		100		100	

Table III.5: EDS spectrum and elemental percent composition for the polymer composite prepared with 5% of BC



ZAF method standarless quantitative analysis					
Fitting coefficient: 0.1682					
Element	(Kev)	Mass (%)	Sigma	Atom (%)	K
Ca K	3.690	0.01	0.00	0.00	0.0178
Fe K	6.398	0.01	0.01	0.00	0.0191
Si K	1.739	0.02	0.01	0.01	0.0310
S K	2.307	0.05	0.00	0.02	0.1057
Al K	1.486	0.29	0.01	0.15	0.3891
N K	0.392	29.90	0.13	29.13	37.7454
O K	0.525	30.06	0.09	25.63	16.5793
C K	0.277	39.66	0.02	45.06	45.1147

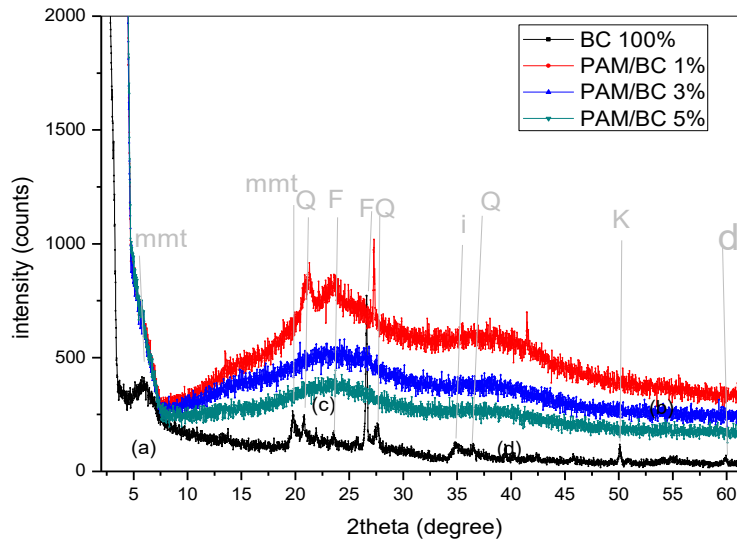
III-4-RD analyses for polymer composites with different ratio of BC/PAM

Figure III.2 : XRD scans of: (a) - BC; 2 theta from [0, 70]; I_{max} for the first peak 400cps. (b)- Composite prepared with 1% of BC; the quartz peak appears at 2 theta = 27° with $I_{max}=1000cps$. (c)- Composite prepared at 3% of BC. (d)- Composite prepared at 5% of BC

The XRD diffractogram of bentonite shows the presence of peaks relative to montmorillonite in particular at 2 theta 6.04°, 19.67°, and crystalline impurities of quartz kaolinite, feldspar and the illite, dollite designed respectively at angles (20.89°, 27.52°, 36.55°), 40.01°, (23.5°, 26.7°), 50.11°, 59.5° that allows us to ensure product identity as being maghnia bentonite [6]. Using bragg equation the distance between the crystal layers was calculated from the first peak at the lowest angle 6.04° that corresponds to 14.6Å. The maximum intensity for this one was 400cps.

The disappearance of peaks (shown in xrd diffractogram of composites prepared at 3% and 5% of BC figure III.2-c and figure III.2-d) indicate that these bentonite layers could be exfoliated and dispersed in the polyacrylamide matrix, as a nanometer scale composite [7,8,9,10]. Furth more, the intensity was reduced approximately between 300 and 400 counts.

On other hand the XRD spectra of a composite prepared with 1% of BC (figure III.2-b) reveals a special structure of this system (PAM 99/BC 1wt%), therefore, a quartz, feldspar, mmt peaks appeared in the spectrum at the angles equal to 20.89°, 27°, 23.5°,41.4°, which means that the blechy clay was partially exfoliated in the polymer matrix. This result was already interpreted by SEM of the polymer composite with one percent in weight of BC.

III-4-3. DSC thermal analysis of the different samples prepared

A second scanning heating was carried out between 30° and 250°C.

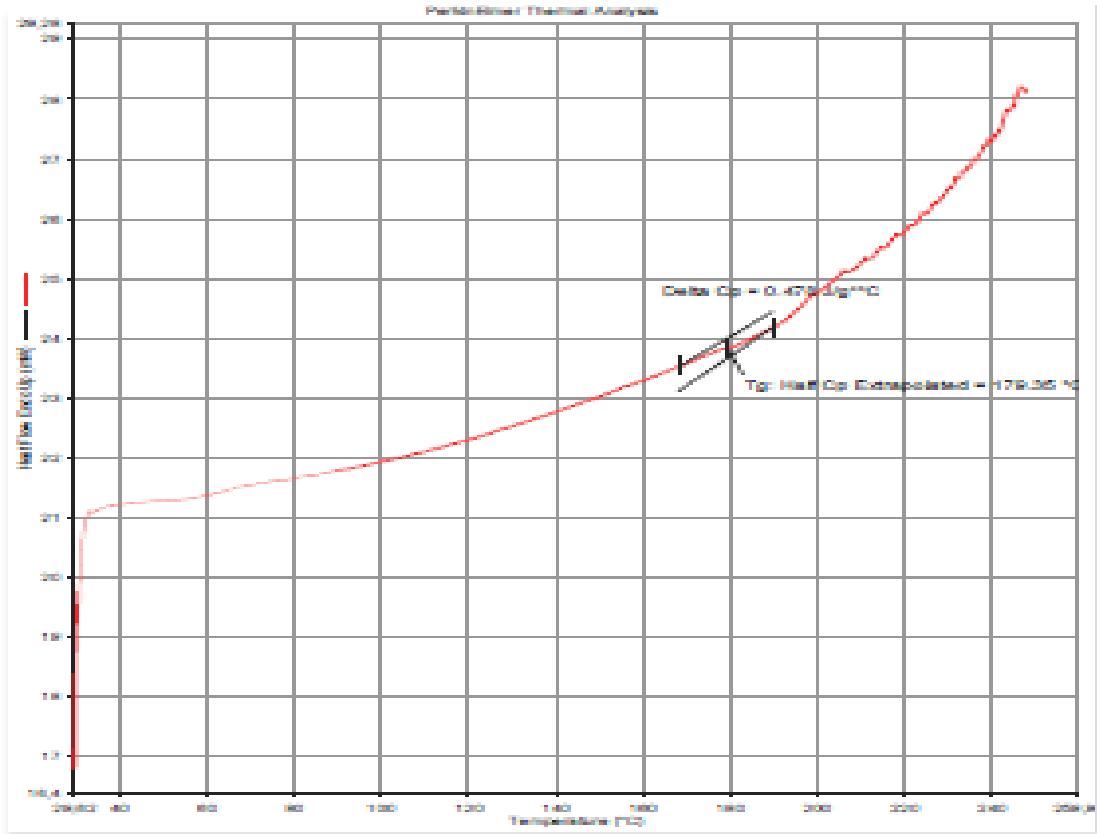


Figure III.3: DSC scan obtained for the composite prepared with 1 percent in weight of BC, Heating speed =5°C/min, Delta Cp = 0.478 J/g*°C, Tg= 179,35°C.

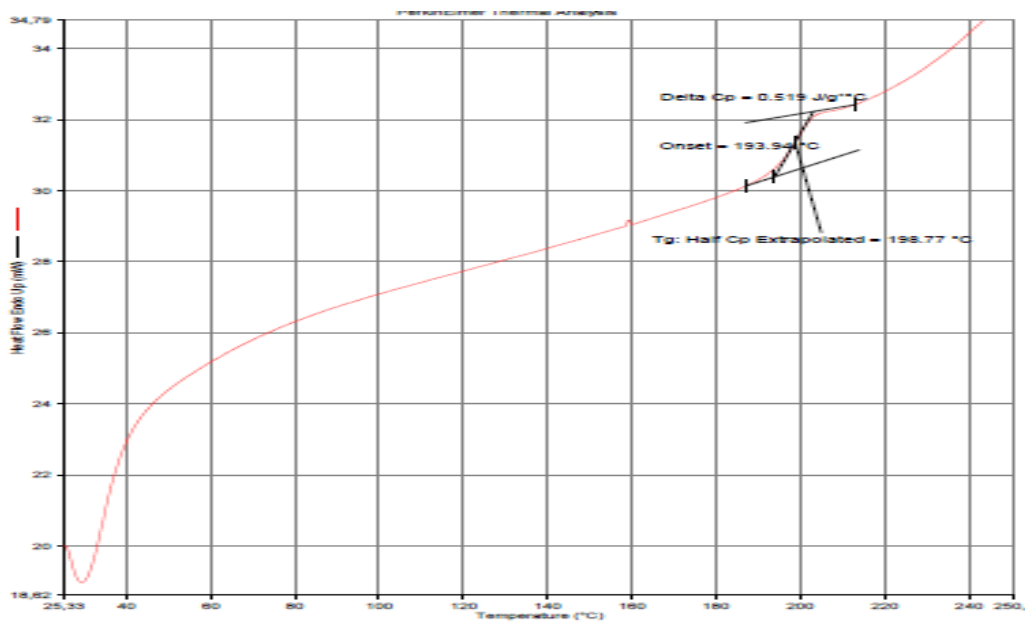


Figure III.4: DSC scan obtained for the composite PAM/ BC 3% Heating speed =20°C/min, Delta Cp = 0.519 J/g*°C, Tg= 198.77 °C.

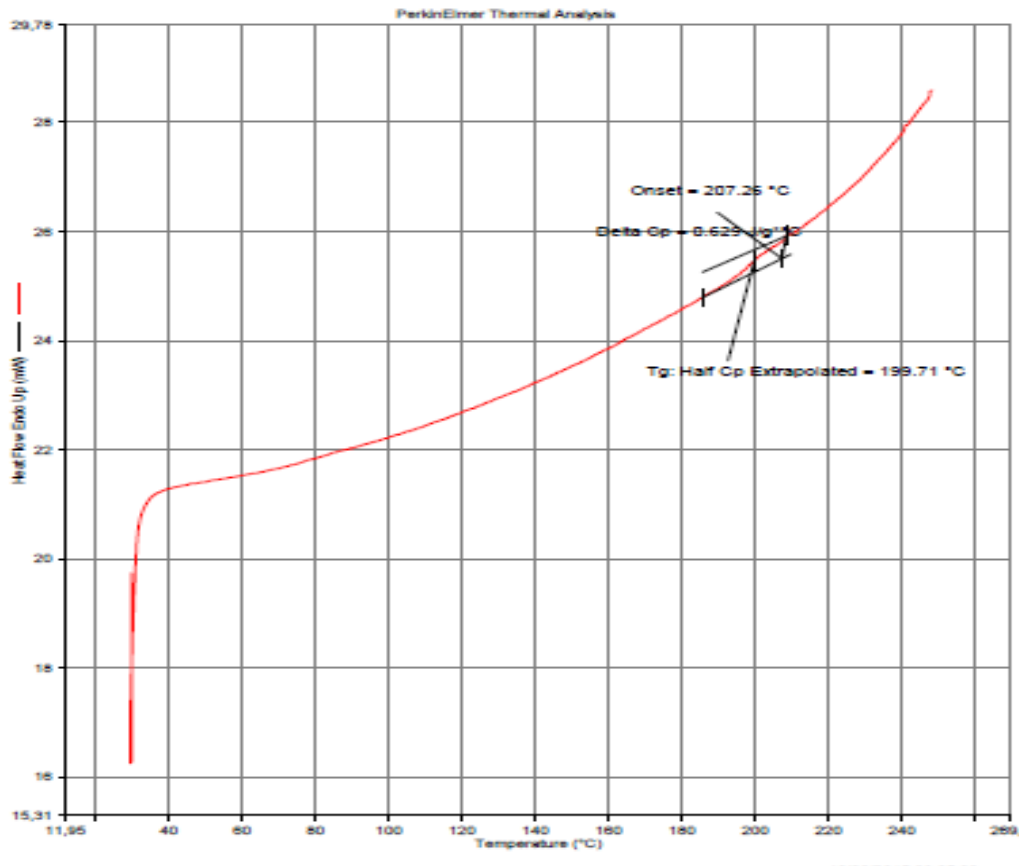


Figure III.5: DSC scan obtained for the composite PAM/BC 5%, Heating speed =20°C/min, $\Delta C_p = 0.587 \text{ J/g} \cdot ^\circ\text{C}$, $T_g = 199,71 \text{ } ^\circ\text{C}$

DSC heating scans of PAM 99/1 BC, PAM 97/3, PAM 95/5 are reported in Figures III.3, III.4, III.5 [11]. Heating temperature was between 30° and 250°. Heating speed was fixed at 5°C/min for the first specimen prepared with 1 percent in weight of BC and it was 20°C/min for PAM 97/BC3, and PAM 95/BC5.

Increasing of delta Cp, with increasing of bentonite content, reveals that the crystallinity index is inversely proportional to BC content. In fact, the exfoliation degree increases with rising weight fraction of blechy clay.

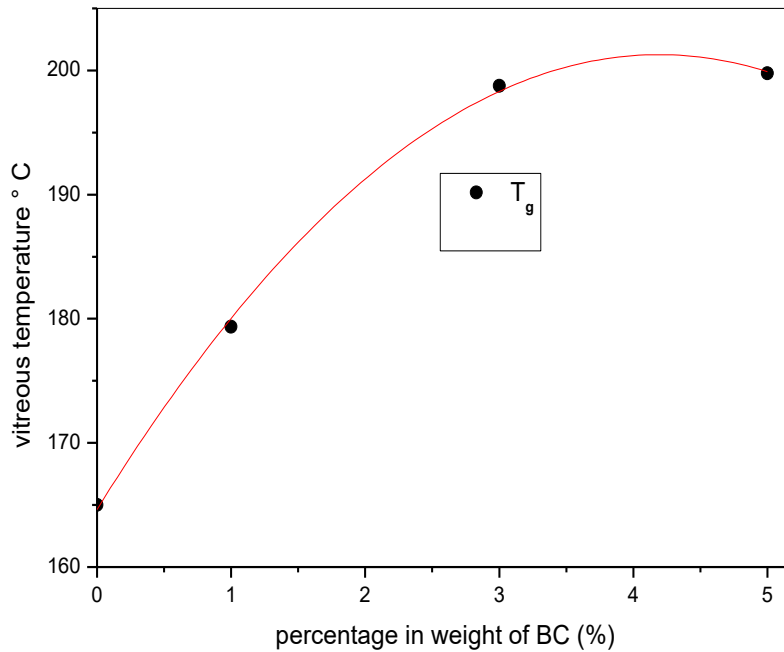


Figure III.6: Glass transition temperature as a function of weight percentage of BC.

Figure III.6 shows the variation of glass transition temperature with the percentage in weight of BC. As shown in this curve, the glass temperature increases with percentage in weight of Bleached clay. This means that percentage in weight of composition influences the thermal properties. Indeed, T_g depends on the structure of our material and the increase in the glass temperature was associated with constraints on molecular mobility of the polymer chains imposed [12] by the presence of BC sheets and agglomerations.

Increasing of glass transition temperature with BC content, may be interpreted by an important restriction of polymer chains mobility due to the presence of BC nano-sheets. The dispersion of the nano layers in the matrix provides and overcomes the Van Der Waals interactions between the Polyacrylamide chains and BC particles. Variation and rising of T_g with percentage in weight of BC is directly related to augmentation of intermolecular interactions between the component of our materials.

III-4-4. Micro-indentation results

A Vickers square-based diamond indenter was employed to measure the microhardness (H) from the residual impression on the sample surface after an indentation time of 6s loads of 250, 500 mN were used to derive a load indenting value of H (MPa). For all samples, 10 imprints were taken for each load. Equations used were mentioned in chapter II paragraph II-5-1-3

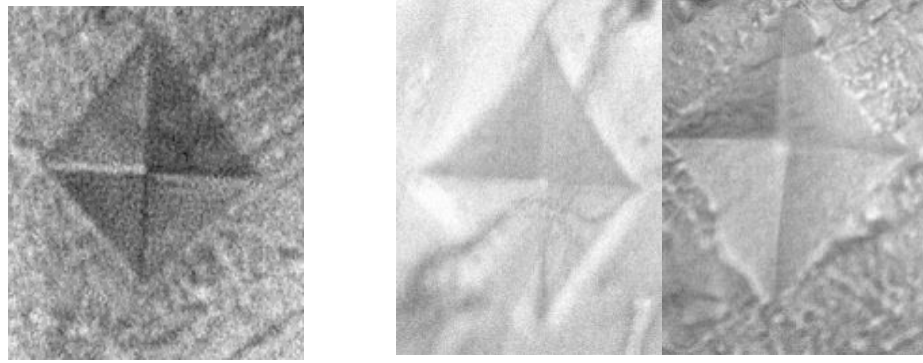


Figure III.7: The residual indentation on samples prepared with 1, 3 and 5 percent in weight of BC.

Figure III.7 represents the residual indentation on samples prepared with 1, 3 and 5 percent of BC

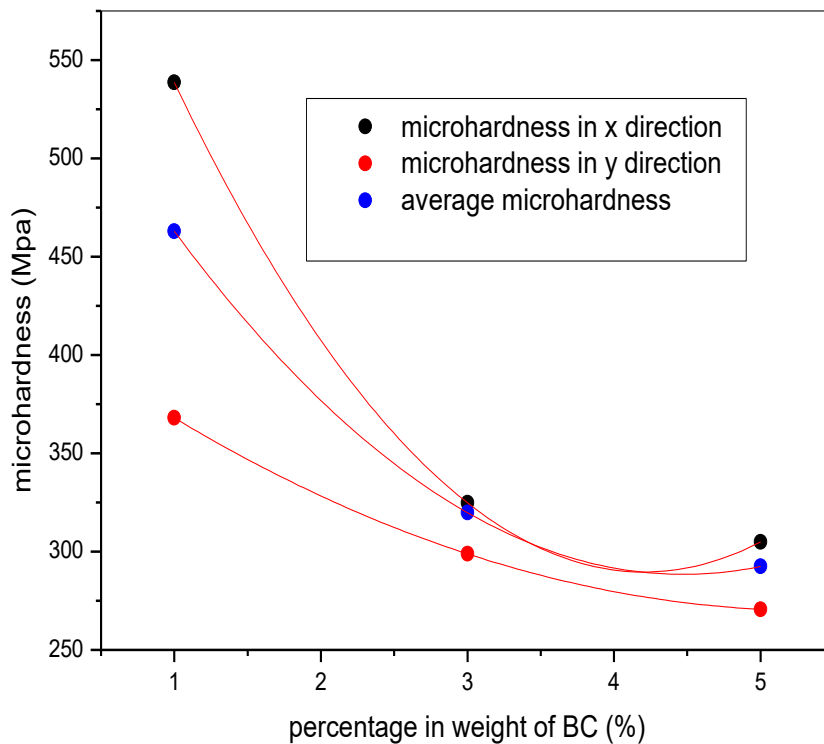


Figure III.8: Micro-hardness variation in x (parallel) and y (perpendicular) direction with percentage in weight. Average micro hardness variation with percentage in weight of BC.

Figure III.8 represents the micro-hardness variation in x direction and y direction, average value with the percentage in weight of BC.

Decreasing of micro hardness values in x direction from 538,6 MPa to 304,91 MPa with increasing of bentonite content varied from 1 wt% to 5 wt% in composite polymer.

Micro hardness variation in y direction shows the same behavior as that for the x axis, reducing from ~375MPa to ~270MPa with a change in BC percentage in weight from 1% wt to 5% wt.

Additionally, average micro hardness was calculated and represented in figure III-8. They varied from 457 MPa to 288 MPa with variation of BC percent in weight (1 wt % - 3 wt % - 5 wt %).

In y direction, the micro hardness values show some discrepancy with the measurements obtained in the x one. This explains why the response of the polymer matrix to the stress field is not the same in both directions. This anomaly is due to the structure of the crystalline phase BC, which has a hexagonal shape. Moreover, the anisotropy between x and y data probably occur owing to disorder orientation between bentonite sheets and macromolecular chains direction.

The lessening of micro hardness in both ways is necessarily due to the composition of agglomerations and dispersion of BC sheets in the polymer matrix. Undeniably, exfoliation degrees and morphology influence the micro-hardness of PAM/BC.

II-4-5. Nano-indentation results

Thickness film about 200 micrometers to 350 micrometers.

Measurements effectuated on the surface of samples are represented in figures I.9 , figure I.10 and figure I.11. figure I.12 (a) (b) (c) correspond to the variation of nanohandress, storage modulus and tangent of load as function of percentage in weight of bleachy clay.

The percentages are respectively 1%, 3% and 5%. Interpretation of results are described in the discussions of curves.

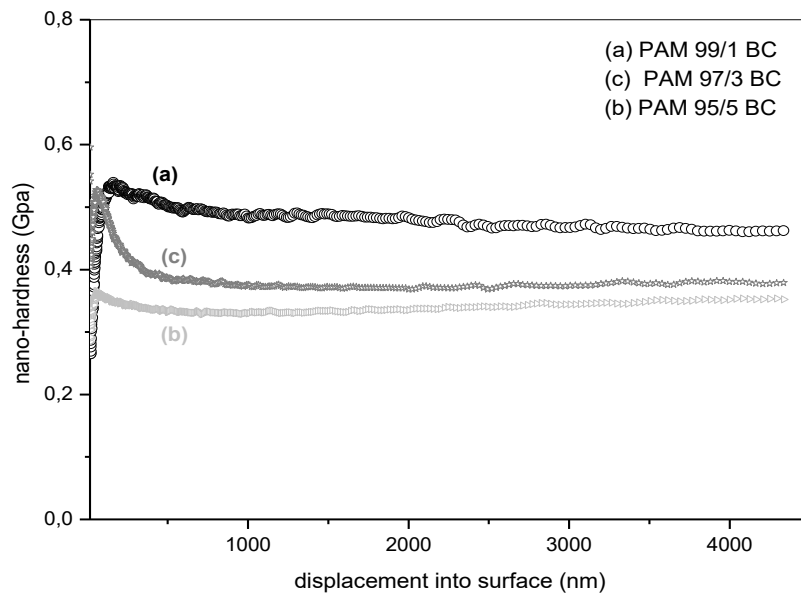


Figure III.9: Nano-hardness (GPa) variation with displacement into surface (nm) for weight percent of BC: **(a)**BC=1%, **(b)**BC=3%, **(c)**BC=5% at $T= 25-26^{\circ}\text{C}$, Relative humidity (RH)=34%).

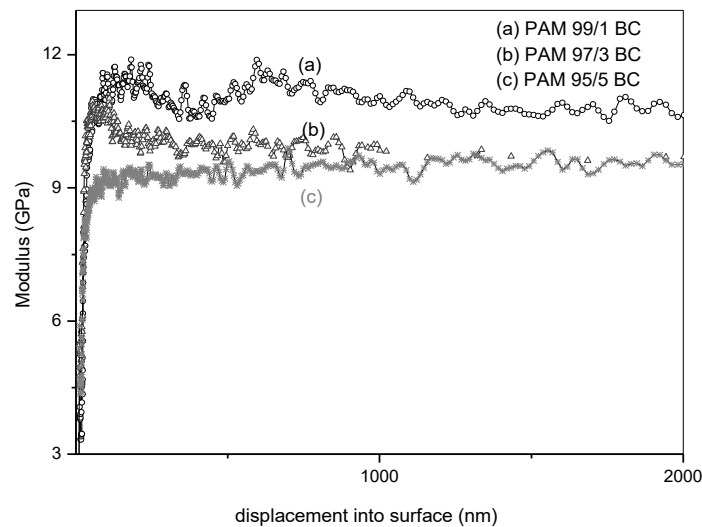


Figure III.10: Modulus (GPa) variation with displacement into surface (nm), for weight percent of BC:**(a)**BC=1%, **(b)**BC=3%, **(c)**BC=5% at $T= 25-26^{\circ}\text{C}$, RH=34%.

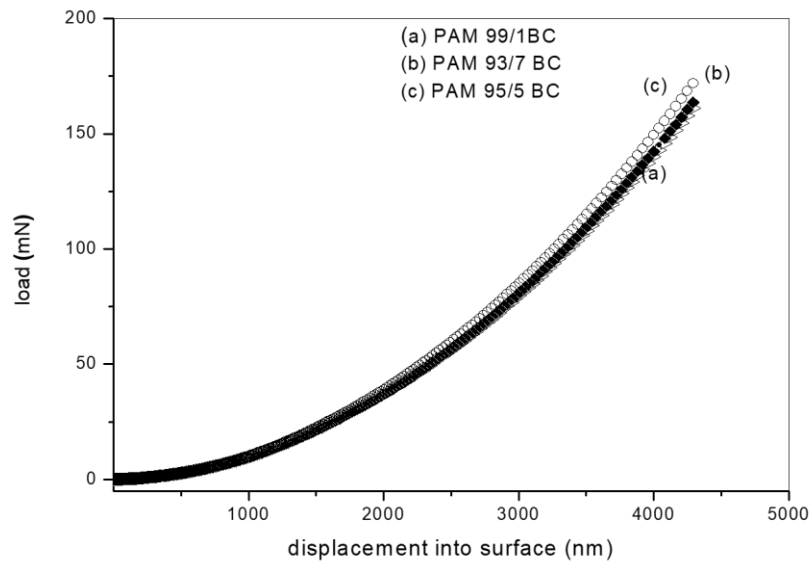


Figure III.11: Load (mN) variation with displacement into surface (nm).

Curves represented in Figure III.9 show the variation of nano-hardness with displacement into the surface for different ratios in weight of PAM/BC and the measurements of the nano-hardness by the nano-indentation technique.

From the data represented in figure III.9 and (Figure. III.12.b), it can be observed that nano-hardness decreases with the percentage of BC in the polymer composite. Increasing of bleaching clay loading in weight induces a fragility of PAM/BC.

These results are attributed to the interaction type created between the bentonite sheets and matrix polymer or dispersion of clay particles in PAM matrix.

This significantly indicates a formation of Van Der Waals bonds among the constituents of our material and agglomerations of BC sheets.

The variation of the nano-hardness as a function of the depth in surface at the surface shows a constant trend for all the measurements carried out on the different samples.

Figure III.10 represents the modulus variation with the displacement into the surface for different ratios weight of PAM/BC.

In each curve of storage modulus, we observe some fluctuations that can be related to the increase of sample surface roughness under load ≈ 200 mN [9].

Figure III.11 shows the evolution of load applied in the surface of PAM/BC for each value of percentage in weight of BC.

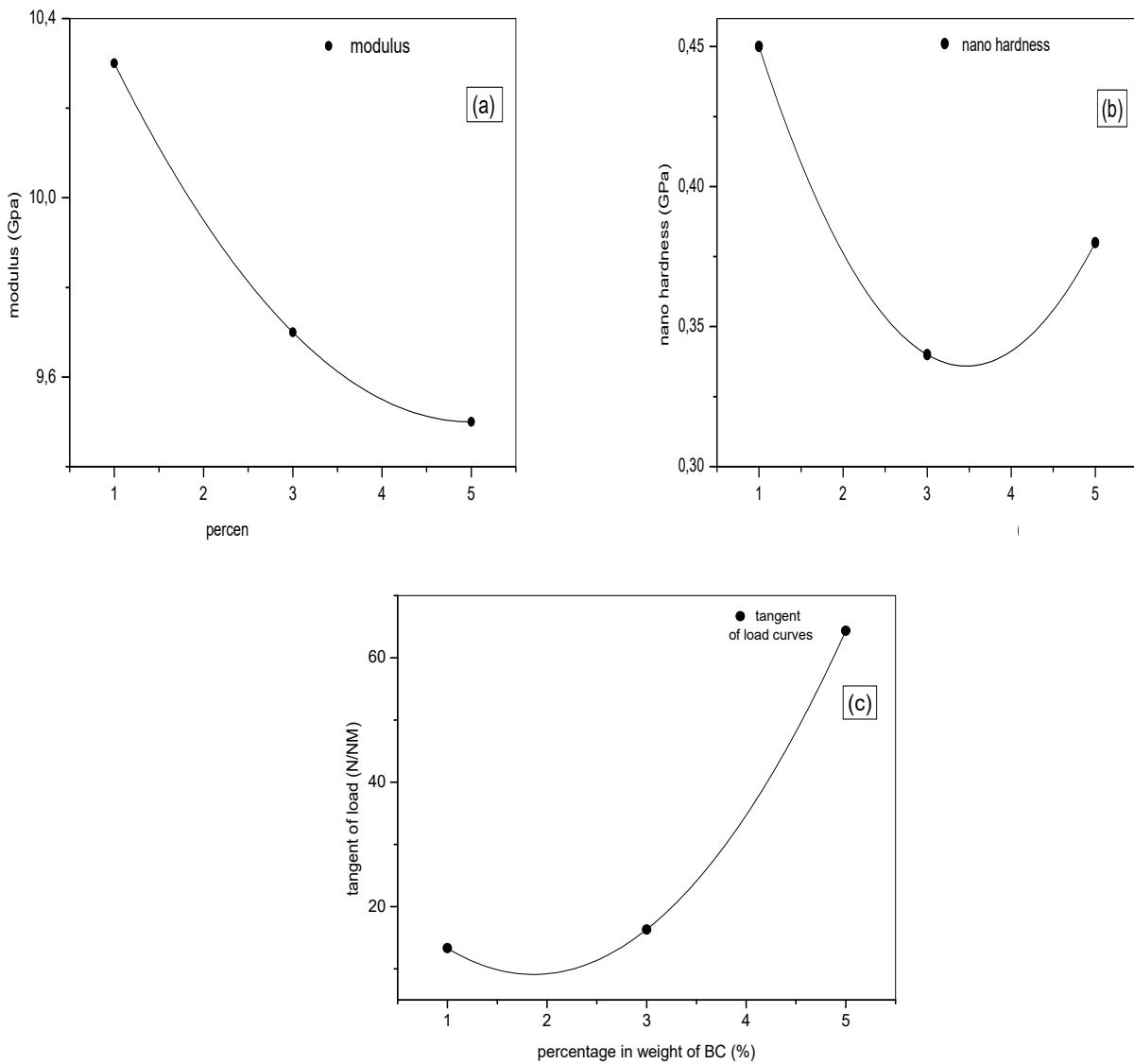


Figure III.12: (a) Storage modulus variation with percentage in weight of BC, (b) Nano hardness variation with percentage in weight of BC, (c) Tangent of curve load variation with percentage in weight of BC.

In figure III.12 (a) is shown decreasing of storage modulus from 10.4 GPa to 9 GPa with increasing of clay content in polymer composites from 0.5 to 5% wt.

Reduction of nano-hardness from 450 MPa to 335 MPa with increasing of BC wt % from 1 to 3% after this value we observed clearly a small gain of nano-hardness from 335 MPa to 400 MPa (figure III.12 (b)).

Augmentation of tangent load as function of loading clay weight %, which varied respectively, from 10 to 70 N/nm and 0,5 to 5 wt% (figure 5 c).

Result obtained in figure III-12 (a) resumed that the storage modulus of our material reduced with augmentation of BC percentage. Storage modulus depends on BC sheet distribution and their organization in the matrix polymer. In fact, correlation between the stress fields applied on the sample and orientation of BC sheet in the matrix polymer displays an important factor in this data.

The remarkable increase in the tangent of load curve (figure III-12 c) as function of loading clay content % depends firstly to the resistance of composite polymer surface to stress. and secondly to dislocations to assemble and dispersion of BC particle in the matrix [10]. The shape of this curve confirms that resistance against the load applied increase with growing of weight fraction of BC.

CONCLUSION

From the data discussion, it can be concluded that:

The morphology and the structure obtained with polymer prepared with one percent in weight of BC present the most important mechanical thermal and structural properties.

Micro indentation measurements and DSC analysis reveal somewhat strong contacts between BC sheet and PAM, this conclusion interprets the increasing of Tg with augmentation of BC % in weight. However, the Van Der Waals bonds and the structure of the polymer composite are the dominant factors in decreasing of micro hardness with content of BC% wt. The storage modulus decreases with the percentage weight of BC in the composite. The load tangent increases with %BC in the polymer, the nano-hardness decreases for the two starting values of the percentage of weight in BC (1% and 3%), then it comes a little increase from 3% to 5% percent of BC. These variations depend on the structure and surface roughness of samples. The effect of amount of BC and the level of reticulation PAM on the structure and physical properties of PAM/BC will be studied in a separate work.

References

- [1] B Bouras, A Mansri, L Tennouga, B. Grassl, Res Chem Intermed, 41:5839 (2015)
- [2] ZZhu, O. Jian, S. Paillet, J. Desbrières, B. Grassl, Eur. Polym. J, 43:824 (2007)
- [3] B Bouras, doctorat thesis, university abou bekr belkais Tlemcen, (2015).
- [4] A Mansri, A. Beladraoua, B. Bouras, J Mater Environ Sci, 7:808 (2016)
- [5] B. Long, C. Wang, W. Lin, Y. Huang, J. Sun, Composites Science and Technology , 67: 2770 (2007)
- [6] A Mansri, S. Ramdani, Res Chem Intermed, 41: 1765 (2015)
- [7] H Haiyan, P. mingwang, L. Xiucuo, S. Xudong, Z. liuchang, poly mint, 53:225 (2004)
- [8] E P Giannelis, R. Krishnamoorti, E. Manias, springer berlin Heidelberg, 107 (1999)
- [9] A B. Morgan, J. W. Gilman, applied polymer, 87:1329 (2003)
- [10] X Zhao, Q. Zhang, D. Chen, Macromolecules, 43:2357 (2010)
- [11] J Dandurand, V. Samouillan, C. Lacabane, A. Pepe, B. Bochicchio, Journal of Thermal Analysis and Calorimetry, 1:120 (2015)
- [12] M Naum Andres Perez, Etude Calorimétrique et Diélectrique de Nanocomposites Silicones . Institut National Polytechnique de Grenoble France (2008)

chapter IV
amount of Bc
effect on the PAM/BC properties

IV-1 INTRODUCTION

The principal objectif in this section is to study the influence of amount of bentonite and the rate of cristallinity on the mechanical thermal and structural properties. The percentage in weight choose are 10%, 25%,50% of bentontinte. Using the sames conditions of polymerization. The films obtained by evaporation solution are characterized by SEM micrograph, DSC analysis, XRD scans, microindentation and nanoindentation measurements for the mechanical behavior of PAM/BC with differents percentage in weight.

IV-2. RESULTS AND DISCUSSION

IV-2-1. SEM of polymer nanocomposites at different ratios of BC/AM

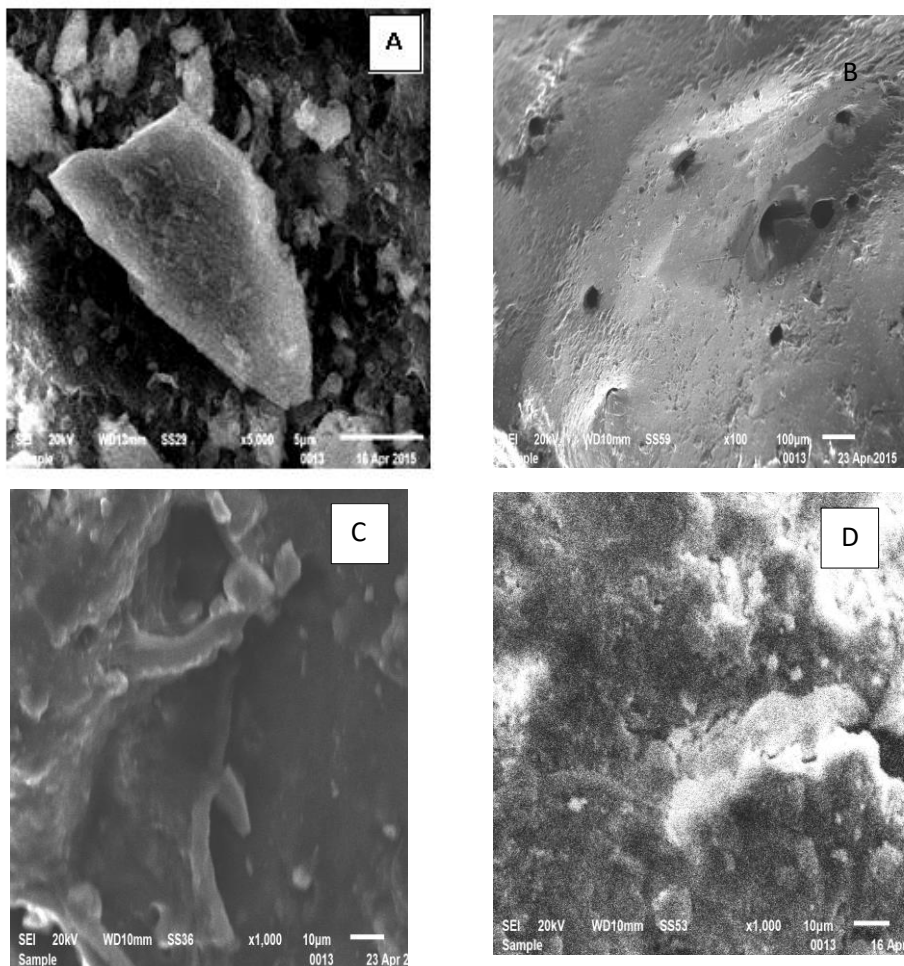


Figure IV.1: SEM micrographs of (A): pure bentonite (magnification x5000) (B): PAM/BC 10% (x100) (C): PAM/BC 25% (x1000) and (D): PAM/BC 50% (x1000)

Figure IV.1 (A) shows the SEM micrograph of pure BC without polymer (5 μm scale bar) and using a voltage of 20kV.

Figure IV.1 (B) exposes the SEM micrograph of PAM90/BC10 (100 μm scale bar) and the same voltage as before. In this figure, it is noteworthy that the morphology of our materials prepared at 10 % in weight of BC is not defined in this case. While, at the SEM test the the analysis of the surface of our sample was invalid and we had not any information of the dispersion situation of BC. it can be interpreted that the particle bc was polymerized at the matrix and it was grafted on the chain polymer.

Figure IV.1 (C) shows the SEM image of PAM95/BC25 (10 μm scale bar), taken at a voltage of 20kV. The results reveal an exfoliation structure of our sample prepared at 25% in weight of BC.

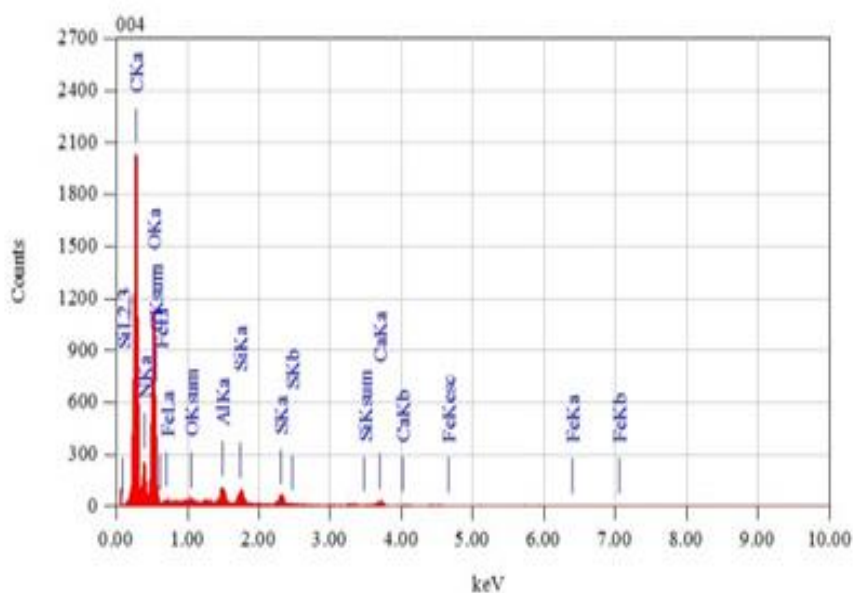
Figure IV.1 (D) shows a SEM image of PAM95/BC 5 (10 μm scale bar, voltage fixed at 20kV).

The intercalation structure is observed in the micrograph of sample prepared with 50% in weight of BC. This result is confirmed by the displacement of pic in drx analyses.

Energy Dispersive X-ray Spectroscopy (EDS) results are presented in tables (IV. 1, IV.2 and IV.3) , with elemental percent composition in polymers nanocomposites PAM/BC at different percentage in weight of BC 10%, 25%; 50%.

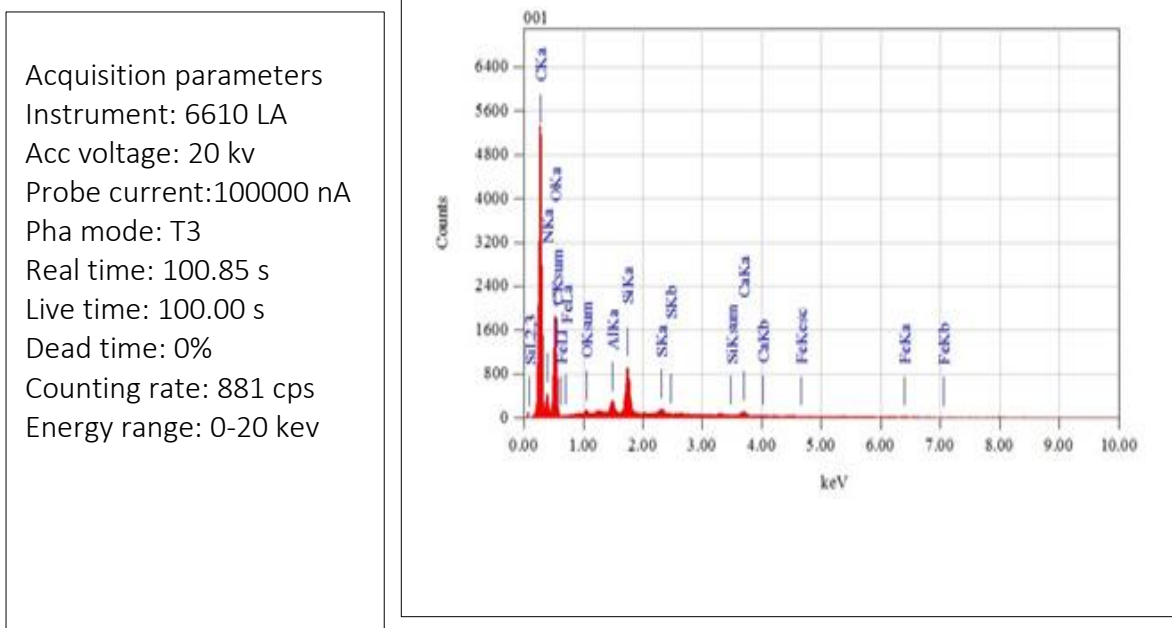
Table IV.1: EDS spectrum and elemental percent composition for the polymer composite prepared with 10% of BC.

Acquisition parameters
 Instrument: 6610 LA
 Acc voltage: 20 kv
 Probe current:100000 nA
 Pha mode: T3
 Real time: 100.35 s
 Live time: 100.00 s
 Dead time: 0%
 Counting rate: 315 cps
 Energy range: 0-20 keV



ZAF method standarless quantitative analysis					
Fitting coefficient: 0.1682					
Element	(Kev)	Mass (%)	Sigma	Atom (%)	K
Ca K	3.690	0.017	0.001	0.06	0.3740
Fe K	6.398	0.01	0.01	0.00	0.0191
Si K	1.739	0.36	0.02	0.018	0.5828
S K	2.307	0.29	0.01	0.13	0.6235
Al K	1.486	0.42	0.02	0.21	0.5443
N K	0.392	24.82	0.21	24.6	34.88
O K	0.525	37.73	0.16	32.82	25.27
C K	0.277	36.22	0.04	41.96	37.71
Total		100		100	

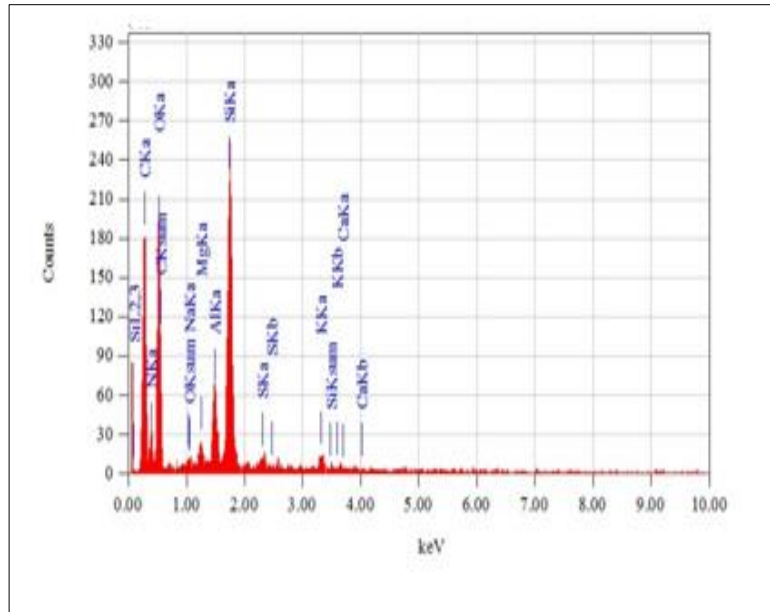
Table IV.2: EDS spectrum and elemental percent composition for the polymer composite prepared with 25% of BC.



ZAF method standarless quantitative analysis					
Fitting coefficient: 0.1682					
Element	(Kev)	Mass (%)	Sigma	Atom (%)	K
Ca K	3.690	0.27	0.001	0.09	0.6377
Fe K	6.398	0.08	0.01	0.02	0.1465
Si K	1.739	1.68	0.02	0.82	2.9836
S K	2.307	0.19	0.01	0.02	0.1465
Al K	1.486	0.43	0.01	0.22	0.6379
N K	0.392	23.54	0.15	23.06	27.9431
O K	0.525	30.19	0.10	25.89	19.62
C K	0.277	43.62	0.03	49.82	47.58
Total		100		100	

Table IV.3: EDS spectrum and elemental percent composition for the polymer composite prepared with 50% of BC

Acquisition parameters
 Instrument: 6610 LA
 Acc voltage: 20 kv
 Probe current: 100000 nA
 Pha mode: T3
 Real time: 100.25 s
 Live time: 100.00 s
 Dead time: 0%
 Counting rate: 104 cps
 Energy range: 0-20 keV



ZAF method standarless quantitative analysis					
Fitting coefficient: 0.2738					
Element	(Kev)	Mass (%)	Sigma	Atom (%)	K
Ca K*	3,69	0,10	0,03	0,04	0,2284
S K*	2,307	0,28	0,03	0,13	0,6243
na K*	1,041	0,32	0,06	0,20	0,4478
K K*	3,312	0,45	0,04	0,17	1,0062
Mg k*	1,253	0,49	0,05	0,29	0,6165
AL k*	1,486	1,65	0,07	0,90	2,5082
SI k*	1,739	6,94	0,13	3,61	12,3356
N k*	0,392	19,51	0,47	20,35	28,5782
O k	0,277	33,44	0,12	40,68	23,1744
C k	0,525	36,82	0,37	33,63	30,4806
Total		100		100	

Table IV.1, IV.2 and IV.3 correspond to the EDS spectrums and elemental composition of polymer composites prepared with ratios of PAM 90/BC 1 , PAM 85/ BC 25, PAM 50/ BC 50. As shown in these tables, the most important element composition was carbon.

IV-2-2 . XRD analyses for polymer composites with different ratio of BC/PAM

Xrd scan for the samples structure are represented in figure IV.4

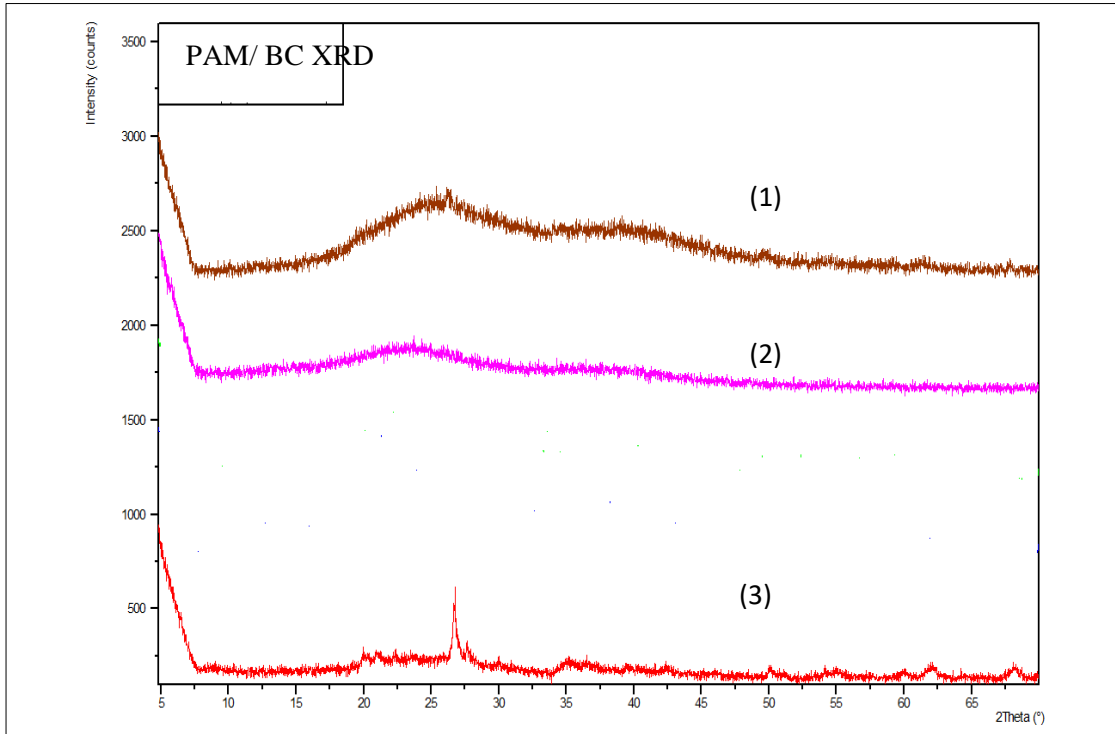


Figure IV.2 : XRD scans of: (1)- Composite prepared with 10% of BC; cps. (2)- Composite prepared at 25% of BC. (3)- Composite prepared at 50% of BC.

The disappearance of peaks in the spectrum xrd of composites prepared at 10% and 25% of BC indicate that the structure of this polymer is amorphous wish confirm that the polymer was not intercalated in the interlayer space of BC

The spectrum shows that the structure of these polymers is amorphous wish we can inform that the polymer was not penetrated in the gallery clay.

Xrd scan of PAM/BC 50 reveal cairely a crystalline structure and there is a moving angle from 6.04° to 3.61° reflects a widening of the interlamellar space, the increase in the distance between crystal layers which passes from $14,6 \text{ \AA}$ To $24,44 \text{ \AA}$. It is due to the penetration of the polymer into the galleries of clay which retains its crystalline structure layers.

IV-2-3. DSC thermal analysis of the different samples prepared

A second scanning heating was carried out between 30° and 250°C.

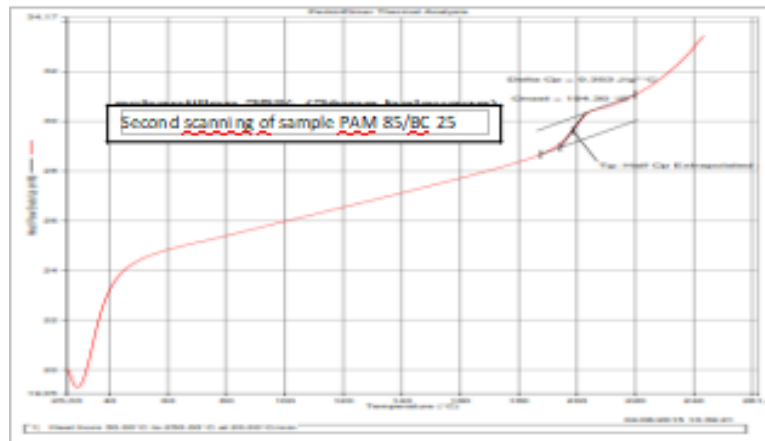


Figure IV.3: DSC scan obtained for the composite PAM/ BC 10% Heating speed =20°C/min,
0.353 J/g*°C Tg = 199,07 °C

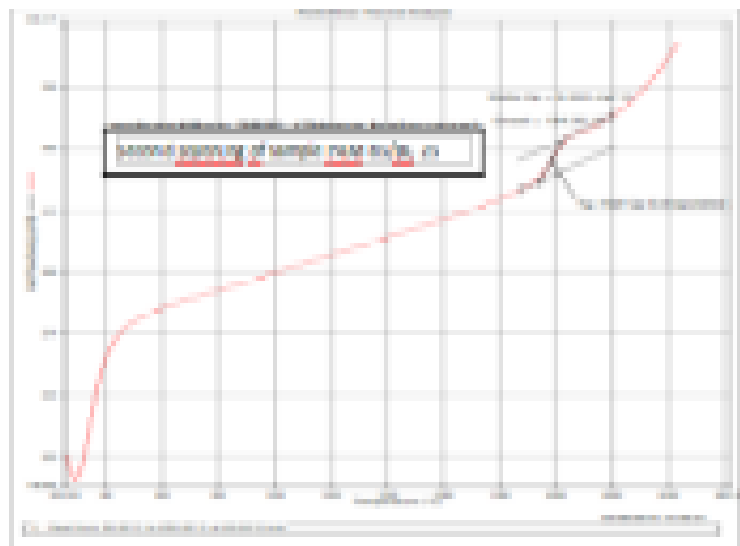


Figure IV.4: DSC scan obtained for the composite PAM/ BC 50% Heating speed =20°C/min,
0.150 J/g*°C Tg = 201.87 °C

DSC heating scans of PAM 85/ BC 25, PAM 50/ BC 50, are exposed in Figures IV.3, IV.4, Heating temperature was between 30° and 250°. Decreasing of delta Cp, with increasing of bentonite content, reveals that the crystallinity index is inversely proportional to BC content.

In fact, the exfoliation degree decreases with rising weight fraction of bleachy clay.

IV-2-4. Micro-indentation results

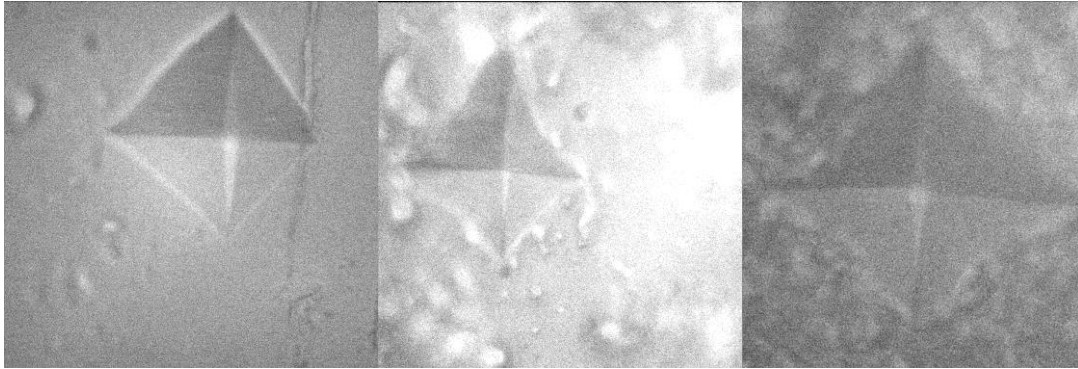


Figure IV.5: The residual indentation on samples prepared with 10, 25 and 50 percent in weight of BC.

Figure IV.5 represents the diagonals empreints registered on the surface samples prepared with 10, 25 and 50 percent in weight of BC.

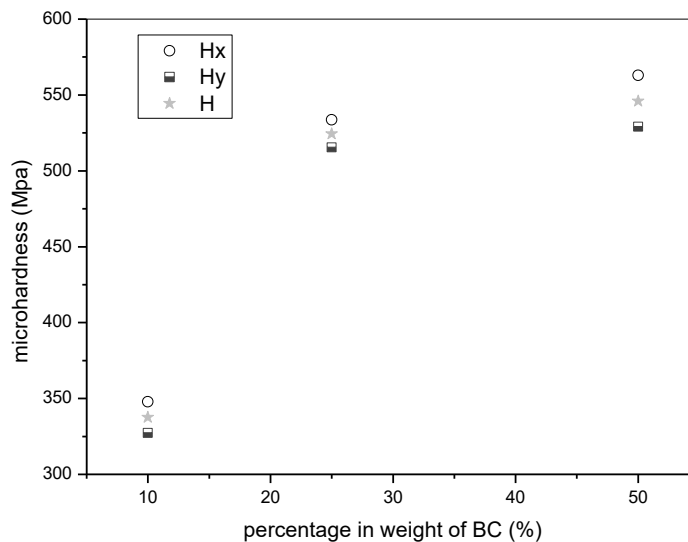


Figure IV.6: Micro-hardness variation in x (parallel) and y (perpendicular) direction with percentage in weight. Average micro hardness variation with percentage in weight of BC.:

Figure IV.6 represents the micro-hardness variation in x direction and y direction, average value with the percentage in weight of BC.

Increasing of micro hardness values in x direction from ~350 MPa to ~575 MPa with rising of bentonite content varied from 10 wt% to 50 wt% in composite polymer.

Micro hardness variation in y direction shows the same behavior as that for the x axis, augmentation from ~325MPa to ~545MPa with a change in BC percentage in weight from 10% wt to 50%wt. Additionally, average micro hardness was calculated and represented in the same plot. They changed from ~347 MPa to ~530 MPa with augmentation of BC percent in weight (10 wt % - 25 wt % - 50wt %). In y direction, the micro hardness values show some differences with the measurements obtained in the x one. This is due to the structure of the crystalline phase BC, which has a hexagonal shape. The rissing of micro hardness in both ways is necessarily due to the amount of crystalline particles in our samples.

Incontrovertibly, cristanility rate and structure influence the micro-hardness of PAM/BC.

IV-2-5. Nano-indentation results

Using the sames conditions and instrumentations parameters the nano indentation measurements of PAM/BC, prepared at 10%, 25%, 50% in weight of BC, are exposed in figures IV.7, IV.8, IV.9 and figure IV.10 .

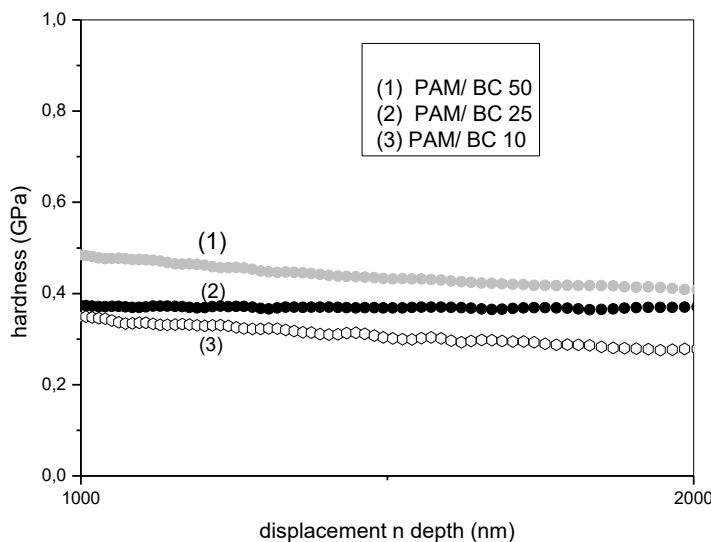


Figure IV.7: Nano-hardness (GPa) variation with displacement into surface (nm) for weight percent of BC: (a)BC=10%, (b)BC=25%, (c)BC=50% at $T= 25-26^{\circ}\text{C}$, Relative humidity (RH)=34%).

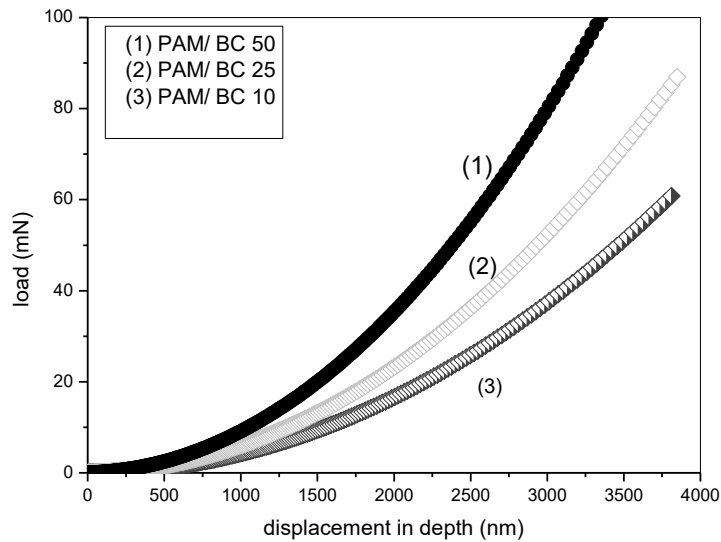


Figure IV.8: Load (mN) variation with displacement into surface (nm).

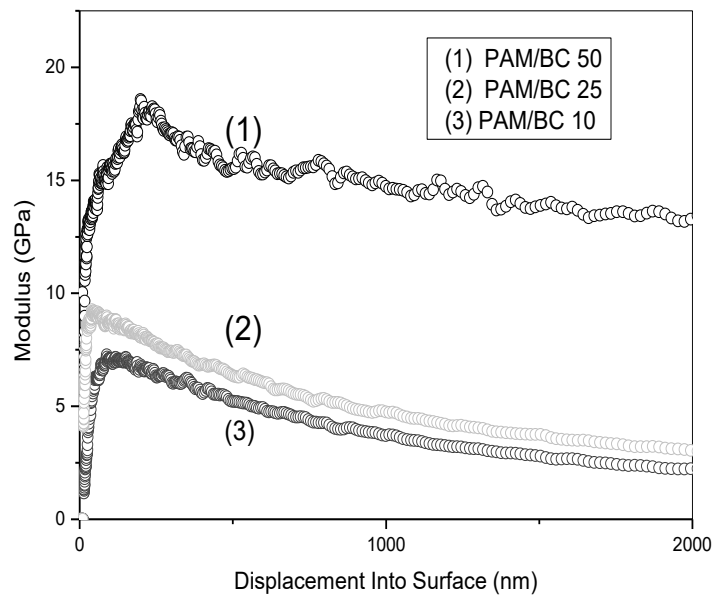


Figure IV.9: Modulus (GPa) variation with displacement into surface (nm), for weight percent of BC: (a) BC=10%, (b) BC=25%, (c) BC=50% at $T=25-26^{\circ}\text{C}$, $\text{RH}=34\%$.

Figure IV.7 represents the variation of nano-hardness with displacement into the surface for different ratios in weight of PAM/BC and the measurements of the nano-hardness by the nano-indentation technique. From the data exposed in fig IV.7 and (Fig. IV.10.1), it can be observed that nano-hardness increases with the percentage of BC in the polymer composite.

Increasing of bleachy clay amount in weight induces a cristanility rate augmentation. This is why the nano hardness has the way to increasing. This significantly indicates the domination of strong bonds among the constituents of our material. The variation of the nano-hardness as a function of the depth in surface at the surface shows a constant trend for all the measurements carried out on the different samples. Figure IV.8 shows the growth of load applied in the surface of PAM/BC for respectively 10%, 25% and 50% of percentage in weight of BC. Figure IV/9 represents the modulus variation with the displacement into the surface for different ratios weight of PAM/BC. In each curve of storage modulus, we observe some fluctuations that can be related to the increase of sample surface roughness under load ≈ 200 mN. It is observed from the results obtained in this figure that the storage modulus vary propotionnally with the amount of bleachy clay in the PAM/BC.

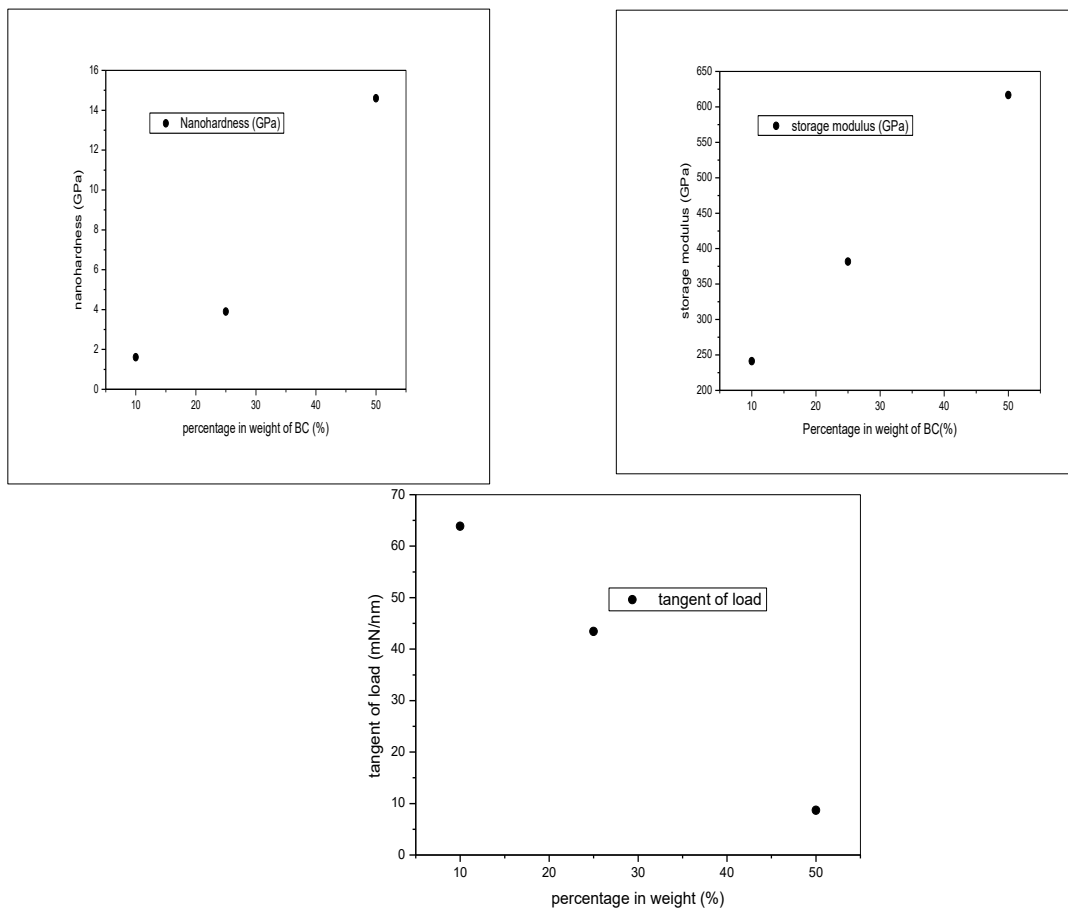


Figure IV.10: (1) hardness variation with percentage in weight of BC, (2) Storage modulus variation with percentage in weight of BC Nano, (3) Tangent of curve load variation with percentage in weight of BC.

Rising of nano-hardness from 241,25 MPa to 381 MPa with increasing of BC wt % from 10 to 25% after this value we observed clearly a great gain of nano-hardness from 381 MPa to 616,66 MPa (figure IV-10 (1)).

Figure IV.10(2) represents the evolution of storage modulus within percentage in weight of bleachy clay. From this data it is observed that the value of storage modulus growth respectively from 1,6 GPa to 14,6 GPa with augmentation of amount BC from 10% to 50%.

Reduction of tangent load as function of loading clay weight %, which varied respectively, from 63,86 to 8,69 mN/nm and 10 to 50 wt% .

Result obtained in figure IV-10 resumed that the storage modulus, nanohardness of our material augments with augmentation of BC amount. In fact, correlation between the stress fields applied on the sample within cristanility rate influence greatly in test measurments.

Deacrising in the tangent of load curve (figure IV-10 3) as function of loading clay content % depends firstly to the resistance of composite polymer surface to stress. and secondly to orientation and organization of our materials. The data obtained from this result confirms that resistance against the load applied reduces with growing of weight fraction of BC. Fragility of material is principally due to the links Inter and intra-molecular types.

CONCLUSION

It can be concluded that the rate of cristanility has a great influences in in the micro indentation results and nano indentation measurements. The xrd scans show an amorphous structure for sample prepared with 10 % and 25% in weight of BC. A crystalline structure for the materials preapred with 50% in weight of bentonite was observed with xrd analysis. DSC thermogrammes show that the variation in cp decrease with percentage in weight of BC which confirme an proportionality of cristanility degree and the amout of BC presented in the polymer nanocomposites.

Proportionality variation of micro hardness, nano hardness and storage modulus with variation of amount of bentonite in the PAM/BC.

The tangent in load vary inverssaly with BC amount existing in the PAM/BC nano composites.

References

- [1] B Bouras, A Mansri, L Tennouga, B. Grassl, Res Chem Intermed, 41:5839 (2015)
- [2] Z Zhu, O. Jian, S. Paillet, J. Desbrières, B. Grassl, Eur. Polym. J, 43:824 (2007)
- [3] B Bouras, doctorat thesis, university abou bekr belkais Tlemcen, (2015).
- [4] A Mansri, A. Beladroua, B Bouras, J Mater Environ Sci, 7:808 (2016)
- [5] B. Long, C. Wang, W. Lin, Y. Huang, J. Sun, Composites Science and Technology , 67: 2770 (2007)
- [6] A Mansri, S Ramdani, Res Chem Intermed, 41: 1765 (2015)
- [7] H Haiyan, P mingwang, L Xiucuo, S Xudong, Z liuchang, poly mint, 53:225 (2004)
- [8] E P Giannelis, R. Krishnamoorti, E Manias, springer berlin Heidelberg, 107 (1999)
- [9] A B Morgan, J W Gilman, applied polymer, 87:1329 (2003)
- [10] X Zhao, Q Zhang, D Chen, Macromolecules, 43:2357 (2010)
- [11] J Dandurand, V Samouillan, C. Lacabane, A Pepe, B Boichichio, Journal of Thermal Analysis and Calorimetry, 1:120 (2015)
- [12] M Naum Andres Perez, Etude Calorimétrique et Diélectrique de Nanocomposites Silicones . Institut National Polytechnique de Grenoble France (2008)

chapter V
LOAD APPLIED AND TIME
INDENTATION EFFECT
ON THE MECHANICAL BEHAVIOR
OF PAM/BC NANOCOMPOSITES

V-1- INTRODUCTION

A number of reviews of methods for the determination of hardness and viscoelastic properties of coatings have been published, as well

as standards for the determination of hardness. There has, naturally enough, been an emphasis on making such methods more sensitive and automated, particularly with reference to indentation tests [1].

We interested in our work specially in this section to the sensibility the mechanical behavior of PAM/BC with load applied at the surface of our materials and time of indentation. While, The content of bleachy clay (BC) was fixed at one percent in weight, the ammonium persulfate used as initiator to propagate the radicalar polymerization. The obtained polymer nanocomposite was transformed to film using an evaporization solution. The thickness of this film was over range 250 μm . The structural and morphological behavior was examined by X-ray diffraction (XRD) and scanning electron microscopy (SEM) techniques, the results is already shown in the previous chapters. The mechanical behavior was performed by the micro indentation technique varying independably the load applied and the time of indentation. The micro-indentation results prove that the load applied and the time indentation influence on the mechanical properties of the sample (PAM 99wt/1wt% BC) and (PAM/50% wt BC). Therefore, the response of the matrix polymer was changed with exchanging of load and time loading on the surface of sample. The choice of percentage in weight was taken in order to compare the mechanical behavior of PAM/BC at low amount of bentonite and at important quantity of bleachy clay.

V-2- MICRO-INDENTATION RESULTS

The Vickers hardness of materials is calculated using this equation:

$$H_v = 1.854 (P/d^2) \quad \text{eq (V.1)}$$

The constant value of each equation is calculated from the specific geometry of the indenter; P represents the indentation load (g), and d the diagonal of the indentation (μm) [2,3].

From the H_v equation, the micro hardness value should be constant when loads and time indentation are varied, because the indentation size increases with augmentation in the load and the expression of H have no dependence in time loading [4]. However, in previous studies of micro-hardness results have shown no constant variation.

PAM/1BC has specific microstructures; thus, their hardness may depend upon indentation times and represent a particular variation with increasing in time loading. This characteristic can be certified to elastic recovery or the viscoelastic nature [5], the grain size effect [6], indentation cracks, surface texture, or diagonal measurement errors [7]. The aim of this study was to evaluate the effect of indentation times on Vickers micro-hardness tests of (PAM/1 wt BC).

Figure V.1 represent the indentation marques registered at the sample surface of (PAM/ 50% wt BC) at different time indentation $t= 6s, t=20s, t=99s$ and load was fixed at $f=500mN$.

Figure V.2 show the indentation diagonals registered at the sample surface of (PAM/ 50% wt BC) at $t= 6s$ and different load applies $F=500mN, F= 250mN$.

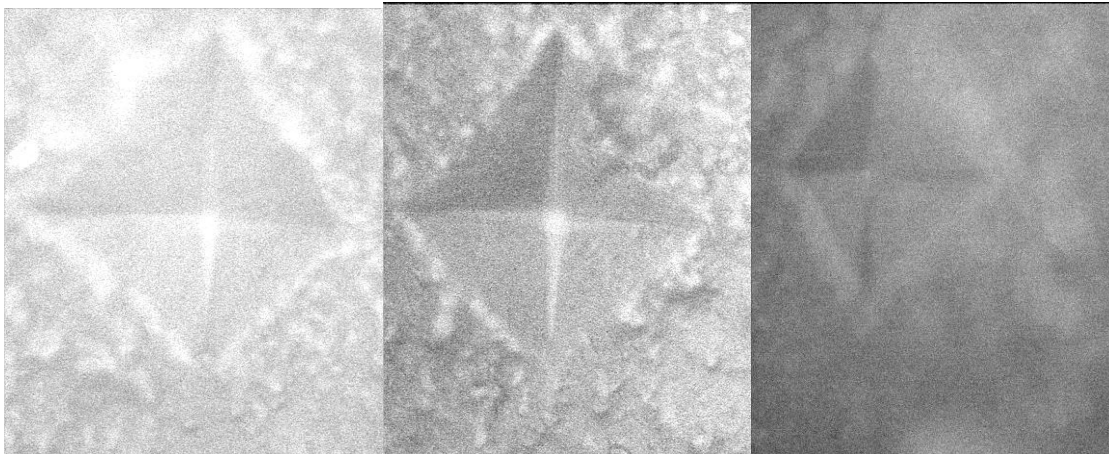


Figure V.1: residual indents at the sample surface of (PAM/ 50% wt BC) at different time indentation $t= 6s, t=20s, t=99s$

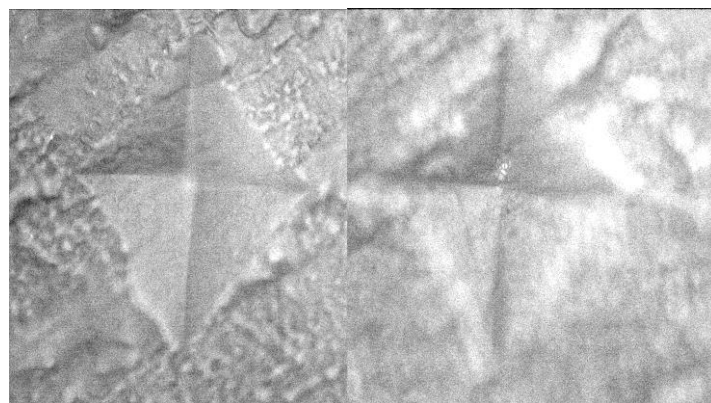


Figure IV.2: residual indents at the sample surface of (PAM/ 1% wt BC) at different load applied $F=500mN, F=250mN$.

Micro indentation results are reported in table V.1 and table V.2 for applied load of 250 mN and 500mN at different indentation time 6s, 20s, 99S respectively for polymer nanocomposite prepared with one percent in weight of BC and fifty percent in weight of Bleachy clay. Table V.3 and V.4 represent the micro indentations data of PAM/BC prepared with one and fifty percent in weight of Bleachy clay at indentation time of 6s for two different values of applied load 250 mN and 500 mN.

Table V.1: micro-hardness data of (PAM/1%wt BC) for different indentation time values for applied load of 250 mN.

PAM/1% wt BC	Time indentation	$H_{\square/\square}$ MPa	H_{\perp} MPa	ΔH MPa	Hv (by microscope)	Average H MPa
1	6 S	363,1	329,4	0,21	466,66	346,25
2	20 S	321,12	354,03	0,17	247,83	337,57
3	99 S	370,4	381,87	0,05	274,07	381,13

Table V.2: micro-hardness data of (PAM/1%wt BC) for two different load values (250 mN and 500 mN) at indentation time of 6S.

PAM/1% wt BC	Load applied	$H_{\square/\square}$ MPa	H_{\perp} MPa	ΔH MPa	Hv (by microscope)	Average H MPa
1	250 mN	363,1	329,4	0,21	466,66	346,25
2	500 mN	538,64	368	1,14	550,97	453,32

Hv: represent the visual micro-hardness calculated by the manipulator from the microscope.

Table V.3: micro-hardness data of (PAM/50% wt BC) for different indentation time values for applied load of 250 mN.

PAM/1% wt BC	Time indentation	$H_{\square/\square}$ MPa	H_{\perp} MPa	ΔH MPa	Hv (by microscope)	Average H MPa
1	6 S	562,88	462,22	0,48	529,1	512,55
2	20 S	426,14	440,33	0,06	416,64	433,235
3	99 S	485,80	487,08	0,005	467,6	486,44

TableV.4: micro-hardness data of (PAM/50%wt BC) for two different load values (250 mN and 500 mN) at indentation time of 6S.

PAM/1% wt BC	Load applied	$H_{\square/\square}$ MPa	H_{\perp} MPa	ΔH MPa	Hv (by microscope)	Average H MPa
1	250 mN	562,88	462,22	0,48	529,1	512,55
2	500 mN	508,02	573,8	0,21	562,14	540,91

Hv: represent the visual micro-hardness calculated by the manipulator from the microscope.

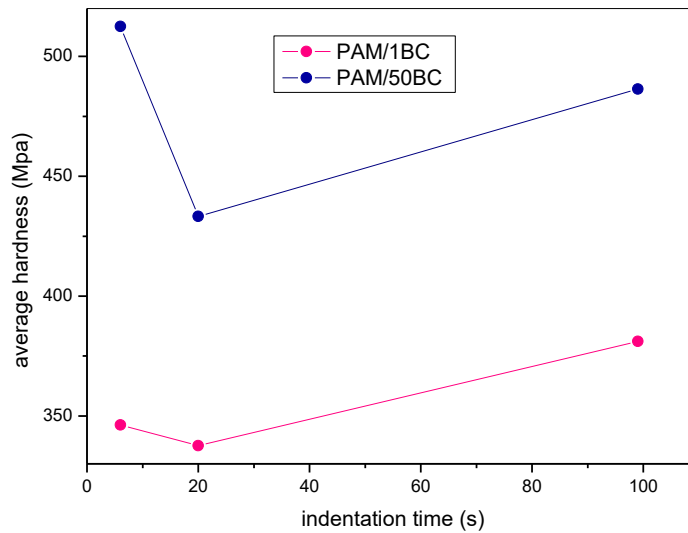


Figure V.3 : average hardness variation with indentation time for (PAM/1wt BC) and (PAM/50wt BC)

The figure represents the average hardness variation with increasing of indentation time. The range of hardness of PAM/1wt BC and PAM/50wt BC was respectively at 466.66 Mpa, 247.83 Mpa, 274.07 Mpa and 529 Mpa, 416.64 Mpa, 467.6 Mpa with increasing in time loading 6S, 20S, 99S.

The figure V-3 reveals a particular behavior of micro-hardness with exchanging in indentation time. This characteristic can be affected to cristalinity, memory shape, microstructure, elastic recovery or the viscoelastic nature of our material, the grain size effect, indentation cracks, and surface texture. In fact, the variation of micro hardness with Increasing in time loading prove that our material have a special behavior, this data show a decreasing in Hv with increasing in indentation time from 6s to 20s, while an augmentation of Hv values with loading time rising from 20 s to 99s. this exchanging nature may depend to time recrystallinity of our matrix polymer and reorganization of distribution of BC particle with polyacrylamid polymer, that why there is decreasing of Hv from 6s to 20s, it mean that 20s was insufficient to the self structural reorganization of our polymer PAM/BC nanocomposite prepared at one percent and fifty percent in weight of BC, and 99s was widely adequate for self recrystanility and augmentation of micro hardness at this loading time. This variation should be essentially affected to the nature of polymer and their specific characteristic when it's combining with Bentonite clay.

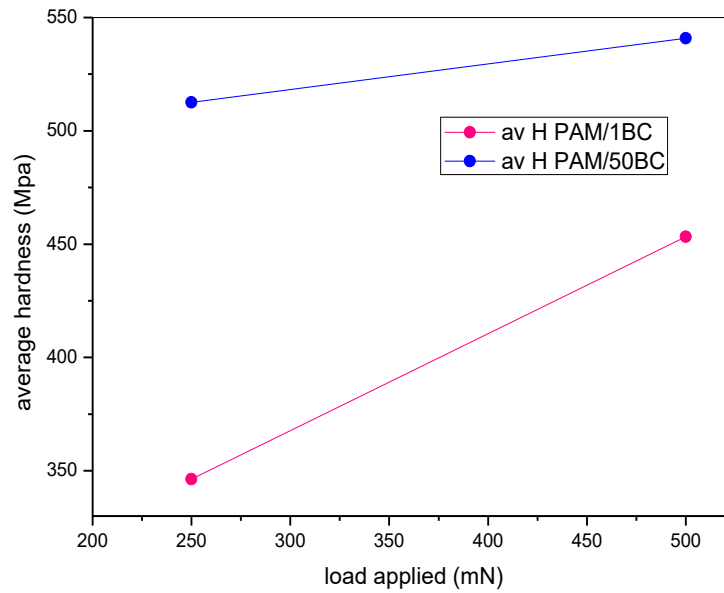


Figure V.4: Average hardness variation with load applied for (PAM/1wt BC) and (PAM/50wt BC).

Figure V.4 shows the average hardness evolution with two different load applied values.

The plotted data proves that mechanical behavior depended on load applied. There for, this hardness tendency reveals that the elasticity recovers increase with increasing of constraint applied. Results illustrate the same tendency of hardness with varied load applied for both of PAM/1 wt BC and PAM/50 wt BC. Other Hens, there is no signified interpretation of this dependence.

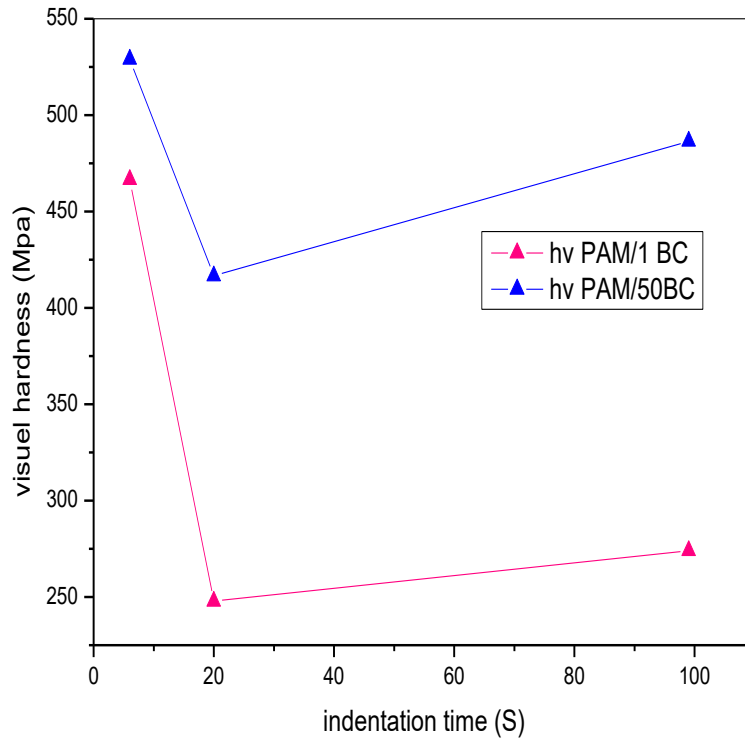


Figure V.5: Visual hardness variation with time loading for (PAM/1wt BC) and (PAM/50wt BC).

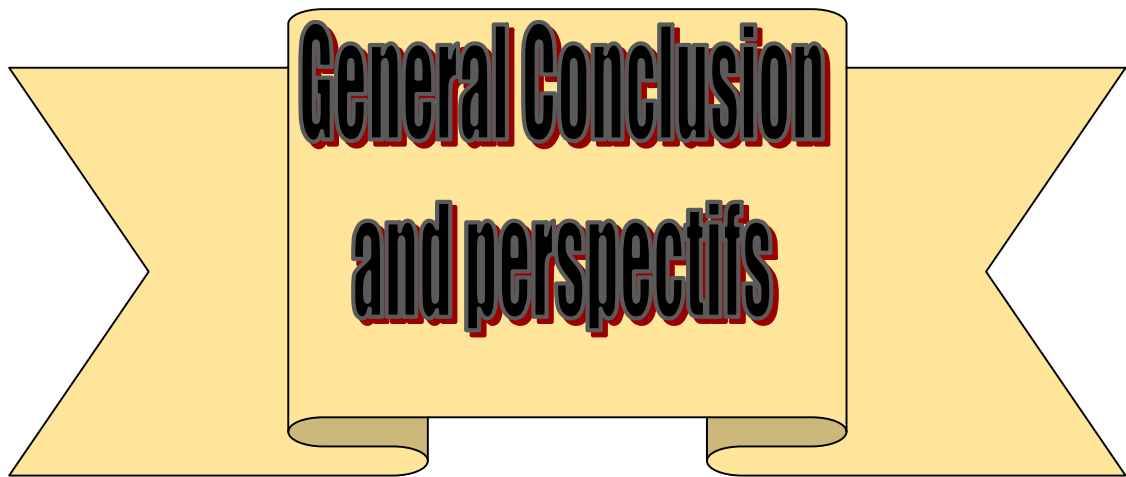
The plots demonstrate the same allure of hardness dependency on time loading and load applied. The measures appears some different in comparison with measures presented in figure 1, it's due to the manipulation and diagonal calculus errors.

CONCLUSION

The results of this study showed that the difference of indentation times was influential on VH values of PAM/1 %BC and PAM/50% wt BC for the same indentation loads. These results are affected to the structure of our material, and the size of BC particle. The variation of micro-hardness with increasing in indentation time prove that our material present a particular characteristic and mechanical behavior.

References

- [1] T A Strivens, Mechanical properties of paints and coatings, in Paint and Surface Coatings (Second Edition), (1999).
- [2] M F Mina, G H Michler, F J Baltá-Calleja, Journal of Bangladesh Academy of Sciences 33, 15 (2009).
- [3] F Ania, G Broza, M F Mina, K Schulte, F.J. Baltá-Calleja, Composite Interfaces 13:33 (2006).
- [4] P Benjakul, P Daosodsai, C Chuenarrom, Mat. Res, 12:4 (2009).
- [5] K Sangwal , B Surowska, P Blaziak P, Materials Chemistry and Physics, 77(2):511-520 (2003).
- [6] Low IM. Effects of load and time on the hardness of a viscoelastic polymer. Materials Research Bulletin. 33(12):1753-1758, (1998).
- [7] G Quinn, Hardness testing of ceramics. Advanced Materials & Processes, 54.(1998).



**General Conclusion
and perspectives**

CONCLUSION

The main objectives of this work is to synthesize new polymers nanocomposites of strong masses based on acrylamide and bentonite of maghnia in aqueous solution and provide a contribution to understanding their mechanical and thermal, physical and chemical behavior in order to later use as a base material for the various applications.

After a rich bibliographical study which provided us with such important tools than essential on polyacrylamides, bentonite and polymers nanocomposites. We have deemed it necessary and essential to synthesize these polymers nanocomposites PAM/BC by a new technique of polymerization in aqueous solution.

Thus, we obtained by this new technique of polymerization a series of polymers based on acrylamide and bentonite with different ration in weight (PAM/BC 1) (PAM/BC 3) (PAM/BC 5) (PAM/BC 10) (PAM/BC 25) (PAM/BC 50) using the adiabatic process and radicalar route of polymerization.

At first in order to study the effect of nanostructure in the PAM/BC properties, The percentage by weight of bleaching clay (BC) was fixed at 1%, 3% and 5%. Thin films were obtained using an evaporation solution (thickness of films were in the range 100- 300 micrometer).

These polymers were perfectly characterized by XRD scan, SEM microscopy, DSC analysis, micro indentation tests and nanoindentation measurements.

SEM micrographs show an exfoliated structure in polymer composites that originates from the nature and method of polymerization used (a radical adiabatic polymerization under neutral condition). DSC measurements reveal that the glass transition temperature increases with percentage in weight of BC. The mechanical tests confirm that the obtained materials have high values of hardness. We conclude that our materials have a special nano-structure that determines the good mechanical properties. It is also shown that average micro-hardness decreases with increasing amount of BC which implies some changes from the initial structure.

Mechanical properties of these polymers nanocomposites under 5 percent in weight of BC; were carried out using nano indentation technic. These results confirm that PAM/BC prepared with 1 percent of BC present the best ones. In fact, the slope of load curve, storage modulus, nano hardness was presented as function of BC amount clay. Indeed, we observed that the amount of BC clay presented in PAM/BC nanocomposite influences in the structural, therefore mechanical properties of our samples. Exceeding value of 5% BC it has observed another response of our

materials. After these remarks, We have deemed it necessary to provide information data about the effect of amount BC and rate of cristanility on the PAM/Bc behavior. For this raison, in the second step of our experimental part the amount of BC The amount of bleachy clay was fixed at 10wt%, 25wt%, 50wt%.

SEM micrographs show an exfoliated structure in polymer composites prepared with 10% an 25% of Bc. Contrarily, a crystalline structure obtained in the polymers nanocomposites obtained in 50% of BC. DSC measurements reveal that the delta Cp decrease with percentage in weight of BC. The mechanical tests confirm the proportionality of micro hardness variation and the percentage in weigh of BC exceeding 5%. the obtained materials have high values of hardness. Mechanical properties of these polymers nanocomposites exceeding 5 percent in weight of BC; were carried out using nano indentation technic. These results confirm that PAM/BC prepared with 50 percent of BC present a good agent of our polymers nanocomposites use and application. Indeed, the slope of load curve, storage modulus, nano hardness was presented as function of BC amount clay.

We concluded that the amount of BC clay and rate of crystalline phase presented in PAM/BC nanocomposite influences in the structural, therefore mechanical.

We have already, studied the influence of indentation time and load applied on mechanical properties of PAM /BC nanocomposite. The percentage in weight of BC was fixed at 1 and 50%. The mechanical characterization was performed by the micro indentation technique. The micro-indentation results prove that the load applied and the time indentation influence on the mechanical properties of the sample (PAM 99wt/1wt% BC) and (PAM/50% wt BC). Therefore, the response of the matrix polymer was changed with exchanging of load and time loading on the surface of sample. The choice of percentage in weight was taken in order to compare the mechanical behavior of PAM/BC at low amount of bentonite and at important quantity of bleachy clay. In fact, vicker hardness dependence on time loading and load applied demonstrate the same tendency of our polymer nanocomposite prepared at the two different percentage of BC.

This work foresees a good number of perspectives. While, the real aim of this work is the investigation and exploitation of this data in the fabrication of hip prosthesis based on PAM/BC nanocomposite via it's biocompatibility, legerity, and good thermal and mechanical behavior.

It can be used in the aeronautic field and industrial application. An antimicrobial study will take place in our future studies.

ملخص

يهدف موضوع الأطروحة إلى تطوير مواد نانو مركبة متكونة بالأساس من البنتونيت والأكريلاميد. في الواقع، تمت دراسة خصائص الطين على نطاق واسع وهي مهمة للعديد من التطبيقات. من ناحية أخرى، فإن خواص مادة الأكريلاميد معروفة ويستخدم البولي أكريلاميد على نطاق واسع في مختلف المجالات، وينتج عن تجميع هاتين المادتين مواد مركبة ذات خصائص فيزيائية وكيميائية جديدة تعتمد بشكل وثيق على التركيب الكيميائي للمادة الجديدة. يعتمد هذا الهيكل بدوره على كيفية تحضير هذه المركبات. هدفنا هو الحصول، من خلال تقنية البلمرة الجديدة، على سلسلة من البوليمرات المتكونة من مادة الأكريلاميد والبنتونيت بنسب وزن مختلفة (PAM / BC 1) (PAM / BC 5) (PAM / BC 10) (PAM / BC 25) (PAM / BC 50) الجذرية. تمت تحليل هذه البوليمرات بشكل مثالي بمسح XRD، الفحص المجهر SEM، تحليل DSC، اختبارات المسافة الميكرومترية الدقيقة وقياسات المسافة النانوية. كخطوة أولى لدراسة تأثير البنية النانوية في خصائص PAM / BC، تم تعيين النسبة المئوية بالوزن لطين (BC) عند 1% و 3% و 5%. تم الحصول على الأغشية الرقيقة باستخدام محلول التبخير (بترواح سمك الأغشية بين 100 و 300 ميكرومتر)، وفي الخطوة الثانية، قمنا بتثبيت كمية BC بنسبة 10%، 25%، 50% والنتائج التي تم الحصول عليها تناقش في الفصل الرابع. يكشف تأثير المسافة البادئة الزمنية والحمل المطبق على نتائج السلوك الميكانيكي عن استجابة مهمة لموادنا المختبرة.

Abstract

The present subject thesis consists of the development of nano composite materials based on bentonite and acrylamide. Indeed, the properties of clay are widely studied and are of interest for many applications. On the other hand, the properties of acrylamide are known and polyacrylamides are widely used in various fields. The pooling of these two materials results in composite materials with new physical and chemical properties that are closely dependent on the chemical structure of the new material. Our aim objectif is to obtain via a new technique of polymerization a series of polymers based on acrylamide and bentonite with different ration in weight (PAM/BC 1) (PAM/BC 3) (PAM/BC 5) (PAM/BC 10) (PAM/BC 25) (PAM/BC 50) using the adiabatic process and radicalar route of polymerisation. These polymers were perfectly characterized by XRD scan, SEM microscopy, DSC analysis, micro indentation tests and nanoindentation measurements. At first in order to study the effect of nanstructure in the PAM/BC properties, The percentage by weight of bleaching clay (BC) was fixed at 1%, 3% and 5%. Thin films were obtained using an evaporation solution (thickness of films were in the range 100- 300 micrometer). In seconde time we fixed the rate of BC at 10%, 25%, 50% and results obtained are discussed in chapter IV. Influence of time indentation and load applied on the mechanical behavior results reveal an important response of ou materials elaborated.

Words key: acrylamide, bentonite, nano composite, hardness, mechanical properties, thermal stability.

Résumé

Le présent travail consiste en la mise au point de matériaux nano composites à base de bentonite et d'acrylamide. En effet, les propriétés de l'argile sont largement étudiées et présentent un intérêt pour de nombreuses applications. En revanche, les propriétés de l'acrylamide sont connues et les polyacrylamides sont largement utilisés dans divers domaines tels que le traitement de l'eau, la caractérisation par électrophorèse, etc. La mise en commun de ces deux matériaux aboutit à des matériaux composites aux nouvelles propriétés physiques et chimiques étroitement dépendantes de la structure chimique du nouveau matériau. Cette structure dépend à son tour de la façon dont ces composites sont préparés. Notre objectif objectif est d'obtenir via une nouvelle technique de polymérisation une série de polymères à base d'acrylamide et de bentonite avec différents rapports en poids (PAM / BC 1) (PAM / BC 3) (PAM / BC 5) (PAM / BC 10) (PAM / BC 25) (PAM / BC 50) en utilisant le procédé adiabatique et la voie radicalaire de polymérisation. Ces polymères ont été parfaitement caractérisés par scan XRD, microscopie SEM, analyse DSC, tests de micro indentation et mesures de nanoindentation. Dans un premier temps afin d'étudier l'effet de la nanstructure dans les propriétés PAM / BC, le pourcentage en poids d'argile décolorante (BC) a été fixé à 1%, 3% et 5%. Des films minces ont été obtenus en utilisant une solution d'évaporation (l'épaisseur des films était comprise entre 100 et 300 micromètres). En une seconde étape nous avons fixé le taux de BC à 10%, 25%, 50% et les résultats obtenus sont discutés au chapitre IV. L'influence de l'indentation temporelle et de la charge appliquée sur les résultats de comportement mécanique révèle une réponse importante de nos matériaux élaborés.

MOTS CLES : Acrylamide, Bentonite, nanoComposite, Dureté, Stabilité thermique, Propriétés mécaniques, Structure.